T-68

PULSE TESTING OF SYSTEMS WITH SOME NON-LINEARITIES

by

T.N.Coppedge, Jr. R.L.Wolf

May, 1954

Instrumentation Laboratory,
Massachusetts Institute of Technology

PULSE TESTING OF SYSTEMS WITH SOME NON-LINEARITIES

by

Thomas N. Coppedge, Jr., Commander, U.S. Navy
B.S., U.S. Naval Academy, 1941
B.S. in Aeronautical Engineering
U.S. Naval Postgraduate School, 1953

Robert L. Wolf, Lieutenant Commander, U.S. Navy
B.S., U.S. Naval Academy, 1943
B.S. in Aeronautical Engineering
U.S. Naval Postgraduate School, 1953

SUBMITTED IN PARTIAL FULFILLMENT OF THE
REQUIREMENTS FOR THE DEGREE OF
MASTER OF SCIENCE
at the
MASSACHUSETTS INSTITUTE OF TECHNOLOGY
1954

This thesis, written by the authors while affiliated with the Instrumentation Laboratory, M.I.T., has been reproduced by the offset process using printer's ink in accordance with the following basic authorization received by Dr. C. S. Draper, Director of the Instrumentation Laboratory.

COPY

April 7, 1950

Dr. C. S. Draper
33-103

Dear Dr. Draper:

Mr. L. E. Payne has shown to me a recent printed reproduction of a thesis, in this instance a Master's dissertation, submitted in partial fulfillment of the requirements for the degree of Master of Science at the Massachusetts Institute of Technology.

The sample shown is printed by the offset press using screened illustrations, graphs and other material. For the purposes of the Library which include record and permanent preservation, theses reproduced in this manner are perfectly satisfactory and in my opinion meet all of the physical requirements of the graduate school insofar as they pertain to the preparation of a thesis.

I note that in the sample submitted the signatures have been reproduced along with the text by photo lithography. It is suggested that for the Library record copy the author, thesis supervisor and chairman of the Departmental Committee on Graduate Students affix their signatures in writing as complete authorization of the study. These can be written above the reproduced signature if desired.

Sincerely yours,

(signed)

Vernon D. Tate
Director of Libraries

VDT/jl

cc: Dean Bunker
Mr. Payne

COPY

PULSE TESTING OF SYSTEMS WITH SOME NON-LINEARITIES

by

Thomas N. Coppedge, Jr.

Robert L. Wolf

Submitted to the Department of Aeronautical Engineering on May 24, 1954, in partial fulfillment of the requirements for the degree of Master of Science.

ABSTRACT

Pulse responses have been used to calculate frequency response functions for several years. Questions have been raised whether useful pulse responses are obtainable from systems having backlash and saturation effects. It has been found in this investigation that by proper choice of pulse shape, duration and strength, it is possible to realize useful pulse responses despite system defects.

First it is necessary that the pulse function have continuous derivatives to avoid infinite inputs. Secondly, the pulse strength must be adequate to provide an output large compared to the backlash and other uncertainties. Finally the pulse should endure long enough to introduce a pulse of adequate strength without inducing saturation in the system.

Pulse tests of two simple positional servo - mechanisms were performed. The AVSD system is characterized by angular velocity signal damping and the MAVSD system by modified angular velocity signal damping. Parameters pertinent to the investigation are as follows:

(1) Backlash 0.25 to 1.0 milliradians

(2) Gear Train 100 to 1

(3) Motor FD 84-21-1 Diehl Manufacturing Company

(a) maximum acceleration 9300 rad/sec^2

(b) maximum velocity 415 rad/sec

(4) Pulse functions
    (a) Rectangular
    (b) Displaced cosine
(5) Pulse strength — 0.8 to 3.2 milliradian second
(6) Pulse duration — (PD)(NP)R from 0.1 to 1.0

Rectangular pulse functions were found to be unsuitable because of the discontinuous nature of their derivatives. A displaced cosine pulse function of (PD)(NP)R = 1.0 and a pulse strength of three point two (3.2) milliradian seconds produced negligible response deviations for a backlash of one milliradian in both systems.

Thesis Supervisor: Sidney Lees
Title: Assistant Professor of Aeronautical Engineering

May 24, 1954

Professor Leicester F. Hamilton
Secretary of the Faculty
Massachusetts Institute of Technology
Cambridge 39, Massachusetts

Dear Professor Hamilton,

In accordance with the regulations of the faculty, we hereby submit a thesis entitled Pulse Testing of Systems with Some Non-Linearities in partial fulfillment of the requirements for the degree of Master of Science in Aeronautical Engineering.

ACKNOWLEDGEMENT

The authors express their appreciation to the personnel of the Instrumentation Laboratory, Massachusetts Institute of Technology, who assisted in the preparation of this thesis. Particular thanks are due to Sidney Lees, who, as thesis supervisor, inspired and guided the entire project, to Winston Markey for his interest and encouragement, and to Leonard Somers and Samuel Giser for their help in the use of the electronic computers.

The graduate work for which this thesis is a partial requirement was performed while the authors were assigned to the U. S. Naval Administrative Unit, Massachusetts Institute of Technology.

TABLE OF CONTENTS

OBJECT

The object of this investigation is to determine a rational basis for the choice of pulse functions to test systems with limited non-linearities.

CHAPTER 1

INTRODUCTION

Testing individual components and complete systems is a necessary phase of engineering. This practice not only enables verification of predicted performance, but also yields new information concerning properties of the system. Prediction of system performance relies on the existing knowledge of component and system properties. However, new inherent properties are frequently disclosed by the correlation of predicted and actual performance. Thus the complementary nature of these two aspects of testing is evident.

Dynamic characteristics of systems and components are investigated by analysis of their responses to specific input quantities. Of the many possible input quantities, two classes are most useful. These consist of transient inducing inputs and sinusoidal inputs. The relationship between the transient response to a pulse input and the steady-state sinusoidal response has been known for many years for systems associated with linear differential equations with constant coefficients. Practical methods for calculating the sinusoidal frequency response from the pulse function transient response were devised by Bromberg[1] and others.

Pulse function testing is particularly valuable when sinusoidal methods are impractical. For example, when the life of the system is short, as in guided missiles, sinusoidal responses cannot be measured directly. Aircraft systems, being subject to changes in environmental conditions during test, do not submit readily to sinusoidal response measurement. However, the time required for pulse testing is much less than that required for sinusoidal techniques. Thus, pulse tests can be completed without materially affecting system life and before significant changes in environment occur. In other instances, damage to

equipment which can result from sinusoidal tests may be avoided with pulse function testing. Recommendations have been made in the interest of economy that pulse techniques be practiced in lieu of sinusoidal for even those occasions when sinusoidal tests are feasible.

Objections have been raised to this recommendation. Statements have been made that physical systems having backlash in the gear train together with velocity and acceleration limits of the motor will yield such poor pulse function responses that the method is useless. Simultaneously, it is asserted that this defect is not as important for sinusoidal tests. These objections were described by Mr. Rawley McCoy of the Reeves Instrument Company, who suggested the subject of this thesis.

From physical reasoning it would appear that pulse techniques should provide results at least as good as those obtained from sinusoidal tests in the presence of the non-linearities outlined above. These non-linearities exist in some measure in every physical system. Successful application of pulse techniques to physical systems are reported by Seamans, Blasingame and Clementson[2], Bollay[3], Gardner and Ross[4] and others. When difficulties appear because of defects in the gear train or limitations of the motor, it seems reasonable to suppose that the difficulties may be overcome by the proper choice of the pulse function input. The purpose of this investigation is to furnish a rational basis for the selection of the pulse function.

Physical systems are subject to interferences which prevent the controlled-member from performing in the ideal manner. Backlash in the gear train is comparable to interferences in this respect. System design practices are to reduce the effect of interferences to a tolerable level described as the level of uncertainty. Similarly, backlash should be minimized, preferably to the level of uncertainty, before the system performs as desired. The strength of the pulse input must be great enough to make the uncertainty and backlash negligible quantities in the response. However, when the maximum value of the physical system response exceeds a critical value, saturation in the velocity or acceleration of the controlled-member occurs. The response magnitude is there-

fore limited if saturation effects are to be avoided. A range of response magnitudes is established by these considerations between a lower limit derived from the backlash or uncertainty level and an upper limit imposed by saturation. The problem is to determine whether or not sufficient latitude exists in this range to provide necessary information for an analysis of the dynamic properties of a given system. In this connection, the influence of pulse shape and pulse duration, as well as pulse strength, has been examined. A qualitative study of the distortion of the response resulting from velocity and acceleration saturation has been made to verify the existence of an upper limit on the response magnitude.

A reasonable surmise is that the deviation from the ideal response arising from backlash will be no greater than that due to the general uncertainty level. The average deviation created by the backlash is expected to be the smaller of the two. This is a consequence of the intermittant nature of backlash as opposed to the continuous nature of the level of uncertainty in a physical system. A consideration of this situation leads to the premise that the effect of backlash on the response will be indistinguishable from the uncertainty level.

Pulse functions, in this investigation, have been applied to two selected systems to provide data for quantitative evaluation of the problems associated with pulse testing physical systems. These two systems have typical closed-chain structures. Selection of the systems was influenced by the relative simplicity of their performance equations and the attendant numerical calculations involved. However, conclusions derived from these cases are believed to be quite general in character.

The investigation reported in this thesis indicates that the responses of physical systems derived from pulse tests will be as satisfactory as those obtained by sinusoidal methods. A definite basis for selecting the proper pulse function is developed. A pulse shape such as a displaced cosine function is desirable. For this type of pulse function, it is found that pulse strength can be increased as the pulse duration is increased. Thus it is possible to avoid saturation effects and yet restrict the response deviation due to a limited amount of backlash. Under these conditions pulse testing of components and complete systems is certainly feasible.

CHAPTER 2

DETERMINATION OF PERFORMANCE OF IDEAL LINEAR SYSTEMS

An ideal linear system is one composed of a set of interacting variables so related that a variation of any one variable causes variation of one or more of the other variables, and in which the principle of superposition applies. Linear systems may be of the open-chain, closed-chain, or multiple loop type. A simple closed-chain linear system is illustrated in Figure 2-1.

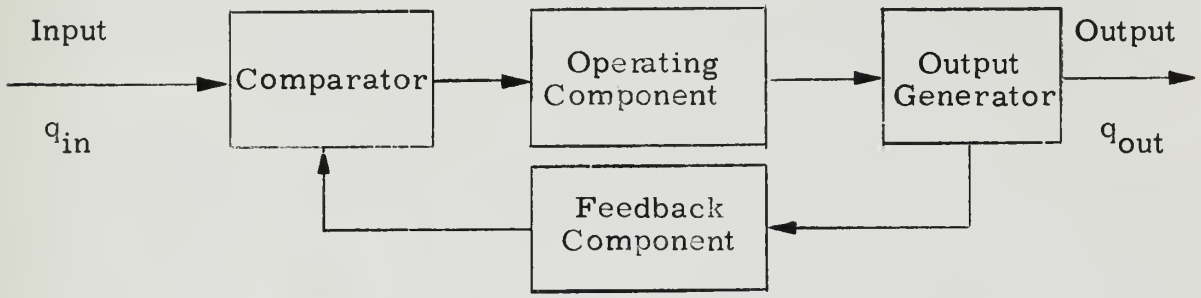

Fig. 2-1 Functional diagram of a closed-chain linear system

The performance of an ideal linear system is defined by Draper, McKay, and Lees[5] as the effects of the system in establishing functional relationships among the physical quantities present. These physical quantities fall into two categories, namely system inputs and outputs. The inputs in general are independent of actions of the system, while the outputs are dependent both upon the inputs and the operation of the system. The performance of the system may then be described by the functional relationships between the outputs and the inputs. The functional relationships are expressed mathematically for linear systems in the form of kinematic and dynamic equations of motion of the system. These equations take the form of linear integro-differential equations with constant coefficients. The coefficients are determined by the parameters of the given system.

Draper et al[5] develop the concept of the performance function which may be derived from the integro-differential equation. The functional relationship between a given input and output may be represented under zero initial conditions as shown below.

$$q_{out} = \left[PF\right]_{id} \left[q_{in};\ q_{out}\right] q_{in}$$

In this expression q_{out} is the output quantity, q_{in} is the input quantity, $\left[PF\right]_{id}$ is the identified performance function. The performance function embodies two components. The first, sensitivity, accounts for magnitude variations between inputs and outputs of the system. The second component, called the response function, represents the time history of the magnitude variations between the inputs and the outputs.

The form of the performance function of particular interest is the steady-state sinusoidal relating function. This form describes the response of an ideal linear system to sinusoidal input variations. Sinusoidal inputs may be represented by the rotating vector complex plane method or by a plot of the sine function with $w_f t$ as its argument and the amplitude of the variation as its coefficient. Both methods are illustrated in Fig. 2-2. In this figure $q_{(in)a}$ is the amplitude, w_f is the angular forcing frequency, and t is time.

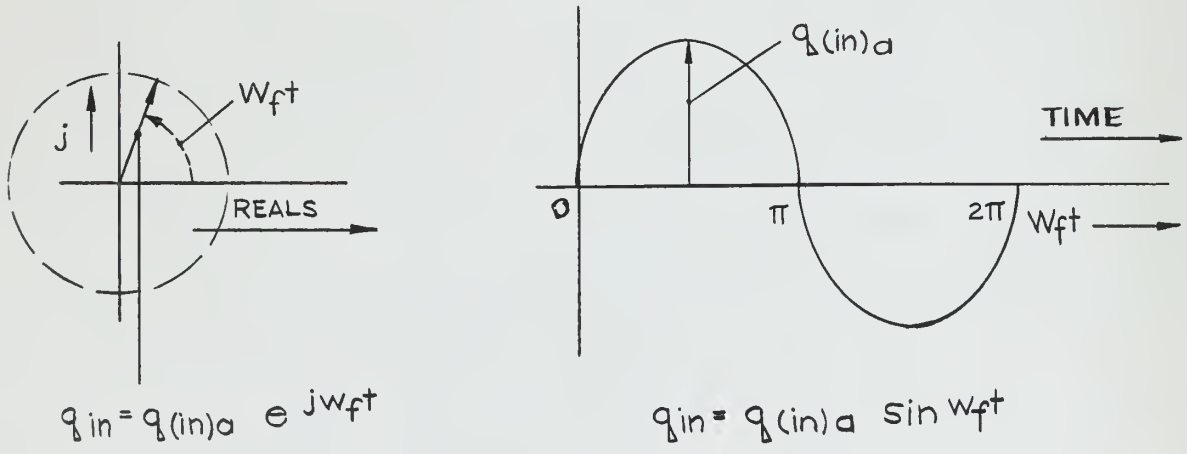

Fig. 2-2 Representation of sinusoidal input functions.

The output or response of the system will also be a sinusoidal function. The response will differ from the forcing function in amplitude and phase angle. Dynamic amplitude ratio (DAR) is the ratio of the response amplitude to the input amplitude. Dynamic response angle (DRA) is the phase shift between the input forcing function (IFF) and the output response (OR). Dynamic amplitude ratio and dynamic response angle are both functions of the forcing frequency. Fig. 2-3 shows a typical steady-state sinusoidal response for an ideal linear system. The steady-state sinusoidal relating function may then be expressed as:

$$\left[PF\right]_{id\left[q_{in};\, q_{out}\right]} = (DAR)_{id\left[q_{in};\, q_{out}\right]}\, e^{j(DRA)_{id\left[q_{in};q_{out}\right]}}$$

The steady-state sinusoidal response may be expressed as

$$q_{out} = \left[PF\right]_{id\left[q_{in};q_{out}\right]}\, q_{(in)a}\, e^{jw_f t}$$

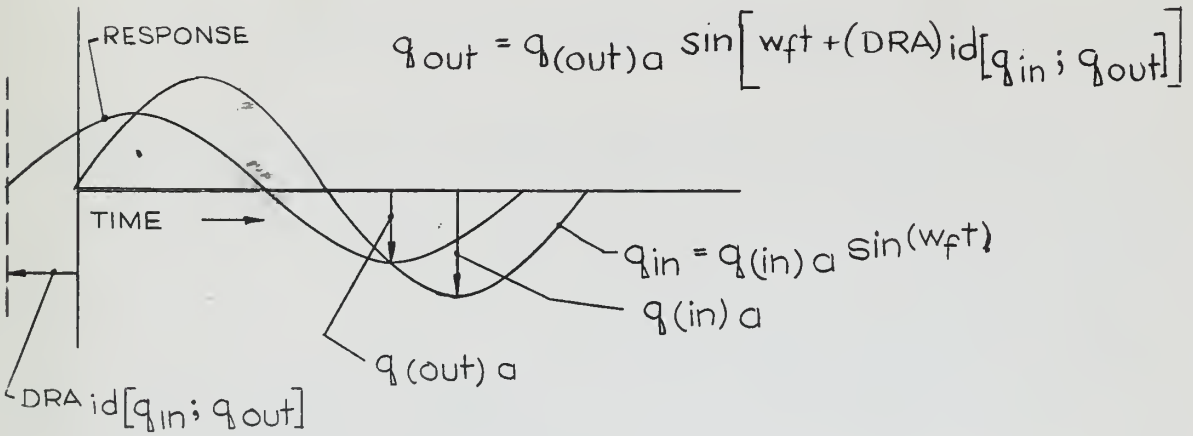

Fig. 2-3 Representation of the steady-state response of an ideal linear system to a sinusoidal input.

The variation of the steady-state relating function with the forcing frequency is the frequency response of the system. Nondimensional performance expressions are derived by dividing the dynamic amplitude ratio by an arbitrarily selected reference amplitude ratio. Performance function derivations and frequency responses for first and second order ideal linear systems are contained in Instrument Engineering[6]. A typical linear scale nondimensional frequency response is shown in Fig. 2-4.

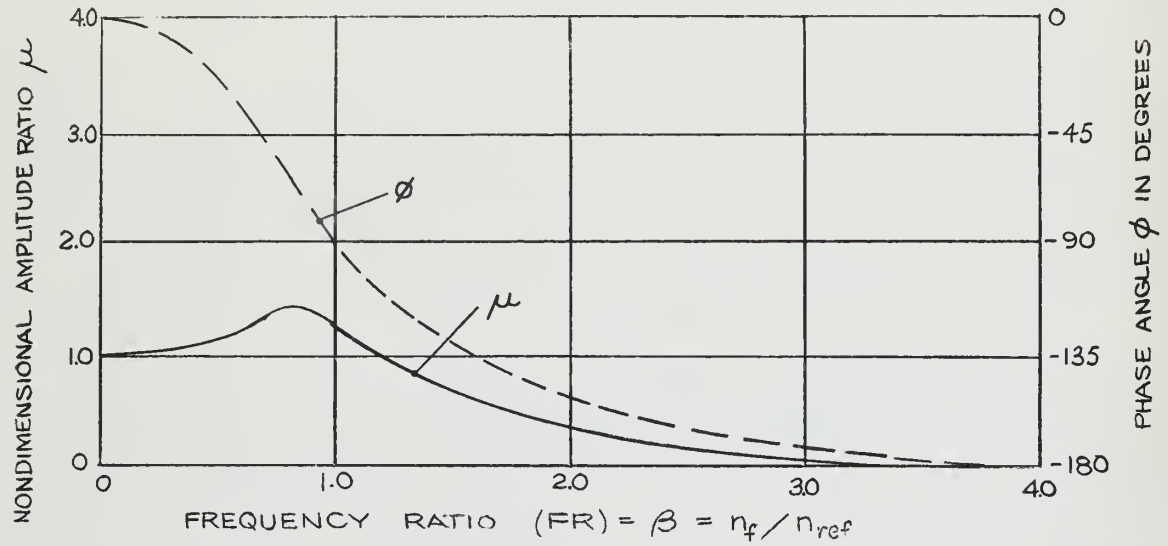

Figure 2-4 Linear scale sinusoidal response characteristics.

Pulse functions may be used as forcing functions for ideal linear systems. Two types of pulse forcing functions are considered by the authors.

2-1 Rectangular pulse function (RPF)

Pulse functions of this type are constant for the duration of the pulse. Discontinuities exist at the beginning and at the end of the pulse. The pulse is described by three attributes. These are pulse height, (PH), pulse duration (PD), and pulse strength (PS). To mathematically define the rectangular pulse function, let u(t) represent the pulse as a function of time, t.

$$u(t) = 0 \; ; \quad t < 0$$

$$u(t) = (PH) \; ; \quad 0 \leq t \leq (PD)$$

$$u(t) = 0 \quad ; \quad t > (PD)$$

Fig. 2-5 shows a representation of a rectangular pulse function

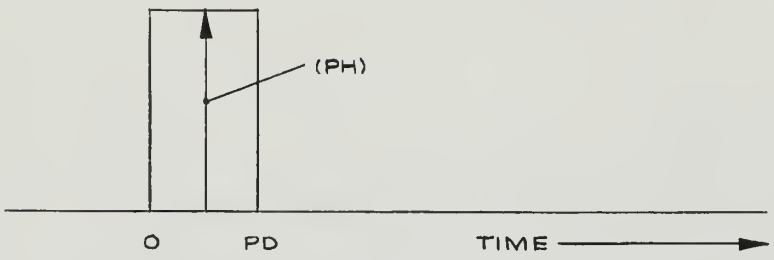

Fig. 2-5 Representation of a rectangular pulse function.

Pulse strength (PS) is defined

$$(PS) = \int_0^{(PD)} (PH)\, dt = (PH)(PD)$$

2-2 Displaced cosine pulse function (DCPF)

Pulse functions of this type vary in magnitude throughout the duration of the pulse. They attain a maximum value only once during the pulse duration. The pulse is described by three characteristics. These are pulse height (PH), pulse duration (PD), and pulse strength (PS). To mathematically define a displaced cosine pulse function, let u(t) represent the pulse as a function of time, t.

$$u(t) = 0 \quad ; \quad t < 0$$

$$u(t) = \frac{(PH)}{2}\left[1 - \cos 2\pi \frac{t}{(PD)}\right] ; \quad 0 \leq t \leq (PD)$$

$$u(t) = 0 \; ; \; t > (PD)$$

Fig. 2-6 shows a representation of a displaced cosine pulse function.

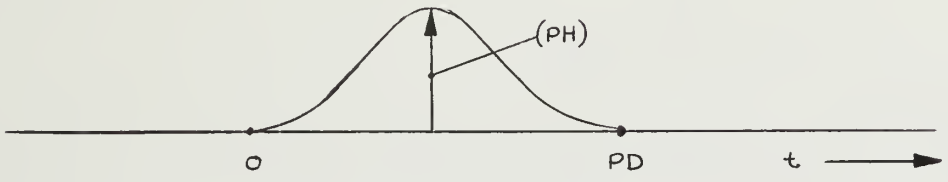

Fig. 2-6 Representation of a displaced cosine pulse function.

Pulse strength (PS) is defined:

$$(PS) = \int_0^{(PD)} \frac{(PH)}{2}\left[1 - \cos 2\pi \frac{t}{(PD)}\right] dt = \frac{(PH)(PD)}{2}$$

Instrument Engineering,[6] Bromberg,[1] Seamans, Blasingame, and Clementson,[2] and others develop numerical and graphical methods for obtaining the frequency response of an ideal linear system from data obtained through pulse testing. Essentially the methods consist of applying a pulse disturbance to the system and recording the input pulse and output response as functions of time. Fig. 2-7 shows illustrative time responses of second order (0;0, 1, 2) linear systems for pulse function inputs. The required performance function form may be determined from the time histories recorded. The procedure is to obtain the Fourier transforms of the input and the response. These transforms may be shown to be continuous functions of frequency. The ratio of the Fourier transform of the response to that of the input is the desired relating function. The relating function thus determined expresses the complete frequency response of the system.

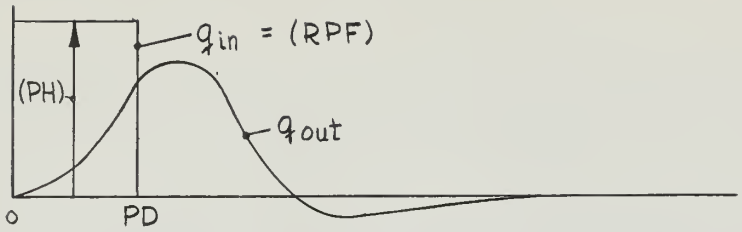

(a) Response to rectangular pulse function

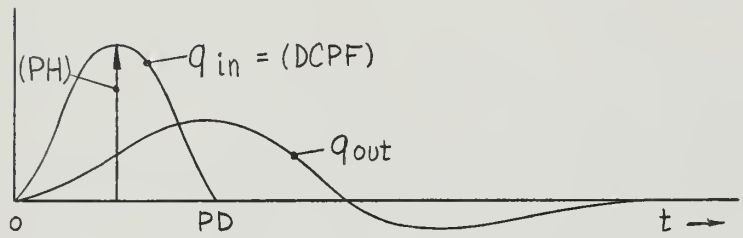

(b) Response to displaced cosine pulse function

Fig. 2-7 Linear second order system time responses to pulse function inputs

From the foregoing it is evident that for an ideal linear system the same criteria may be determined by pulse disturbance methods as can be determined by sinusoidal methods. This is noteworthy since the time required to apply pulse test techniques is much less than that required using sinusoidal methods. Further it is conceivable that pulse techniques can be applied to systems when sinusoidal testing might cause excessive wear or damage to the system whose performance is to be determined.

CHAPTER 3

DESCRIPTION OF THE PERFORMANCE OF SYSTEMS WITH LIMITED NON-LINEARITIES

A non-linearity exists in a system when a dependent variable is determined by an independent variable in accordance with some non-ideal relationship. For example, the independent variable might vary sinusoidally and the dependent variable will then vary periodically but not sinusoidally. This constitutes non-linear dependence. Fig. 3-1 illustrates the non-linear relationship just described.

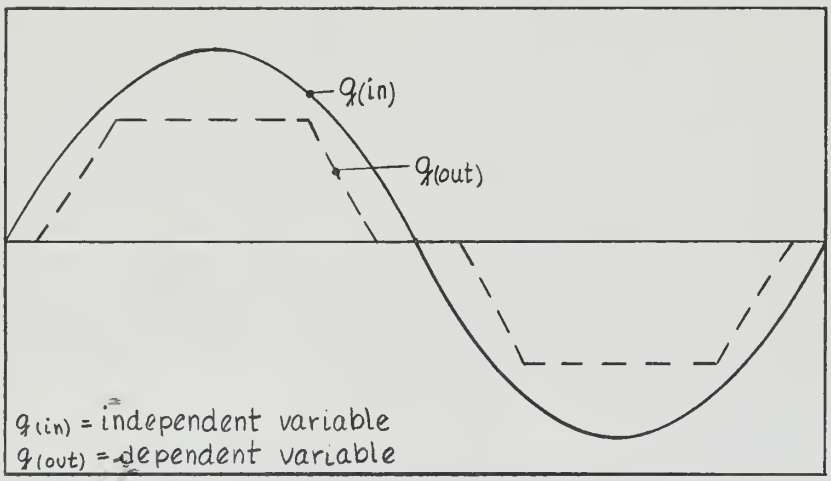

Fig. 3-1 An example of a non-linear response.

The non-linearities considered in this thesis are nominal amounts of backlash in a gear train as well as saturation characteristics of a motor. As noted in Chapter 1, these will exist in some measure in almost every physical system.

A system response forced by a pulse function input is termed a transient response. An example of such a response is shown in Fig. 2-7 of Chapter 2. The transient nature is readily evident. Correspondence of the input and output quantities is attained only when both have returned to zero displacement. The response does not reach a state of continuous

correspondence with the input pulse function prior to this time. Further, it does not follow the pulse function with a constant error. The discussion which follows is concerned only with system transient characteristics.

Fig. 3-2 illustrates schematically the relationship existing between the controlled-member and the torque summing member when backlash is present. The term controlled-member refers to the output member of a feedback control system. The torque summing member is considered to be the next to last gear in the train.

Tustin[7] develops a technique that makes it possible to closely approximate the controlled-member motion when backlash exists in the gear train. It is assumed that some point between the torque summing member and the controlled-member moves in the manner predicted by ideal linear theory. This assumption is reasonable when the backlash constitutes a relatively small part of the total motion of the controlled-member. The location of the point is established by Tustin's method as the mean value of the motions of the controlled-member and the torque summing member. Motion of this point is referred to as mean motion. The actual motion of the controlled-member is calculated by combining the mean motion predicted by ideal linear theory with a deviation calculated from the backlash. The angular displacement of the point performing the mean motion is given by the expression:

$$A_{(mean)} = \frac{I_{(cm)} A_{(cm)} + I_{(tsm)} A_{(tsm)}}{I_{(cm)} + I_{(tsm)}} \qquad (3\text{-}1)$$

where

$I_{(cm)}$ = controlled-member inertia

$I_{(tsm)}$ = torque summing member inertia referred to the control member.

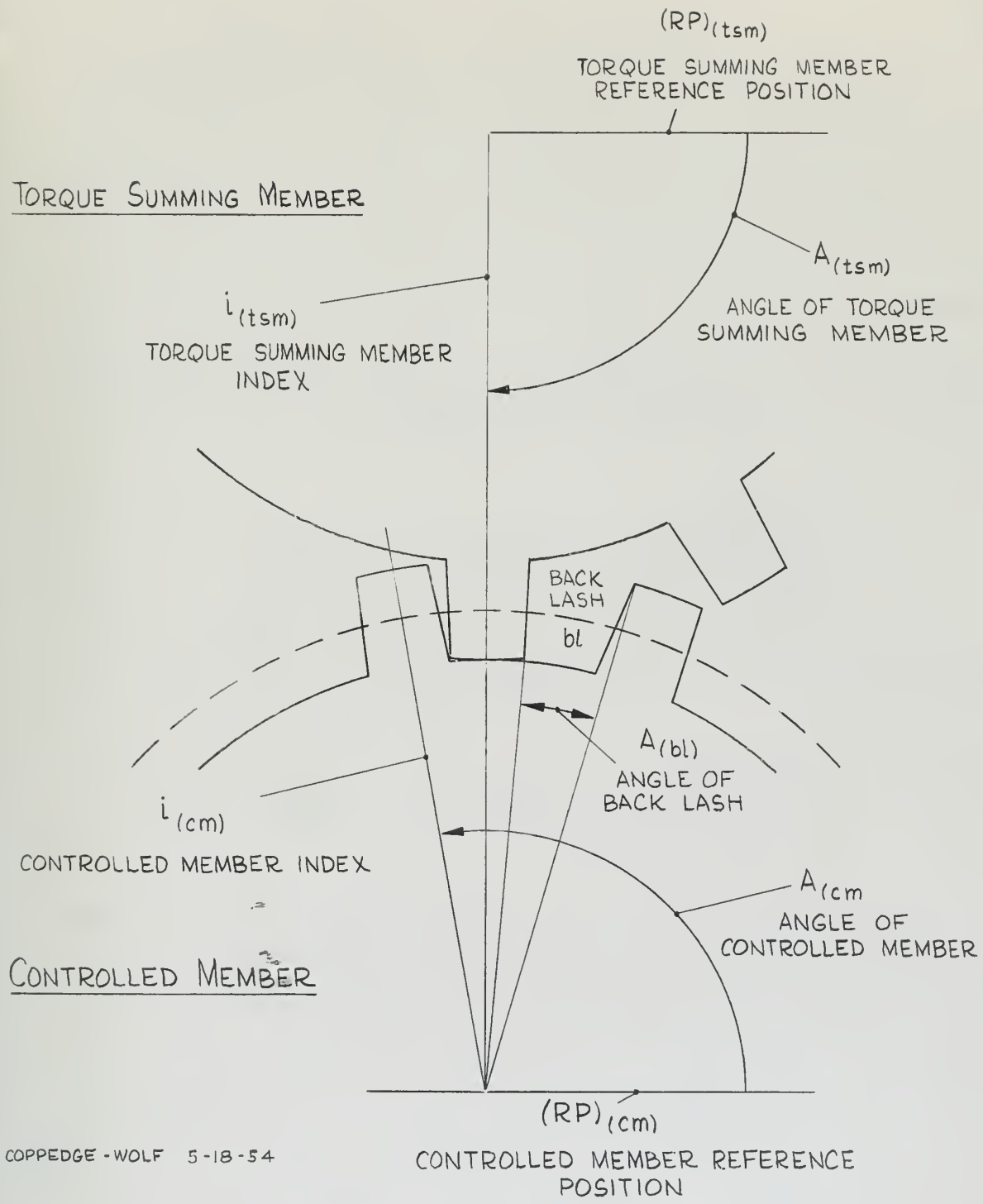

Fig. 3-2 Schematic diagram of the relationship between controlled-member and torque summing member when backlash exists in the gear train.

The motions of the controlled-member and torque summing member are intermittant relative to the mean motion as the backlash is taken up in one direction or the other. When the backlash is small the motion of each member may be represented as a deviation from the mean motion. From the definition of the mean motion, it is noted that the deviation of the torque summing member is opposite to that of the controlled-member when the backlash is being taken up. The sum of these deviations equals the whole backlash. Each member may be considered to take up a fixed proportion of the total relative motion due to backlash. The portion of the backlash taken up by the controlled-member is:

$$\frac{I_{(tsm)}\, A_{(bl)}}{I_{(tsm)} + I_{(cm)}} = A_{(bl)(cm)} \qquad (3\text{-}2)$$

That taken up by the torque summing member is:

$$\frac{I_{(cm)}\, A_{(bl)}}{I_{(tsm)} + I_{(cm)}} = A_{(bl)(tsm)} \qquad (3\text{-}3)$$

It is now possible to describe the motion of the controlled member. Referring to Fig. 3-3a, the decaying transient oscillatory curve represents the velocity of the mean point. The backlash is assumed to be taken up at the initial instant. As a result, the controlled-member velocity duplicates that of the mean point until the first peak occurs. At this instant the mean velocity decreases. However, in the absence of friction, the controlled-member continues to move with a constant velocity because of the backlash. The mean velocity decreases until the effective backlash is taken up at which instant the gear teeth make contact. It is assumed that contact between the gear teeth is achieved without bounce effects. At contact the torque summing member slows down the controlled-member while it in turn speeds up. Fig. 3-3b shows the velocity deviations of the controlled-member relative to the velocity of the mean point.

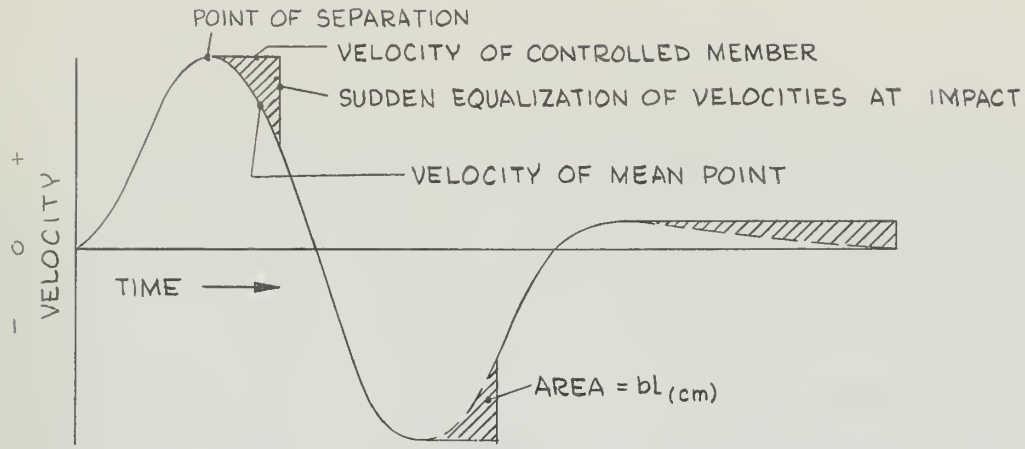

Fig. 3-3a Velocity of the controlled-member relative to the velocity of the mean point for backlash in the gear train.

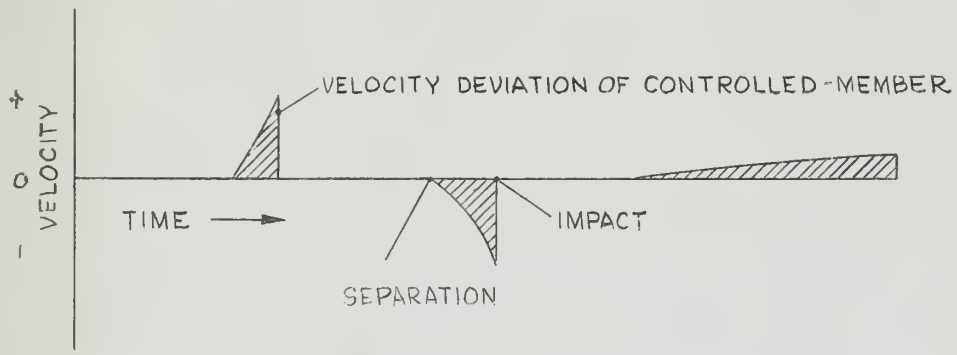

Fig. 3-3b. Deviation velocity of the controlled-member

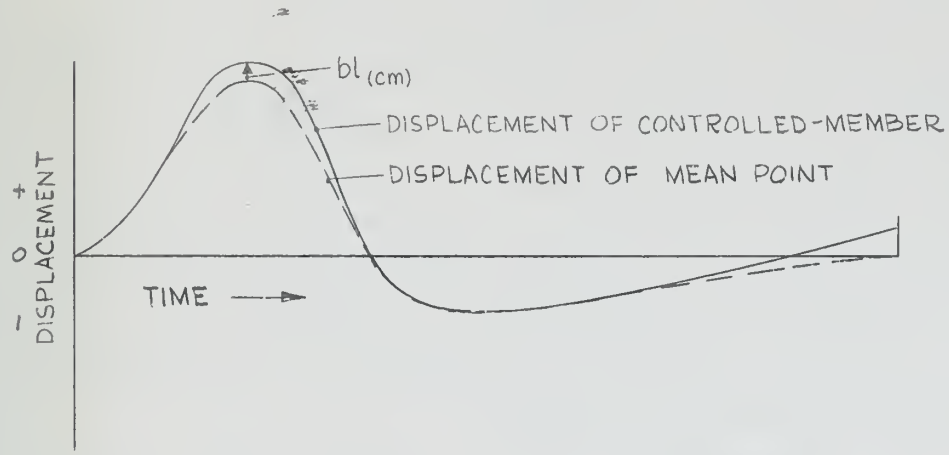

Fig. 3-3c. Displacement of controlled-member relative to the displacement of the mean point.

Figure 3-3. Motion of the controlled-member relative to the mean point for a decaying transient oscillation of the mean point as adapted from Tustin[9]

The controlled-member displacement curve is obtained by integrating the velocity curve of the controlled-member. Fig. 3-3c represents the angular displacement curves corresponding to the velocities in Fig 3-3a. The integral of each of the shaded triangular areas of Fig. 3-3a is equal to the effective backlash experienced by the controlled-member.

From the above discussion, it is apparent that the deviation of the controlled-member displacement never exceeds the effective backlash of the controlled-member. When the backlash itself is small and the peak displacement of the mean point is comparably large the net effect of backlash is insignificant. For this case, the area between the controlled-member and mean point angular displacement curves will be a very small percentage of the area under the mean point curve.

Torque saturation characteristics of the motor may be considered to impose limits on the velocity and acceleration of the controlled-member. The undesirable effects of driving a system into saturation may be seen in Fig. 3-4. This figure shows the ideal linear angular displacement response of a second order system to a rectangular pulse input. Response curves are also included for both velocity and acceleration limiting of the controlled-member. It is noted that velocity and acceleration limiting increase the peak amplitudes of the transient response. Further, a considerable time lag resulting from the limiting is evident. Fig. 3-5 illustrates the effect on the velocity of the controlled-member of velocity limiting and acceleration limiting. Similarly, Fig. 3-6 shows the effect of acceleration limiting on the acceleration of the controlled-member. Certain discontinuities are pointed out in the curves of Figs. 3-5 and 3-6. These are attributed to the effect of the discontinuity in the rectangular pulse function which occurs when it returns to zero. These curves were obtained from the General Purpose Simulator of the Instrumentation Laboratory of M.I.T.

Qualitative study of Fig. 3-4 indicates that distortion of the transient response resulting from either velocity or acceleration saturation is unacceptable. The frequency response calculated by Bromberg's [1]

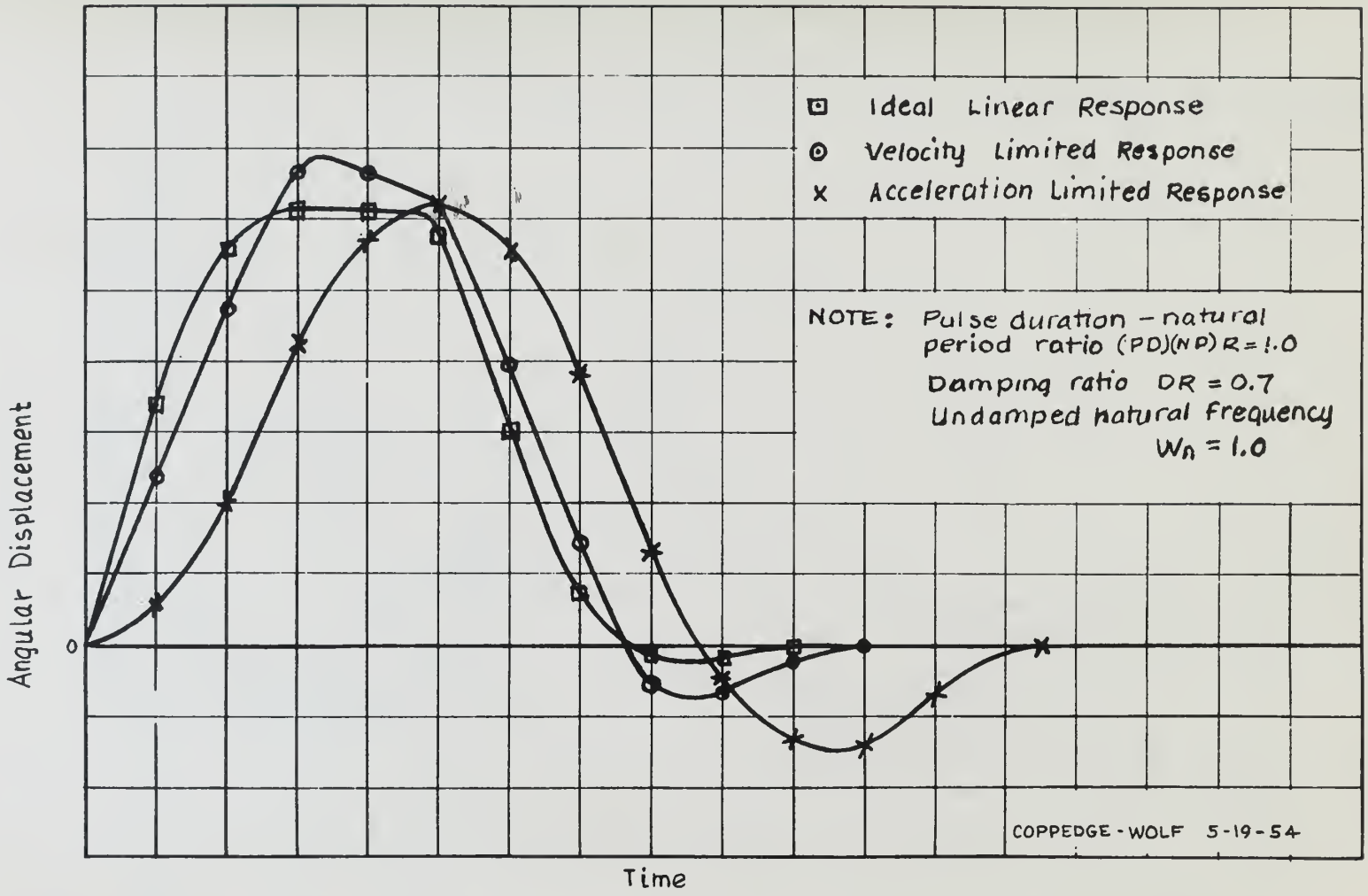

Fig. 3-4 Angular displacement response of a second order (0;0,1,2) system for a rectangular pulse function input illustrating the effect of velocity and acceleration limiting.

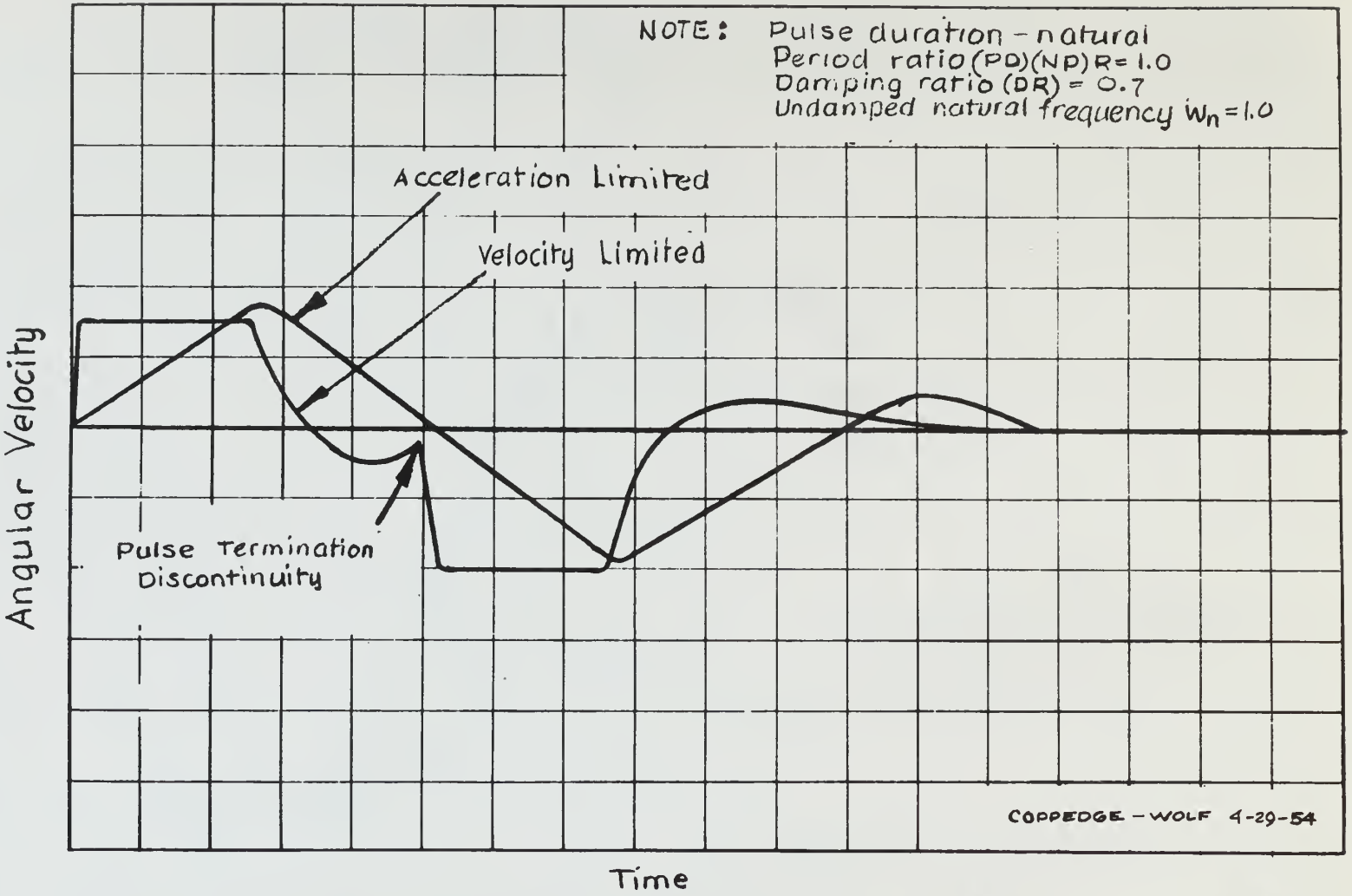

Fig. 3-5 Angular velocity response of a second order (0;0,1,2) system for a rectangular pulse function input illustrating the effect of velocity and acceleration limiting.

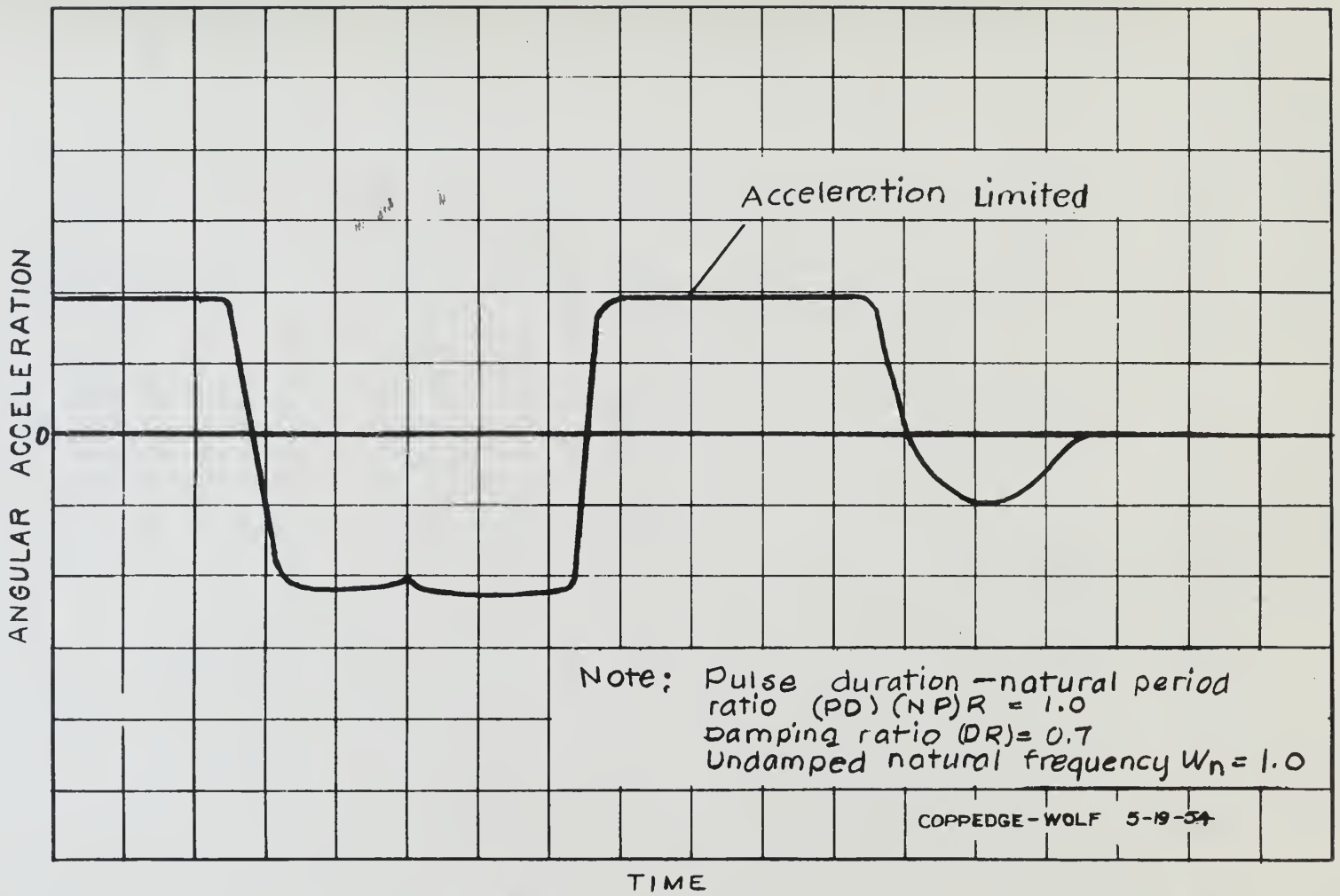

Fig. 3-6 Angular acceleration response of a second order (0;0,1,2) system for a rectangular pulse function input illustrating the effect of acceleration limiting.

method from such a transient response will also be distorted. Satisfactory correlation between the predicted and actual system response under these conditions would be difficult, if possible. It is concluded therefore that the pulse strength must be limited to avoid saturation effects for successful application of pulse test techniques.

The character of the pulse shape, as well as the pulse strength, becomes important if the controlled-member velocity and acceleration are to be prevented from reaching saturation. In this connection, Derivation Summary 3-1 develops the initial accelerations required of representative second and third order systems for a step input. It is evident that a step input to the second order system will demand an acceleration of the controlled-member at the initial instant equal in magnitude to the square of the undamped natural frequency of the system multiplied by the magnitude of the step. For the third order system, the same input demands an acceleration approximately equal to one and three tenths times as great. The argument may be extended to show that a rectangular pulse will force such accelerations at both the beginning and end of the pulse. Consideration of these facts suggests that acceleration, rather than velocity limitations are critical for rectangular pulse functions. The problem clearly will not be alleviated by increasing the pulse duration.

A displaced cosine pulse function, in contrast to the rectangular, possesses no discontinuities. Therefore it is anticipated that the relative importance of the velocity and acceleration limits will depend both on pulse strength and pulse duration.

The discussion presented here is concerned with a method for calculating the angular displacement response of a system with backlash in the gear train. It is suggested that the response deviations from ideal will not exceed the backlash provided velocity and acceleration saturation are not encountered. Acceleration saturation will be difficult to avoid for rectangular pulse inputs. For small amounts of backlash, it is presumed to be possible to obtain sufficiently large peak response amplitudes with a displaced cosine input while avoiding saturation. If this can be done, the non-linearity of the transient response of the physical system may be considered negligible. Close correlation of the predicted and actual system responses then becomes practicable.

Consider the following second order linear differential equation with constant coefficients.

$$('p^2 + 2\zeta\,'w_n\,p + 'w_n^{\,2})\,A_{(out)} = \sigma\,'w_n^{\,2}\,A_{(in)} \qquad (1)$$

where

$'p$ = non-dimensional derivative operator

$A_{(in)}$ = independent variable

$A_{(out)}$ = dependent variable

$'w_n$ = non-dimensional undamped natural angular frequency

ζ = damping ratio

σ = dimensional similarity factor

The Laplace transformation yields:

$$A_{(out)}(\lambda) = \frac{\sigma\,'w_n^{\,2}}{(\lambda^2 + 2\zeta\,'w_n\lambda + 'w_n^{\,2})}\,A_{(in)}(\lambda) \qquad (2)$$

for $\lambda = \alpha + j\,2\pi\beta$

and λ = nondimensional Laplace transform variable

α = real component of λ

$2\pi\beta$ = imaginary component of λ

Let $A_{(in)}$ = unit step function

Then, $A_{(in)}(\lambda) = \frac{1}{\lambda}$ (3)

Substituting in (2)

$$A_{(out)}(\lambda) = \frac{\sigma\,'w_n^{\,2}}{\lambda(\lambda^2 + 2\zeta\,'w_n\lambda + 'w_n^{\,2})} \qquad (4)$$

Derivation Summary 3-1 Initial acceleration of second and third order systems for a step input. (Page 1 of 3)

$$A''_{(out)}(\lambda) = \frac{\sigma\, {}'w_n^{\,2}\, \lambda^2}{\lambda(\lambda^2 + 2\zeta\, {}'w_n \lambda + {}'w_n^{\,2})} \qquad (5)$$

$$A''_{(out)}(\lambda) = \frac{\sigma\, {}'w_n^{\,2}\, \lambda}{(\lambda^2 + 2\zeta\, {}'w_n \lambda + {}'w_n^{\,2})} \qquad (6)$$

For simplicity let ${}'w_n = 1.0$, $\sigma = 1.0$

Substituting for ${}'w_n$ and σ, and expanding in partial fractions

$$A''_{(out)}(\lambda) = \frac{-\zeta + j\sqrt{1-\zeta^2}}{2j\sqrt{1-\zeta^2}\,(\lambda - \lambda_1)} + \frac{-\zeta - j\sqrt{1-\zeta^2}}{2j\sqrt{1-\zeta^2}\,(\lambda - \lambda^*_1)} \qquad (7)$$

Where λ^*_1 is the complex conjugate of λ_1. Taking the inverse transform,

$$A''_{(out)} = \frac{-\zeta + j\sqrt{1-\zeta^2}}{2j\sqrt{1-\zeta^2}}\, e^{\lambda' 1 t} - \frac{-\zeta - j\sqrt{1-\zeta^2}}{2j\sqrt{1-\zeta^2}}\, e^{\lambda^* 1 't} \qquad (8)$$

where $'t$ = non-dimensional running variable.

At $'t = 0$

$$A''_{(out)} = 1.0 = {}'w_n^{\,2} \qquad (9)$$

(a) initial acceleration of a second order (0;0,1,2) system for a step input.

The third order equation similar to (6) is as follows:

$$A''_{(out)}(\lambda) = \frac{\lambda(1 + {}'t_1 \lambda)}{(\lambda^2 + 2\zeta\lambda + 1)(1 + {}'t_2 \lambda)} \qquad (10)$$

when ${}'w_n = \sigma = 1.0$

$'t_1$ and $'t_2$ are first order non-dimensional time constants.

Derivation Summary 3-1 Initial acceleration of second and third order systems for a step input. (Page 2 of 3)

The inverse transform gives:

$$A''_{(out)} = \frac{1}{{}'t_2}\left\{\frac{-\frac{1}{{}'t_2}\left(1-\frac{{}'t_1}{{}'t_2}\right)}{\left(1-\frac{2\zeta}{{}'t_2}+\frac{1}{{}'t_2{}^2}\right)}\; e^{\frac{-{}'t}{{}'t_1}}\right.$$

$$+\frac{(-\zeta+j\sqrt{1-\zeta^2})\left[1-{}'t_1(\zeta-j\sqrt{1-\zeta^2})\right]}{2j\sqrt{1-\zeta^2}\,(\frac{1}{{}'t_2}-\zeta+j\sqrt{1-\zeta^2})}\; e^{\lambda_1{}'t}$$

$$\left.-\frac{(-\zeta-j\sqrt{1-\zeta^2})\left[1-{}'t_1(\zeta+j\sqrt{1-\zeta^2})\right]}{2j\sqrt{1-\zeta^2}\,(\frac{1}{{}'t_2}-\zeta-j\sqrt{1-\zeta^2})}\; e^{\lambda^*_1{}'t}\right\} \qquad (11)$$

Let $t_1 = \frac{1}{2\pi}$, $t_2 = \frac{1}{1.3(2\pi)}$, $\frac{t_1}{t_2} = 1.3$ and $\zeta = 0.707$.

Then, $A''_{(out)} = 1.3$ for ${}'t = 0$ (12)

or $A''_{(out)} = 1.3\,{}'w_n{}^2$

(b) Initial acceleration of a third order (1,0;0,1,2,3) system for a step input.

Derivation Summary 3-1 Initial acceleration of second and third order systems for a step input. (Page 3 of 3)

CHAPTER 4

GENERAL DESCRIPTION OF TWO SELECTED PHYSICAL SYSTEMS

In Chapter 3, a method is proposed for determining the performance of systems with some non-linearities. In order to find out how practical the techniques are, two physical systems are selected for study. Each is a positional servomechanism with two feedback branches. The first is one associated with a second order (0;0,1,2) performance equation. The other is a system associated with a higher order performance equation, namely a third order (1, 0;0, 1, 2, 3) type. Both systems have as an input angular displacement - $A_{(in)}$. The output of each system is a controlled-member angular displacement -$A_{(cm)}$.

4-1 Ideal Linear Properties of the AVSD and MAVSD Systems

The first system is an angular velocity signal damped positional servomechanism which will be referred to as the AVSD system. A functional diagram of the AVSD system is shown in Figure 4-1. Its ideal linear performance equation is a linear differential equation of the following derivative operator form:

$$\left\{ I_{(cm)eq}\, p^2 + S_{(ps)}[\dot{A}; M]^p \right\} A_{(cm)} = S_{(ps)}[A; M]^{(C)} A_{(cm)} + M_{intfr} \qquad (4\text{-}1)$$

The derivation of the above equation and definitions of the coefficients may be found in Appendix A.

The ASVD system is characterized by the means by which damping is achieved. Negative unity feedback of the controlled-member angular displacement causes generation of a correction signal whenever the displacement is different from that of the input. The existence of signal level elements in the chain of Fig. 4-1 permits reduction of the correction signal by a signal proportional to the torque summing member angular

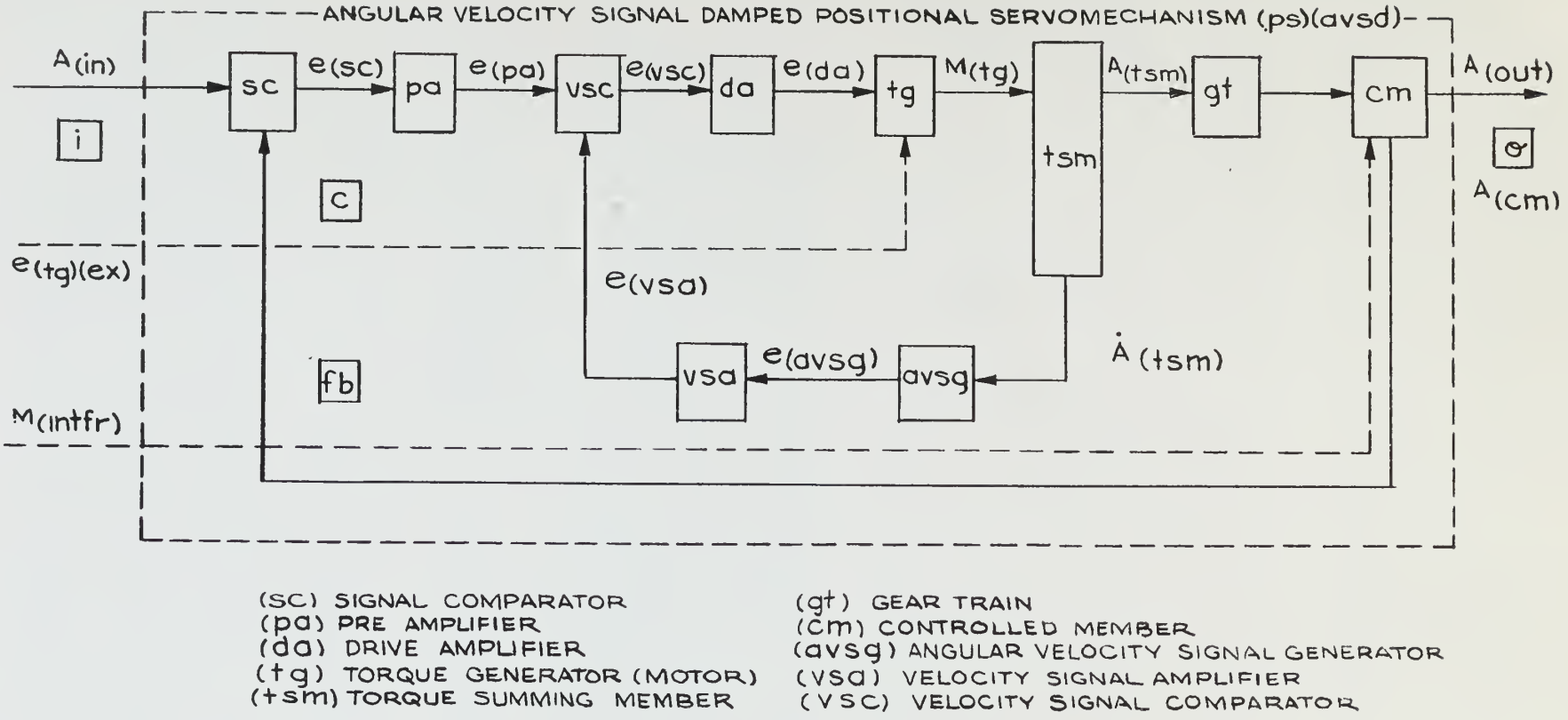

FIG. 4-1 FUNCTIONAL DIAGRAM OF BASIC POSITIONAL SERVO-MECHANISM WITH ANGULAR VELOCITY SIGNAL FEEDBACK DAMPING.

velocity. The reduced correction signal produces an actuating torque in the torque generator which tends to drive the correction signal to zero. Under these conditions, the actuating torque is the difference between a torque proportional to the original correction signal and a torque proportional to the angular velocity of the torque summing member. Thus a damping-like term, introduced at the signal level, is included in the actuating torque. This technique exactly simulates viscous damping while avoiding high power dissipation.

As a final comment on the AVSD system, it can be shown that an error will exist between the output and input shafts when the angular velocity of the controlled-member is constant.

The second system studied is shown in the functional diagram of Fig. 4-2. The diagram differs from that of Fig. 4-1 by the addition of a velocity signal modifier in the angular velocity feedback path. Therefore this system will be referred to as the MAVSD system hereafter.

The velocity signal modifier consists of a passive network differentiating circuit. Incorporating the velocity signal modifier gives the following derivative operator form of the system ideal linear performance equation.

$$\left\{I_{(cm)(eq)}p^2 + S_{(gt)}^2\left[A_{cm};A_{tsm}\right]\left[S_{(tg)}\left[\dot{A};M\right] + \frac{(CT)_{(vsm)}p}{1+(CT)_{(vsm)}p}\,S_{(fb)(av)}\left[\dot{A};M\right]p\right]\right\}A_{(cm)}$$

$$= S_{(ps)}\left[A;M\right](C)\,A_{(cm)} + M_{intfr.} \qquad (4\text{-}2)$$

This equation is equivalent to a third order linear differential equation with constant coefficients. The reader is referred to Appendix A for the derivation of the performance equation and the definition of the coefficients.

A frequency dependent damping characteristic results from the inclusion of the velocity signal modifier in the MAVSD system. The output of the angular velocity signal generator is supplied to the differentiating network of the velocity signal modifier. The resultant output

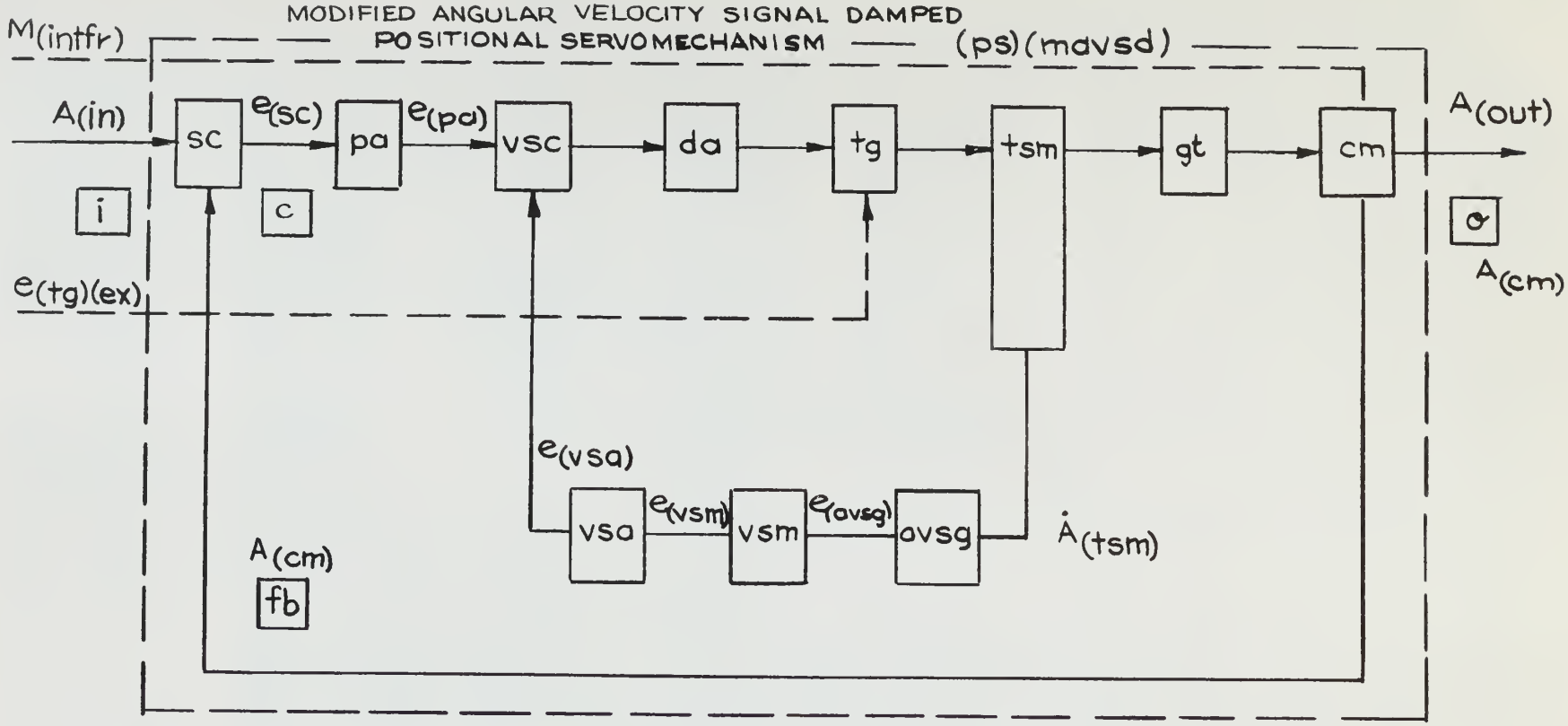

FIG. 4-2 FUNCTIONAL DIAGRAM OF BASIC POSITIONAL SERVOMECHANISM WITH MODIFIED ANGULAR VELOCITY SIGNAL FEEDBACK DAMPING.

is then combined with the correction signal generated from negative unity feedback of the output position.

The frequency-dependence of the velocity signal modifier is apparent in the steady-state frequency response form of its performance function.

$$PF_{(vsm)\ e;e} = \frac{(CT)_{(vsm)}(jw_f)}{1 + (CT)_{(vsm)}(jw_f)}$$

With the characteristic time equal to the undamped natural period, it is evident that the function approaches zero for small values of the forcing frequency. For values of the forcing frequency of the order of the undamped natural frequency, the function approaches unity. The undamped natural frequency referred to is that of the second order system existing before the inclusion of the velocity signal modifier.

The desirability of frequency-dependent damping is developed by Lees[8]. Briefly, it is shown in the reference cited that the damper characteristics should not be prominent for low frequencies, but should become important for frequencies in the range of the undamped natural frequency. This requirement is met by the velocity signal modifier of the MAVSD system.

4-2 Physical Properties of the AVSD and MAVSD Systems

So far no consideration has been given to the physical properties of these two systems. Generalities have been purposely used to ensure wide applicability of possible conclusions. It must be realized that equations 4-1 and 4-2 are not associated solely with the systems shown in Figs 4-1 and 4-2. A variety of components may be chosen. For example, a large range of sensitivities and gear ratios is available. Equations 4-1 and 4-2 are still applicable to describe the performance of the systems. This demonstrates the power of this method of investigation.

To obtain quantitative results from which conclusions may be drawn, it is necessary to specify numerical values of the parameters involved. Appendix A lists the numerical coefficients of the equations of motion of the systems selected for study. These coefficients are derived in Appendix A from physical properties of the systems.

The physical systems chosen use a motor to drive a controlled-member in response to an input command. To drive the controlled-member, a gear train is often needed. The presence of the gear train introduces backlash into the system. In addition interference torques or forces are present. The effects of these physical factors must be considered.

It is known that backlash in a system causes a steady state as well as a transient displacement error. It is apparent that in a well designed system this error must be held to a minimum. To describe this error it is necessary to establish a representative value of backlash to be found in physical systems. Such a value may be determined by considering Fig. 3-2. It is seen that the amount of backlash is the gap between adjacent teeth when gears are meshed. Angular backlash may be expressed in terms of this gap divided by the radius of the gear. Current machining tolerance may be specified in ten-thousandths of an inch. Therefore the gap may be as large as four times the tolerance. Assuming a tolerance of plus or minus one ten-thousandth of an inch and a gear radius of two inches, it is seen that a backlash of approximately one half a milliradian is representative. Therefore in this study the range of backlash is one-fourth to one milliradian.

Motors have limitations on output torque, angular velocity, and angular acceleration. Each of these limitations must be considered. Limited torque specifies a lower limit on the gear ratio that may be used. If too low a gear ratio is specified, the mechanical advantage of the motor will be insufficient to move the heavier controlled-member. A value of gear ratio of one-hundred to one from the motor to the controlled-member is chosen as typical. The value of gear ratio selected limits the controlled-member velocity and acceleration to one one-hundredth of the motor maximum velocity and acceleration if saturation

is to be avoided. Chapter 3 explains why saturation should be avoided. The direct current servo motor with integral tachometer generator FD 84-21-1 built by the Diehl Manufacturing Company is considered representative of the drive motors available. The maximum speed of this motor is 415 radians per second and the maximum acceleration is 9,300 radians per second per second. For the selected gear ratio, the maximum controlled-member velocity is then 4,150 milliradians per second and the maximum acceleration 93,000 miliradians per second per second.

Limitations on controlled-member velocity and acceleration establish a maximum error signal the systems investigated may receive as an input. In actual use of the systems no problem is presented. This is true since the system operates to keep the error signal nulled. In pulse testing, however, a limit is established on the pulse strength that may be used. Since pulse strength is a function both of pulse height and duration, it is possible to introduce too great a pulse height for the duration of the pulse. A pulse of this character will cause saturation of the drive motor velocity or acceleration or both.

The relation between the motor inertia and the controlled-member inertia is an important parameter. In Chapter 3 it was shown that the controlled-member effective backlash is directly proportional to the effective inertia of the motor and inversely proportional to the sum of the effective masses of the motor and the controlled-member. With a gear ratio of one hundredth to one the effective mass of the motor when considered at the controlled-member is ten thousand times its actual value. In this study the effective mass of the motor is made equal to the effective mass of the controlled-member. This makes the effective backlash to be taken up by the controlled- member one half the backlash actually present in the system. Also by this stipulation the actual inertia of the controlled-member is ten thousand times the actual inertia of the motor. It is evident that this inertia ratio is extreme but it is considered desirable. If the actual inertia ratio controlled-member to motor inertia is made smaller, the effective controlled-member backlash will also be reduced. To emphasize the effects of backlash the ratio of effective

inertias for this investigation will be taken as one half.

Deviations in measurement of physical quantities will result. This class of deviations may be described as uncertainties because of their unpredictable nature. A maximum range of the output quantity may be specified which will include all the uncertainties. This range is defined as the uncertainty level. In the systems investigated, the uncertainty level is specified to be one half a milliradian.

CHAPTER 5

PHYSICAL SYSTEM RESPONSES

Physical feedback control systems using a motor and gear train to drive a controlled-member must exhibit non-linear performance characteristics for some operating conditions. For example, when the input quantities are large enough, the motor will exhibit either acceleration or velocity saturation or both. Backlash in the gear train will cause intermittant non-linear operation when the motion is reversed. Chapter 3 outlines a procedure for determining time responses of systems with a little backlash. This method will now be applied to the physical systems described in Chapter 4.

The investigation consists of three phases. The first is the calculation of ideal linear time responses for rectangular and displaced cosine pulse input functions. The second part of the study is the determination of actual responses from computed ideal responses when backlash is varied from one-fourth to one milliradian. The last phase is to evaluate the average error resulting from backlash in time responses as well as frequency responses of physical systems.

5-1 Assumptions

The following assumptions are made to facilitate investigation.

1. The average uncertainty due to interfering forces and torques is considered to be zero. As will be shown later this uncertainty may be larger than the average error caused by backlash. The inclusion of the uncertainties due to interferences in this situation obscures the error caused by backlash.
2. The effects of friction are neglected. The controlled-

member velocity therefore remains constant during take-up of backlash. It is to be noted that Tustin[7] states that the effects of friction are ameliorating.

3. Bounce effects between driving and driven gears are not considered.

4. Motor acceleration and velocity saturation will be prevented. To accomplish this, forcing function pulse strenghts will be limited.

5. All initial conditions are zero. The motor gear is positioned prior to test in contact with the controlled-member gear in the direction the pulse will drive the system when it is first applied. Controlled-member and mean displacement responses will then be identical until separation first occurs.

6. The amplitude of the controlled-member displacement is considered to be essentially zero when the mean motion displacement amplitude has settled to zero. This is a necessary assumption to establish convergence and integrability of the displacement response of the controlled member. It is a reasonable assumption when the uncertainty level is comparable to the controlled-member effective backlash.

5-2 Calculation of Ideal Linear Responses

The Reeves Electronic Analogue Computer (REAC) of the Instrumentation Laboratory, Massachusetts Institute of Technology, was used to calculate the ideal linear time responses. The instrumentation of the REAC is described in Appendix B. Time responses were recorded on the output tables associated with the REAC. Output tables were used to obtain the accuracy required for graphical computation.

Rectangular and displaced cosine pulse functions were applied to the AVSD and MAUSD systems. Pulse duration was one-tenth the natural period of the AVSD system. Time responses were obtained of angular displacement, velocity and acceleration for various damping ratios. Angular velocity and acceleration responses were recorded for use in determining maximum pulse strengths for each system. These responses are shown in nondimensional form in Fig. 5-1 through

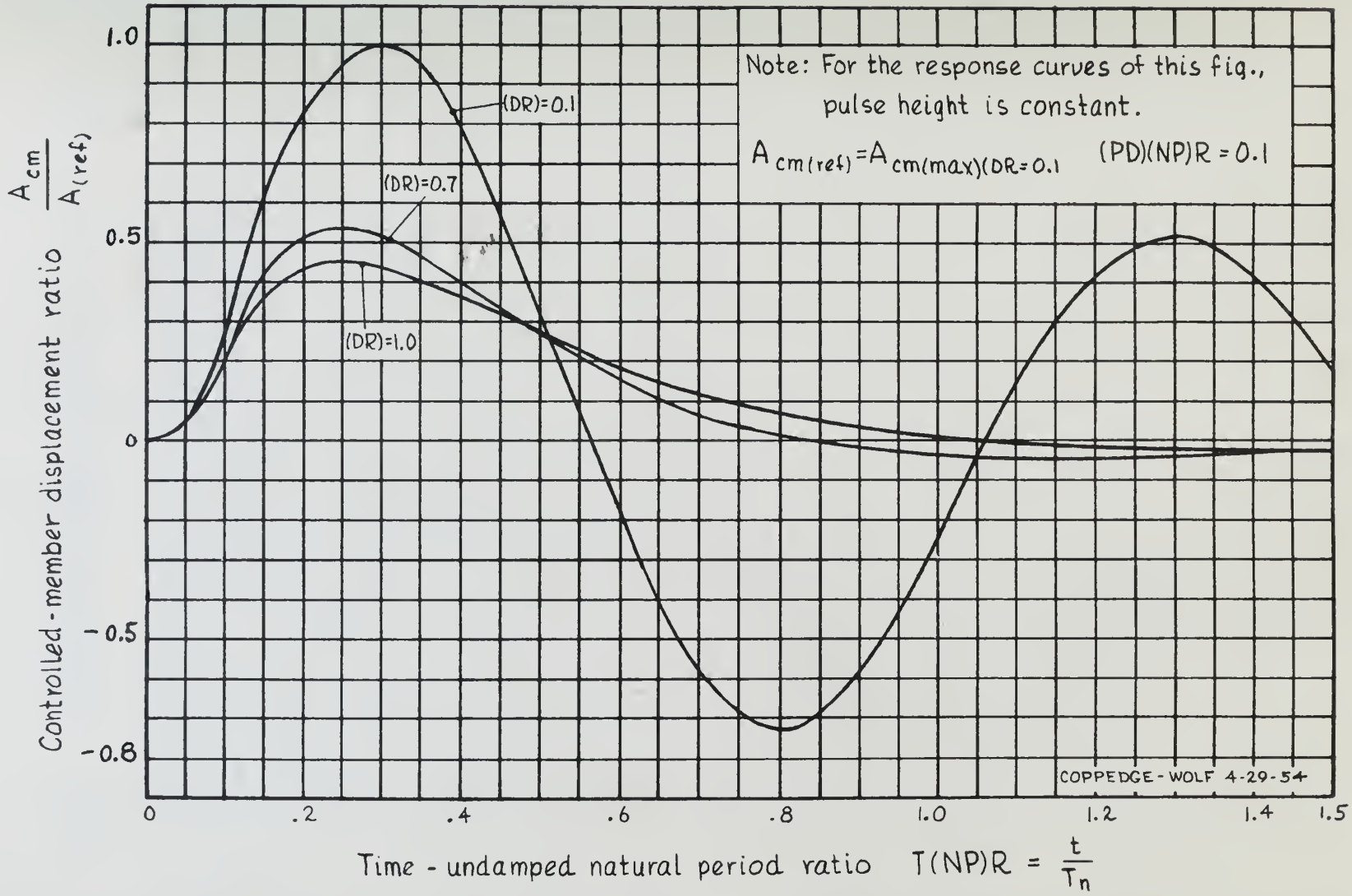

Fig. 5-1 Rectangular pulse function input-angular displacement response curves for the MAVSD system for variation of the damping ratio (DR)

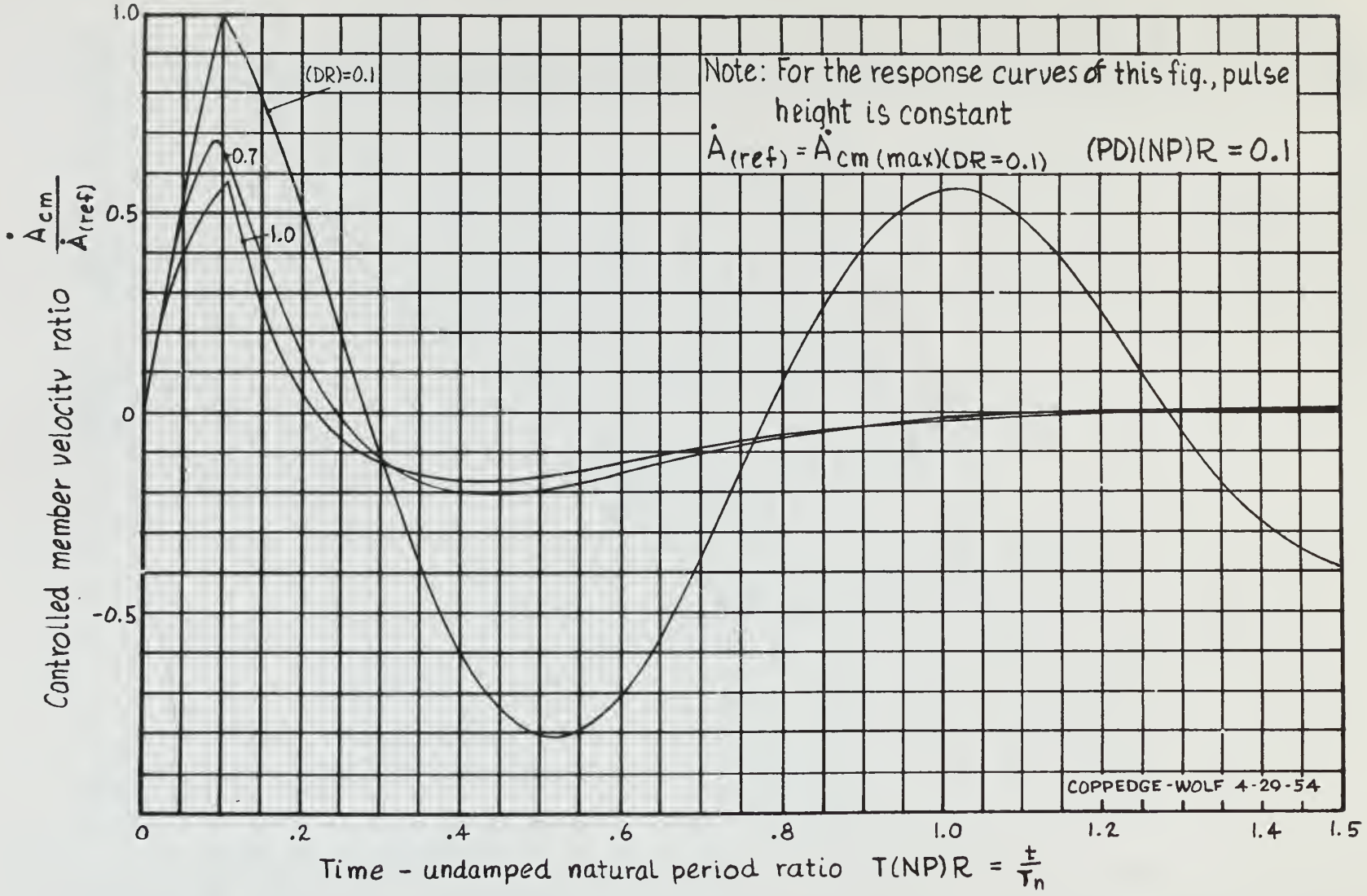

FIG. 5-2 Rectangular pulse function input-angular velocity response curves for the MAVSD system for variation of the damping ratio (DR)

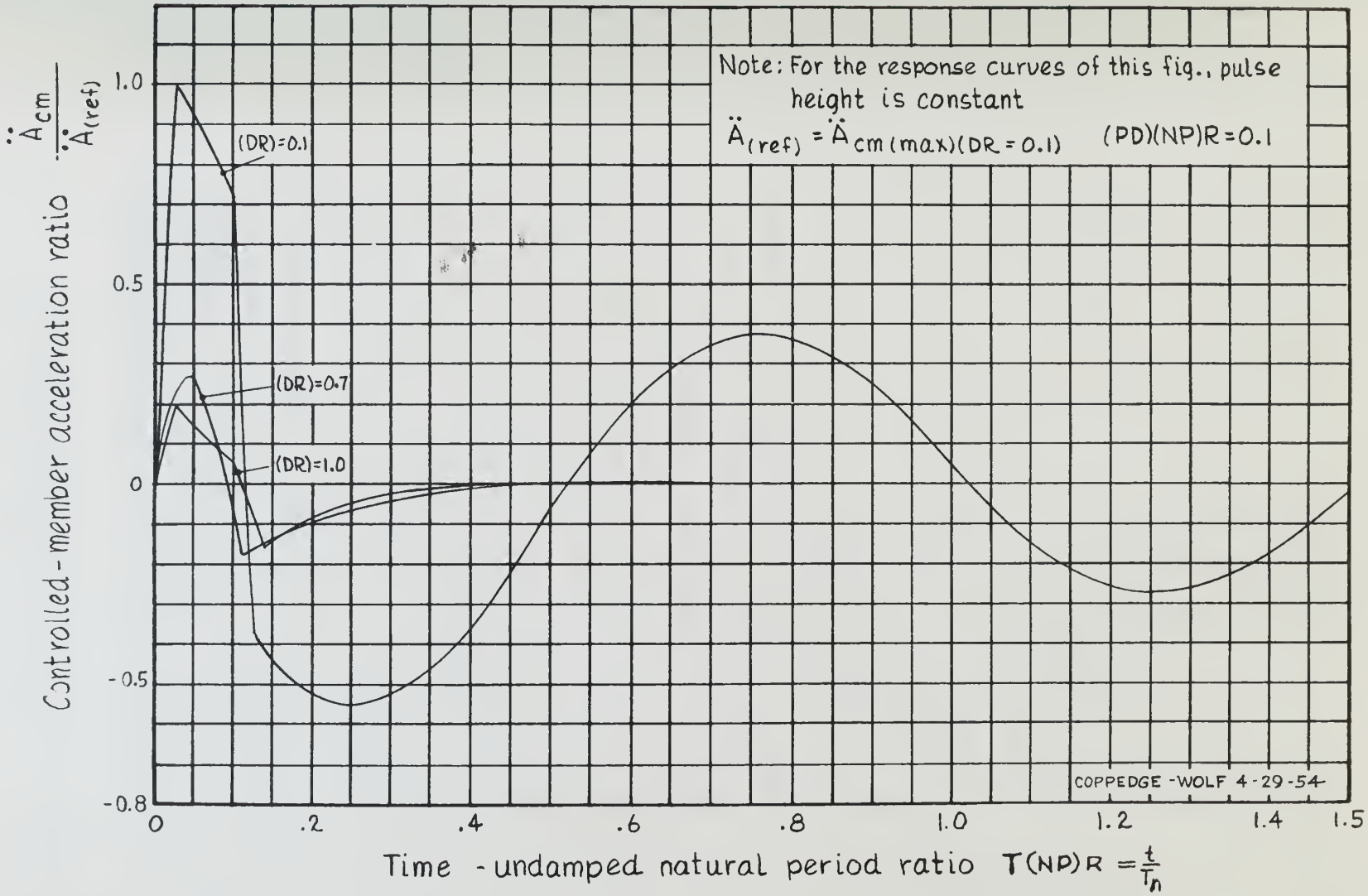

Fig. 5-3 Rectangular pulse function input-angular acceleration response curves for the MAVSD system for variation of the damping ratio(DR).

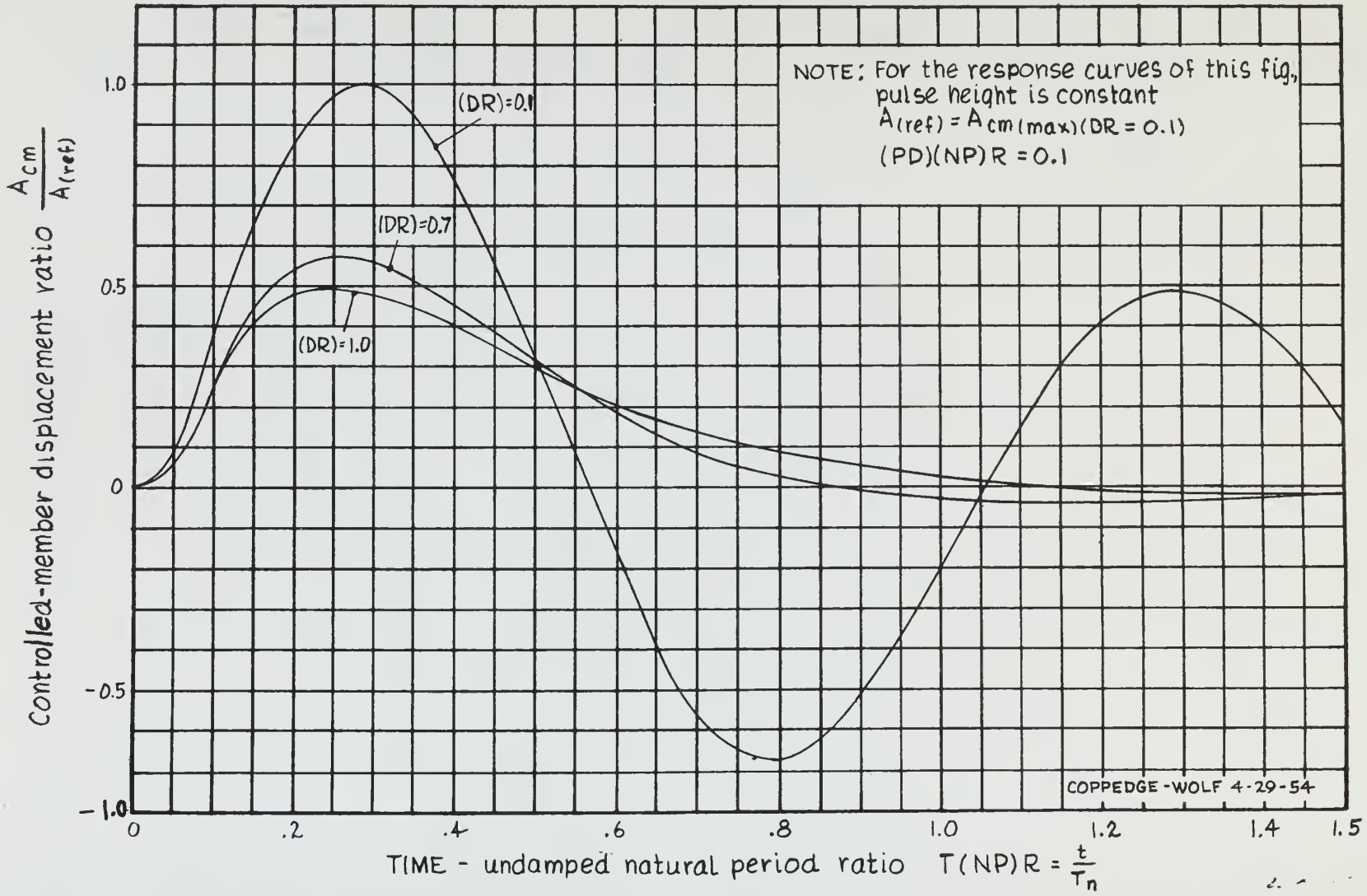

Fig. 5-4 Displaced cosine pulse function input-angular displacement response curves for the AVSD system for variation of the damping ratio (DR).

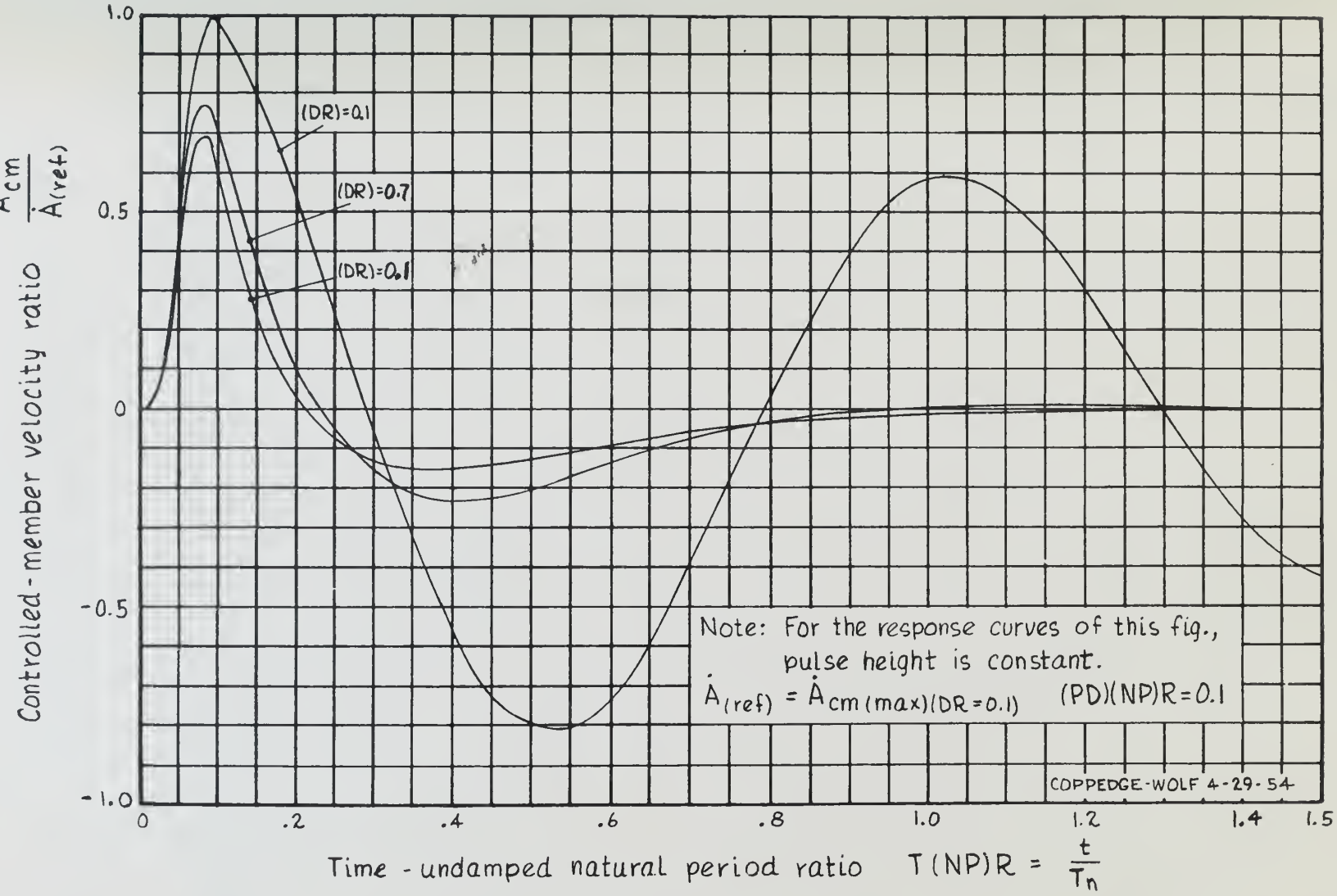

Fig. 5-5 Displaced cosine pulse function input-angular velocity response curves for the AVSD system for variation of the damping ratio (DR)

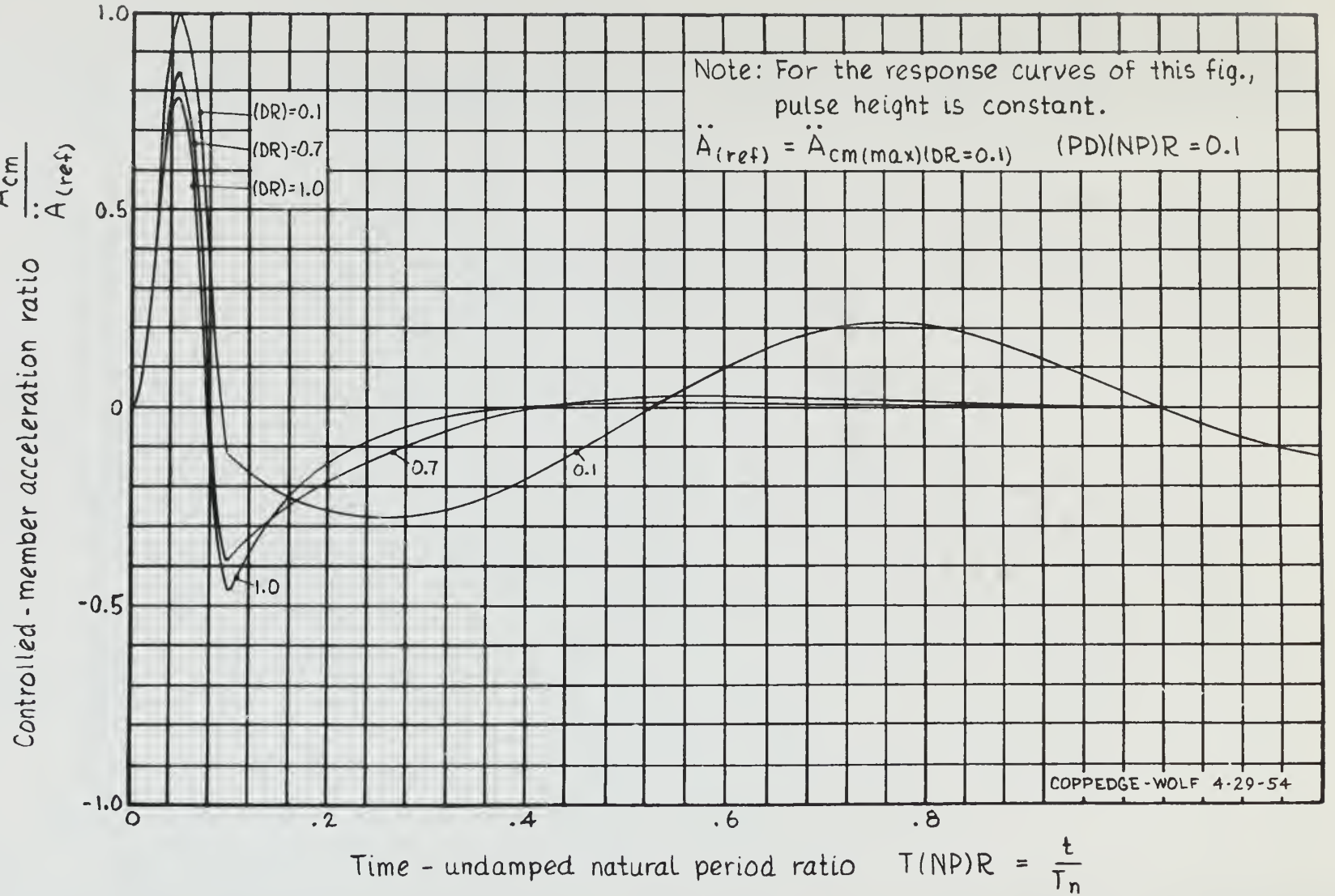

Fig 5-6 Displaced cosine pulse function input—acceleration response curves for the AVSD system for variation of the damping ratio (DR)

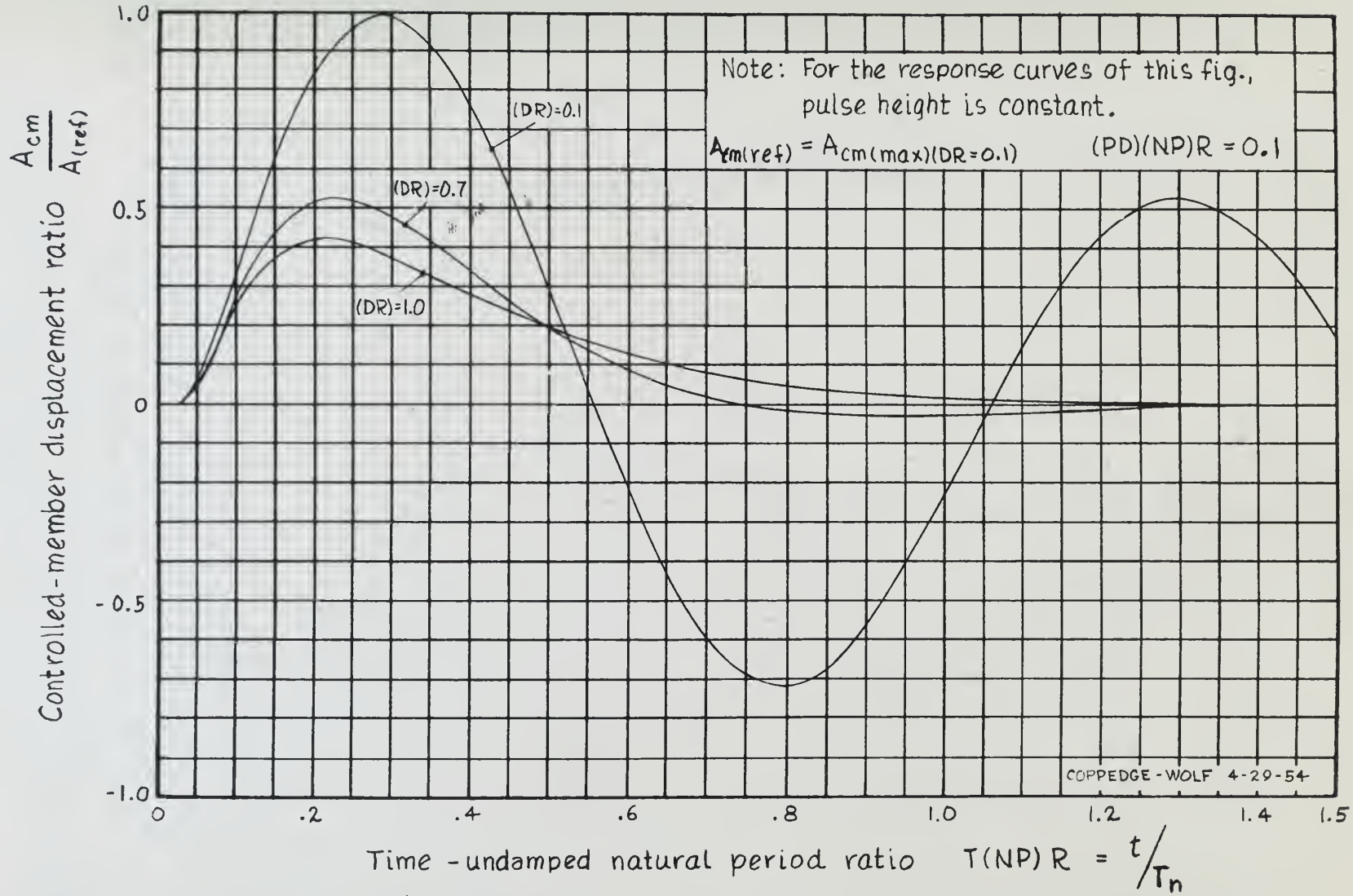

Fig. 5-7 Displaced cosine pulse function input-angular displacement response curves for the MAVSD system for variation of the damping ratio (DR)

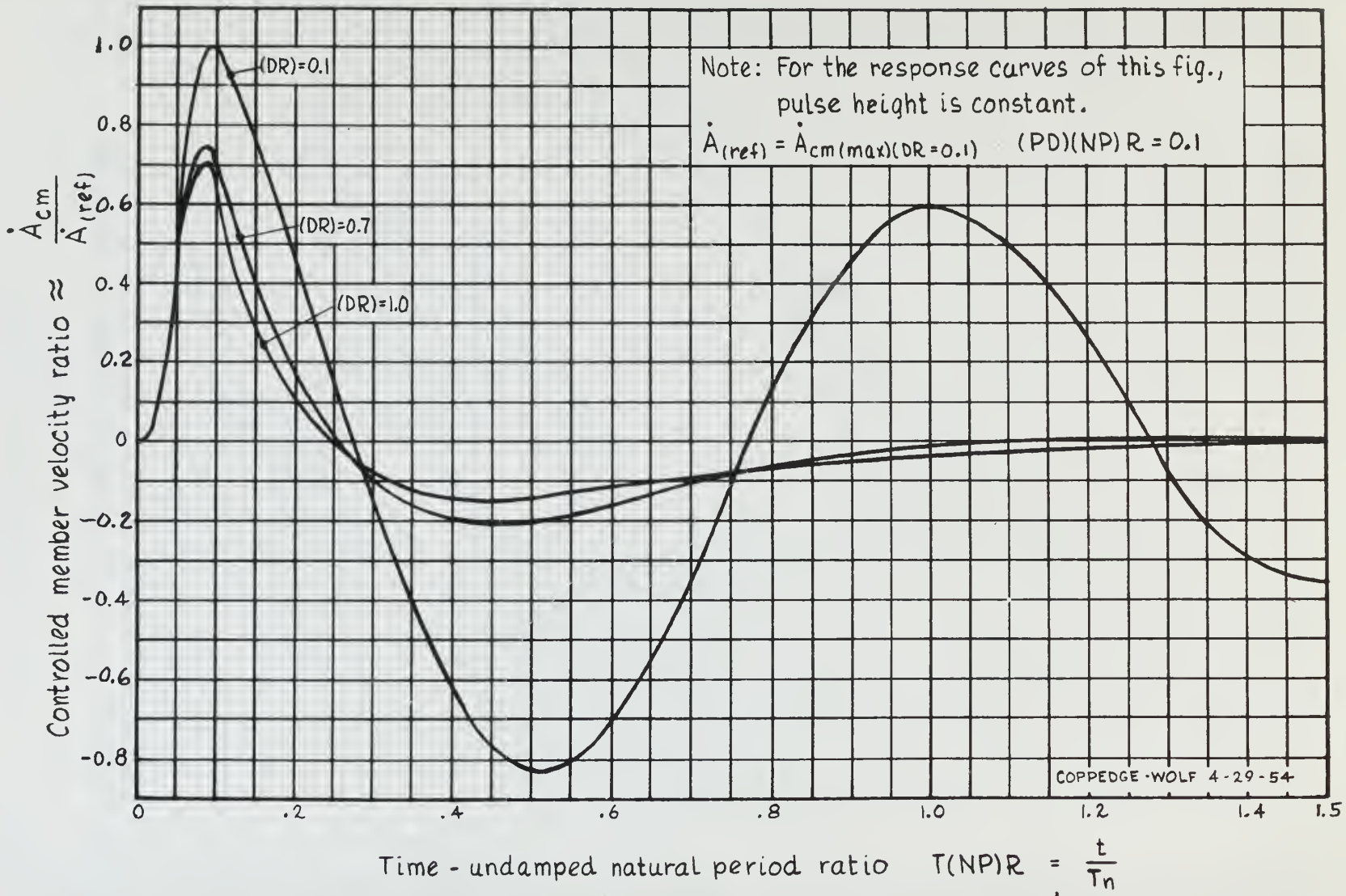

Fig. 5-8 Displaced cosine pulse function input-angular velocity response curves for the MAVSD system for variation of the damping ratio (DR)

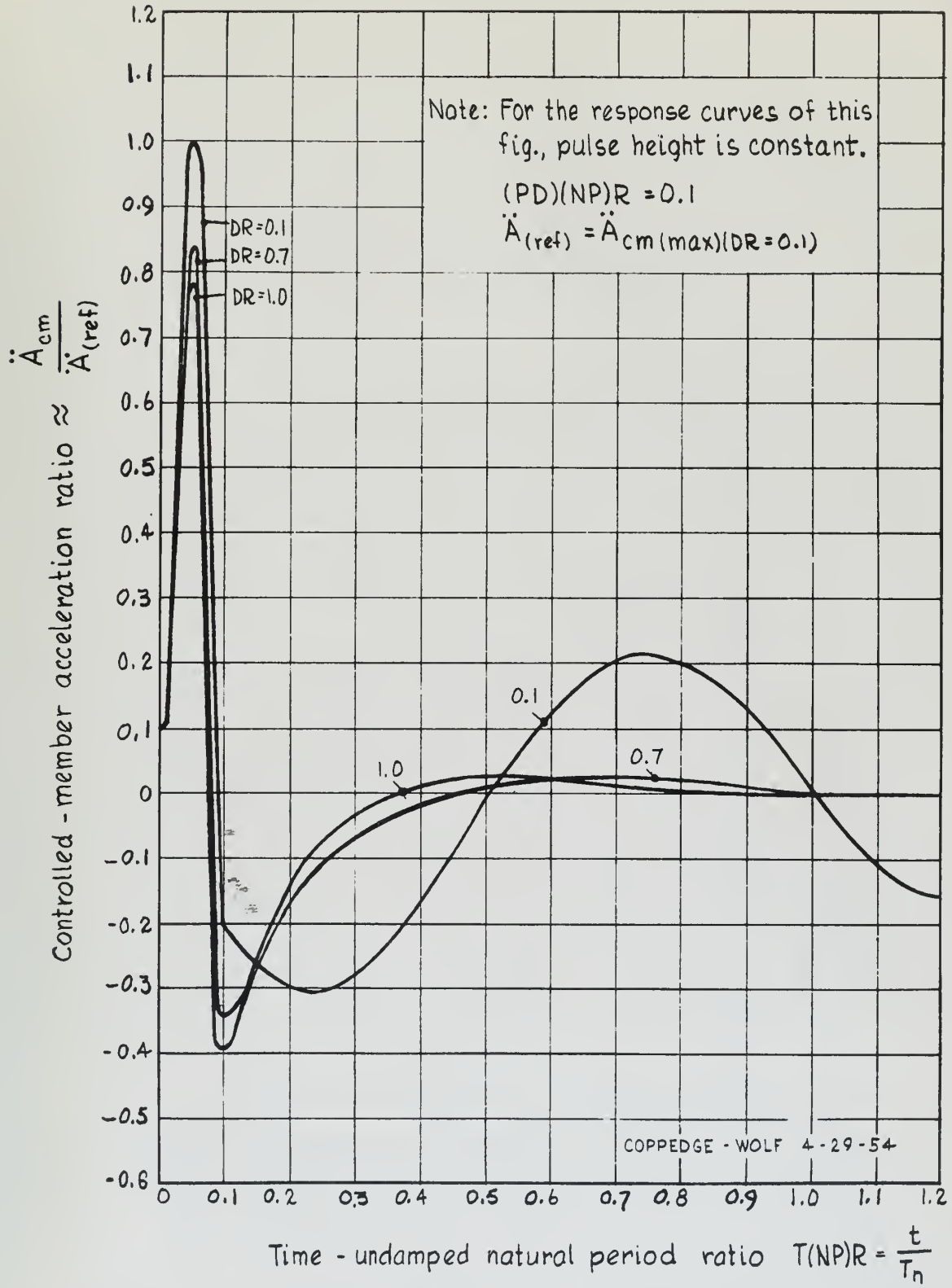

Fig. 5-9 Displaced cosine pulse function input-angular acceleration response curves for the MAVSD system for variation of the damping ratio (DR)

Table 5-1 Numerical values of first peaks of ideal linear response of AVSD and MAVSD systems to rectangular and displaced cosine pulse functions with (PD)(NP)R = 0.1 and PH = 1mr.

	DR	RPF		DCPF	
		AVSD system	MAVSD system	AVSD system	MAVSD system
A_{cm} - mr	1.0	.2175	.2585	.1169	.1276
	0.7	.2690	.3030	.1440	.1485
	0.1	.5020	.5170	.3065	.2812
$\dot{A}_{cm}$ - mr/sec	1.0	21.65	21.65	12.86	13.15
	0.7	24.25	24.50	14.32	14.12
	0.1	33.93	37.10	18.53	18.27
$\ddot{A}_{cm}$ -mr/sec^2	1.0	3590	3170	3035	3092
	0.7	3755	4155	3310	3205
	0.1	4325	18350	3890	3875

Fig. 5-9. Numerical values from which these figures were constructed are tabulated in Appendix C. Table 5-1 shows the numerical values of the response peaks for both systems.

It may be seen from Table 5-1 that neither pulse function of this pulse duration is satisfactory as a forcing function. If a pulse strength sufficient to produce a ratio of one hundred to one peak displacement to effective backlash is used the resulting motor acceleration will exceed its limit and saturation will occur. It is therefore necessary to increase peak displacement response and investigate the effect on acceleration and velocity peaks.

Before discussing this part of the investigation, it is considered necessary to comment on the acceleration peak values caused by the rectangular pulse function. From Derivation Summary 3-1 it may be seen that the acceleration peak values should theoretically be independent of damping ratio and equal to $w_n^2 A_{in}$. w_n^2 for the AVSD system is 4007 radians per second per second. It may be seen from Table 5-1 that the acceleration is dependent on damping ratio for the AVSD system and the value is not constant. Further it may be seen from Derivation Summary 3-1 that the acceleration peak for the MAVSD system should be dependent on damping ratio and should vary from $1.1\ w_n^2 A_{in}$ to $1.4\ w_n^2 A_{in}$ as damping is decreased from critical. w_n^2 for the MAVSD system is 2800 rad/sec^2. Referring again to Table 5-1, it may be seen that the MAVSD acceleration peaks for damping ratios of 1.0 and 0.7 are approximately correct. The peak value for a damping ratio of 0.1 is not to be trusted at all. The cause of this bad reading is attributed to a scale factor omitted in the computer set-up or subsequent calculations. It must also be pointed out that output table dynamics could have contributed to these errors in computation since the acceleration peaks occur at time zero.

From Derivation Summary 3-1 it may be seen that pulse duration has no effect on the acceleration peak caused by a rectangular pulse function. This peak always occurs at the instant the system is disturbed. Its magnitude is directly proportional to the pulse height. It is evident therefore that no decrease in acceleration could result from increasing pulse duration if pulse height were kept constant. It may be

seen from Figs. 5-6 and 5-9 that the maximum acceleration occurs later in the response if a displaced cosine pulse is used. It was therefore postulated that increased pulse duration with constant pulse height could produce decreased maximum acceleration if the forcing function were a displaced cosine pulse.

The investigation was then continued using only the displaced cosine pulse function as the forcing function. Only the seven-tenths critically damped form of each system is studied. Pulse duration is varied from one-tenth to one natural period of the AVSD system. The calculated responses in non-dimensional form are shown in Figs. 5-10 through 5-15 for both systems. Appendix C tabulates the numerical values from which these figures were constructed. From these figures it may be seen that for constant pulse height as the pulse duration increases

1. Angular displacement peak increases.
2. The first angular velocity peak increases until the pulse duration is one half the natural period. Thereafter it decreases.
3. The second angular velocity peak increases.
4. The first angular acceleration peak decreases.
5. The second angular acceleration peak exceeds the first angular acceleration peak when the pulse duration is greater than three-tenths the natural period of the AVSD system.
6. The second angular acceleration peak decreases after the pulse duration exceeds three-tenths the natural period.

The investigation so far has shown that it is possible to increase the controlled member angular displacement peak while decreasing the acceleration peak.

Table 5-2 lists the numerical values of the response peaks of the AVSD system to a displaced cosine pulse function for various values of pulse duration. Table 5-3 lists the same information for the MAVSD system. From these tables it may be seen that the desired ratio of

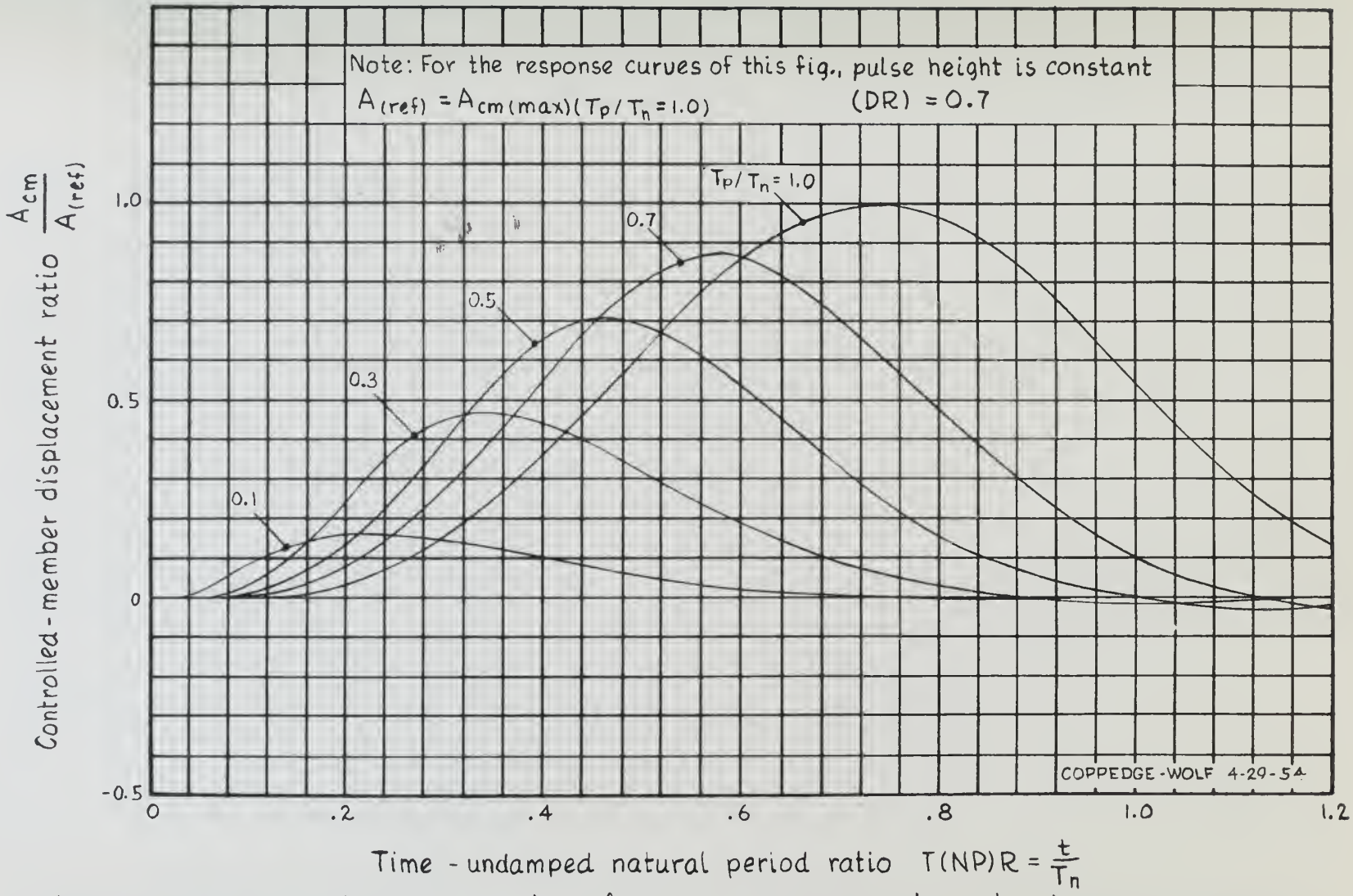

Fig. 5-10 Displaced cosine pulse function input-angular displacement response curves for the AVSD system for variation of the pulse duration (PD)

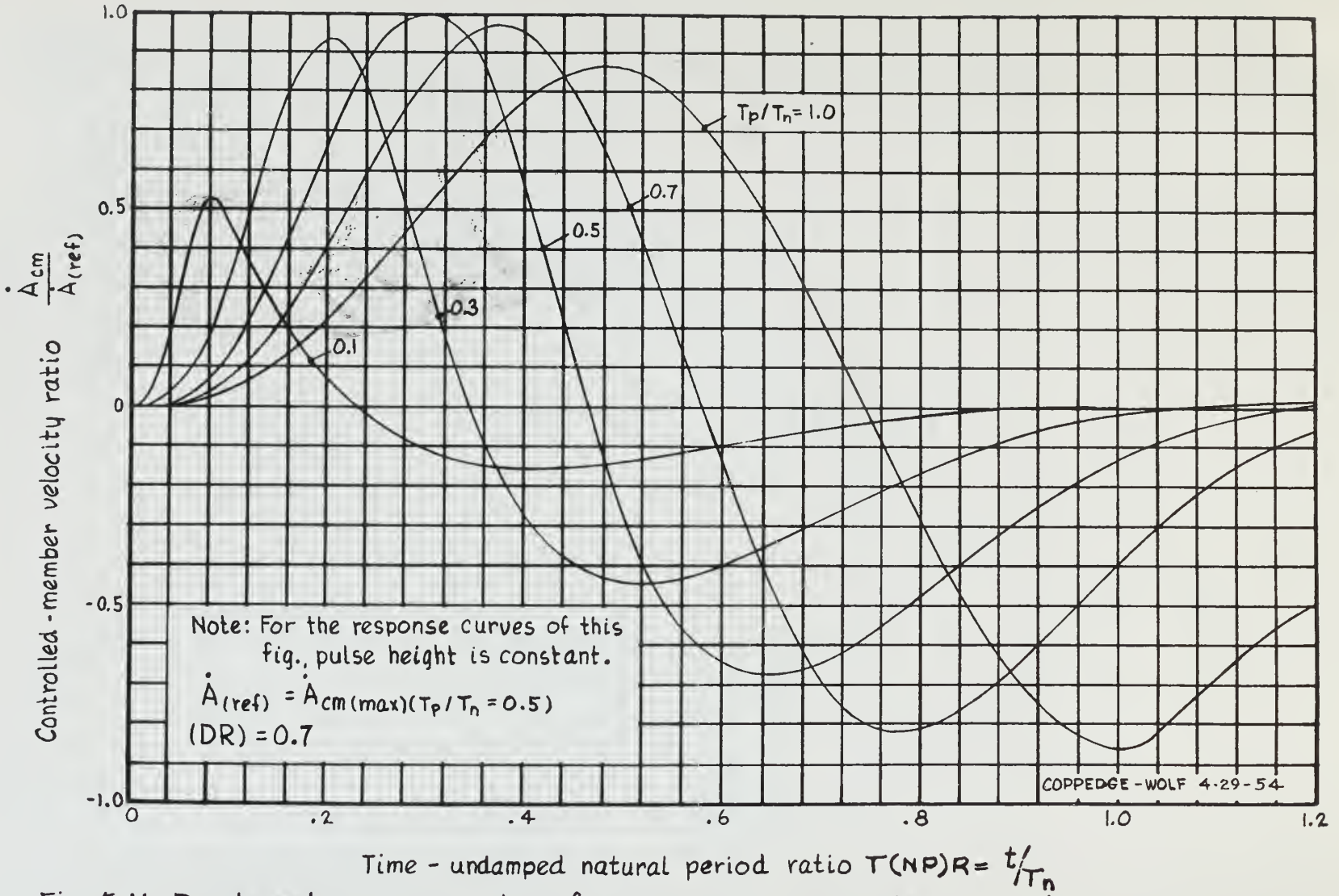

Fig. 5-11 Displaced cosine pulse function input-angular velocity response curves for the AVSD system for variation of the pulse duration (PD).

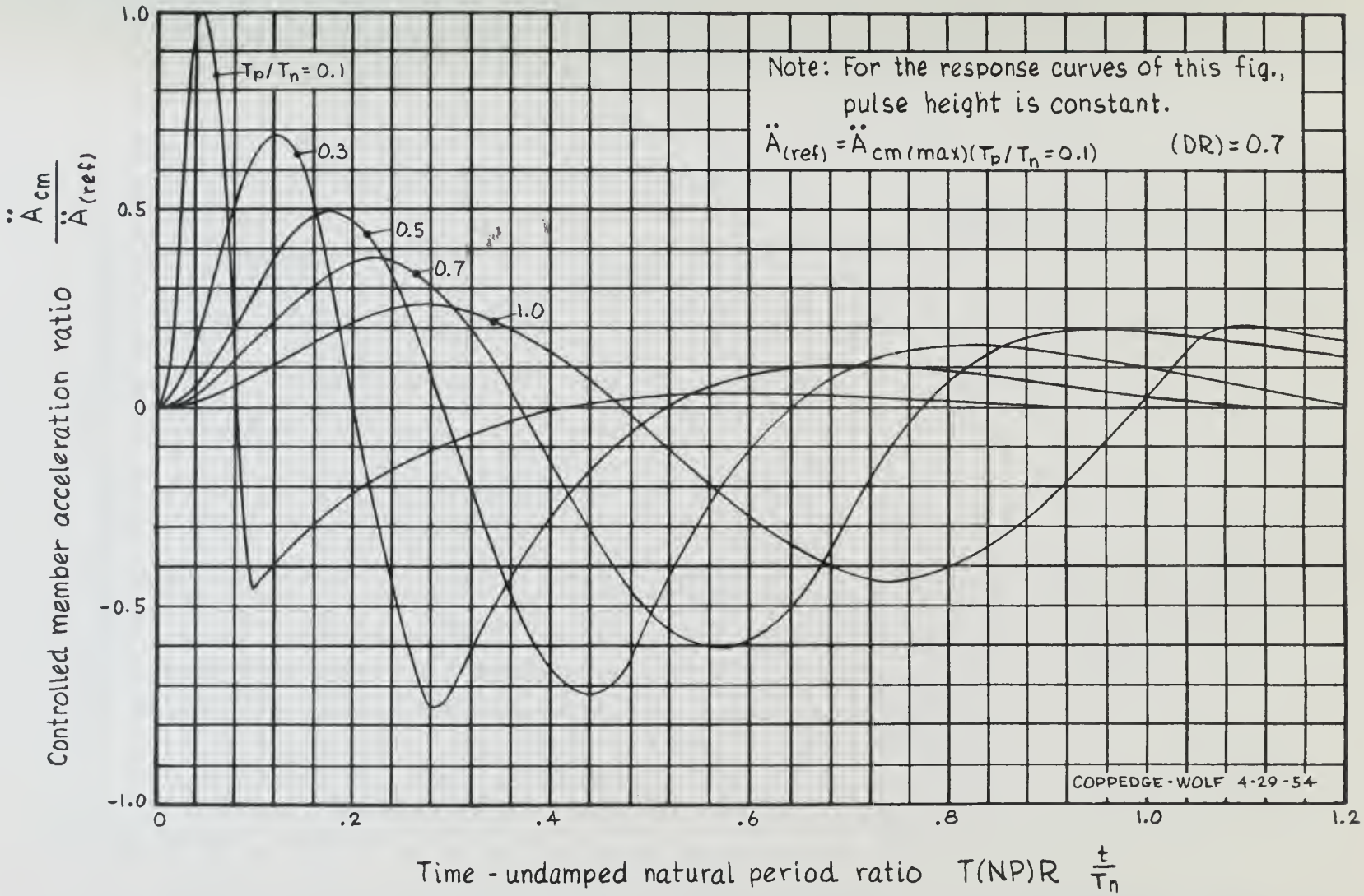

Fig. 5-12 Displaced cosine pulse function input-angular acceleration response curves for the AVSD system for variation of the pulse duration (PD)

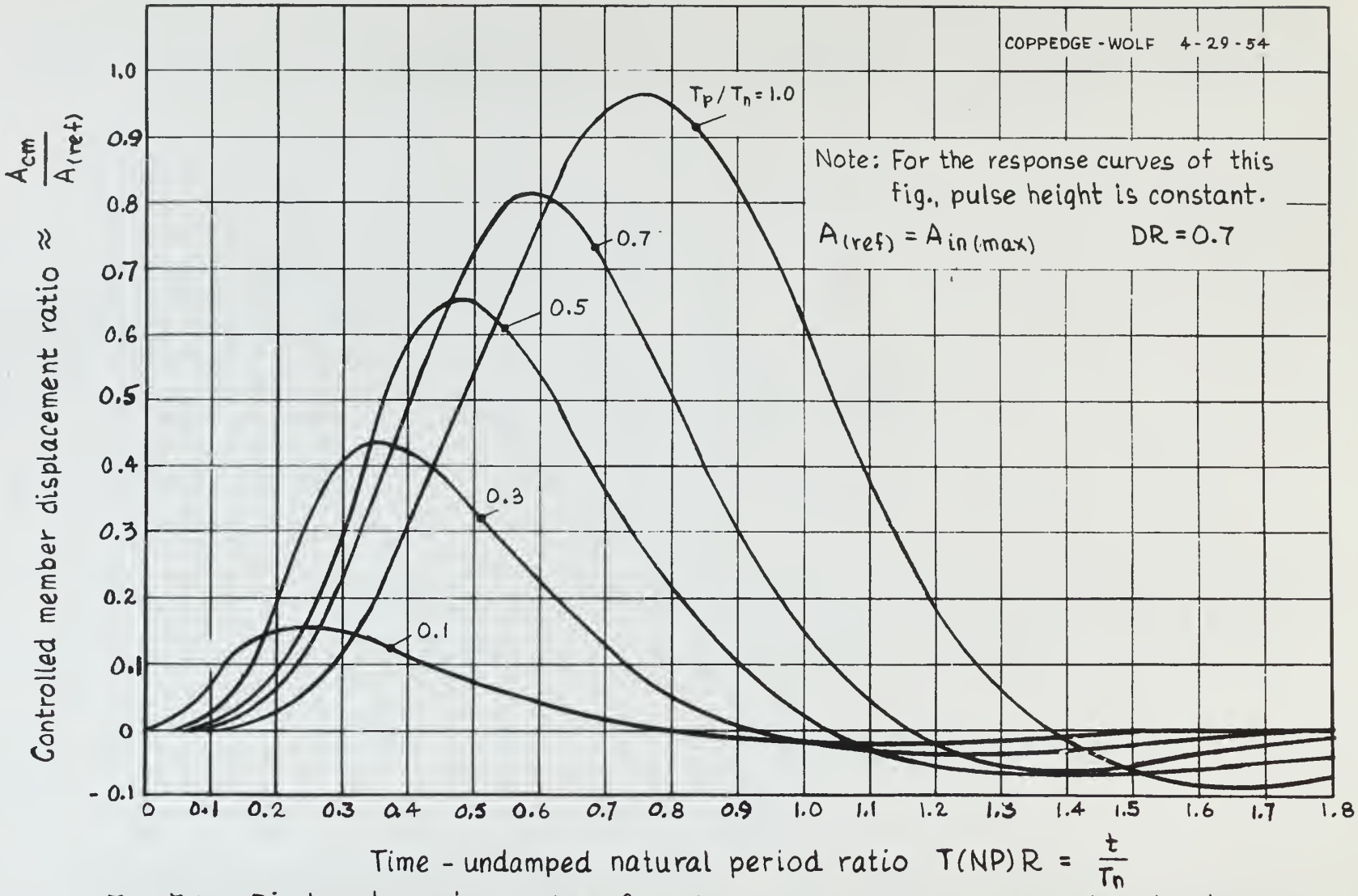

Fig. 5-13 Displaced cosine pulse function response input-angular displacement curves for the MAVSD system for variation of the pulse duration $(PD)^h$

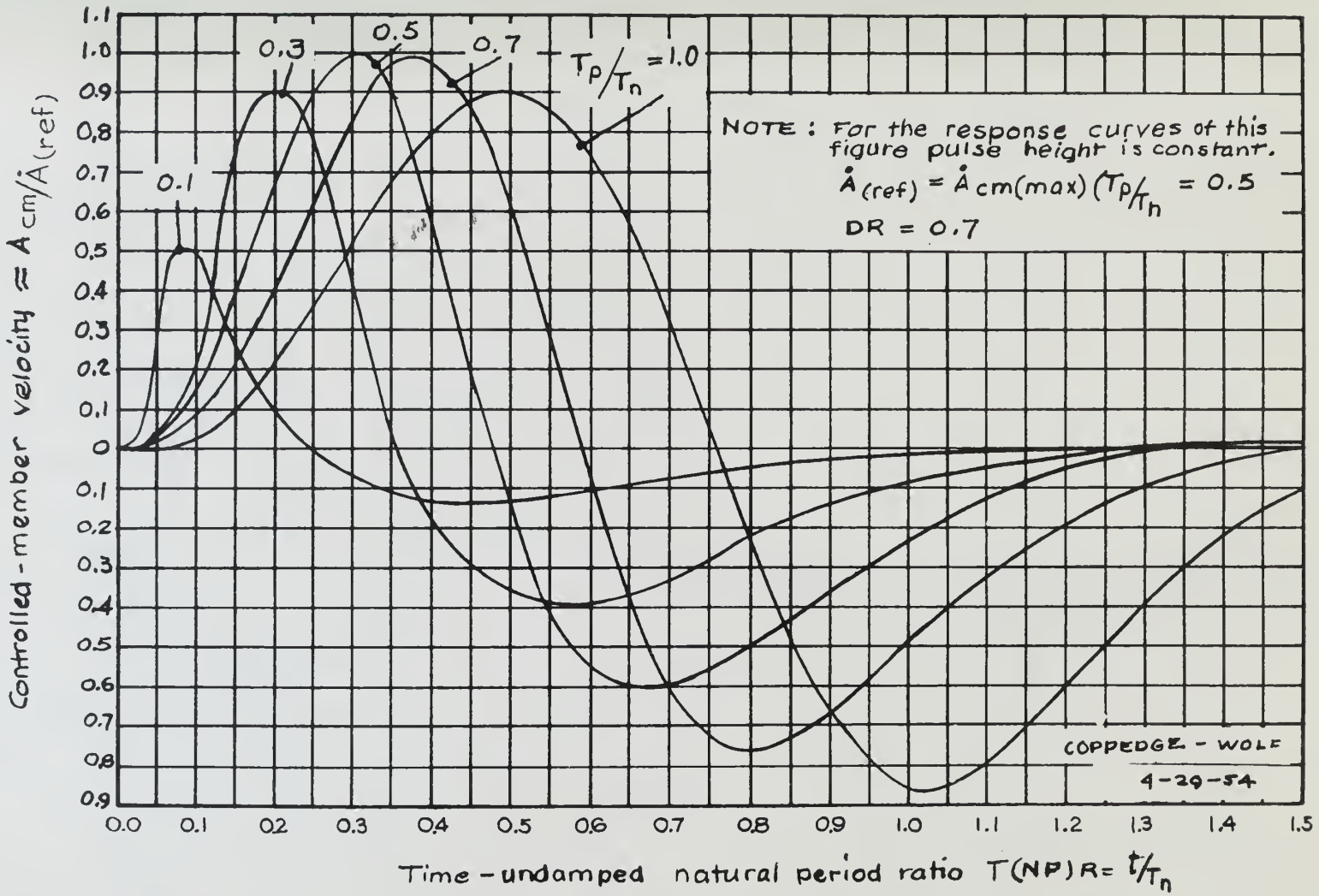

Fig 5-14 Displaced cosine pulse function input-angular velocity response curves for the MAVSD system for variation of the pulse duration (PD)

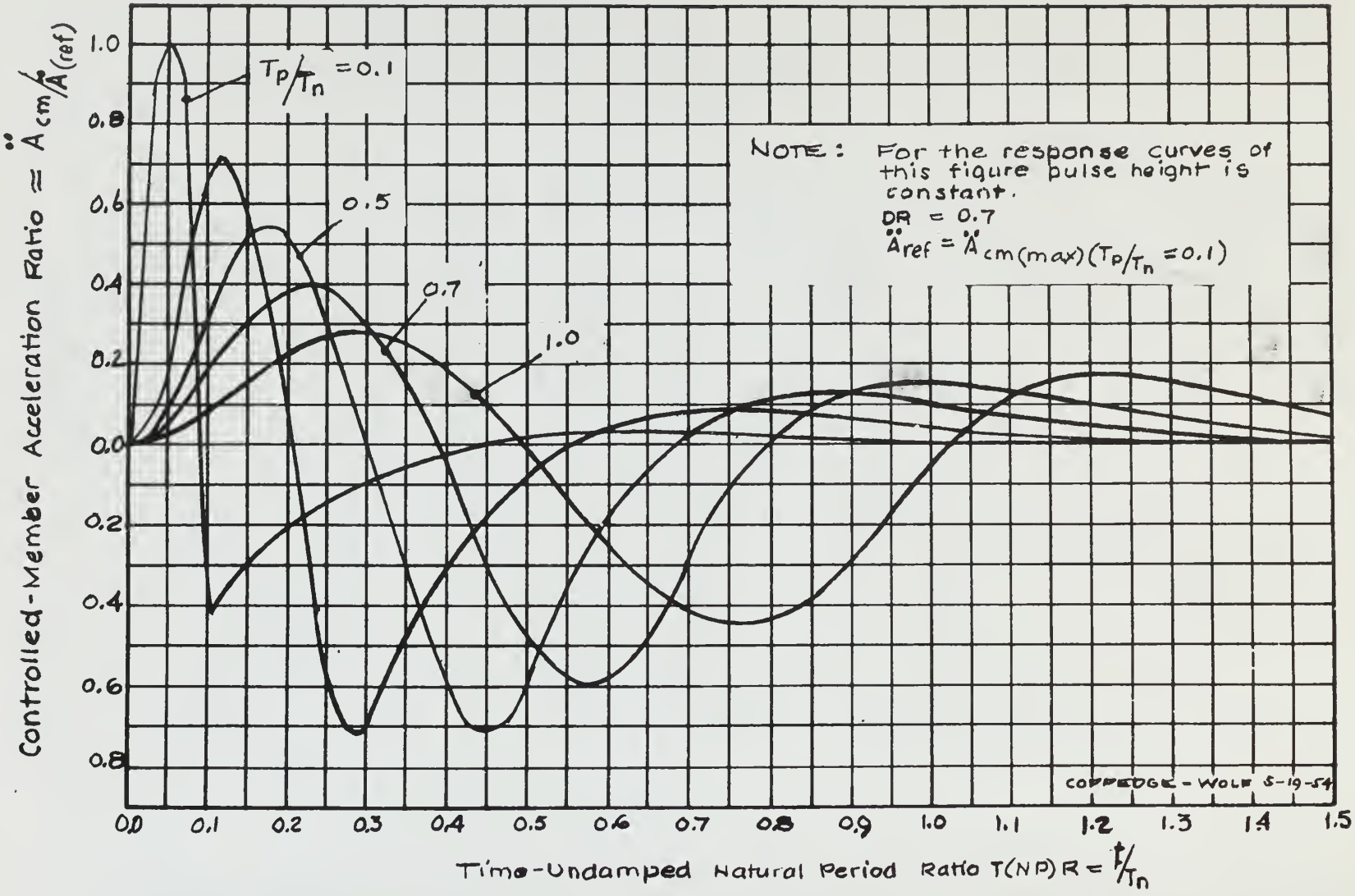

Fig. 5-15 Displaced cosine pulse function input — angular acceleration response curves of the MAVSD system for variation of the pulse duration (PD)

Table 5-2 Numerical values of peaks of ideal linear responses of AVSD system DR = 0.7 to a displaced cosine pulse function.

$\frac{PS}{PS_{(ref)}}$	$\frac{PD}{NP}$	A_{cm} mr.	$\dot{A}_{cm}$ - mr/sec		$\ddot{A}_{cm}$ - mr/sec^2	
			1st Peak	2nd Peak	1st Peak	2nd Peak
1.0	0.1	.1449	14.30	4.31	3305	1502
3.0	0.3	.419	25.35	12.12	2277	2480
5.0	0.5	.633	27.24	18.34	1641	2384
7.0	0.7	.771	26.15	22.04	1249	2004
10.0	1.0	.891	23.54	23.25	858.5	1426
1.0	0.1	.1449	14.30	4.31	3305	1502
1.0	0.3	.1397	8.45	4.04	759	826.6
1.0	0.5	.1266	5.45	3.67	328.2	476.8
1.0	0.7	.1101	3.74	3.15	178.4	286.3
1.0	1.0	.0891	2.35	2.33	85.85	142.6

$PS_{(ref)}$ = 0.00993 mr sec.

Table 5-3 Numerical values of peaks of ideal linear responses of the MAVSD system DR = 0.7 to a displaced cosine pulse function

$\frac{PS}{PS_{(ref)}}$	$\frac{PD}{NP}$	A_{cm} mr.	$\dot{A}_{cm}$ - mr/sec		$\ddot{A}_{cm}$ - mr/sec^2	
			1st Peak	2nd Peak	1st Peak	2nd Peak
1.0	0.1	.1485	14.12	3.75	3215	1343
3.0	0.3	.432	25.25	11.01	2250	2300
5.0	0.5	.657	27.8	16.85	1679	2282
7.0	0.7	.818	27.5	21.0	1257	1930
10.0	1.0	.967	25.0	23.9	888	1441
1.0	0.1	.1485	14.12	3.75	3215	1343
1.0	0.3	.1472	8.43	3.67	750	767
1.0	0.5	.1315	5.56	3.37	336	457
1.0	0.7	.1169	3.93	3.00	179.6	276
1.0	1.0	.0967	2.50	2.39	88.8	144.1

$PS_{(ref)}$ = 0.00993 mr sec.

angular displacement peak to effective backlash may be achieved. Pulse durations of seven-tenths the natural period of the AVSD system or greater may be used. Smaller ratios of displacement peak to effective backlash may be obtained by using shorter pulse durations or smaller pulse strengths at the large values of pulse duration.

5.3 Calculation of Actual Responses

The second part of the investigation deals with the extrapolation to the actual response curves of the AVSD and MAVSD systems. This is accomplished using the method outlined in Chapter 3. The major portion of this phase is graphical integration and construction. In Appendix D will be found the complete calculation of a typical controlled-member angular displacement response curve. This section will consist only of a detailed description of the application of the method outlined in Chapter 3.

The starting point is the ideal linear response peak table. Knowing the acceleration and velocity limits of the motor and the gear ratio of the physical system to be tested, these limits are reflected through the gear ratio. These limits then become the maximum controlled-member velocity and acceleration permissable. These values for the AVSD and MAVSD system are respectively 4,150 milliradians per second and 93,000 milliradians per second per second. The next step is the determination of the maximum pulse height that may be used to disturb the system. In this investigation it can be seen that the acceleration limit is the deciding limit. All calculations are made for a pulse duration equal to the natural period of the AVSD system.

To determine the maximum pulse height, divide the allowable controlled-member velocity and accelerations by those tabulated in Tables 5-2 and 5-3 for the selected pulse duration. It may be seen that this maximum pulse height is 65.2 milliradians for the AVSD system and 64.5 milliradians for the MAVSD system. The mean member angular displacement response may now be computed. This is accomplished by dimensionalizing Fig. 5-10 for the AVSD system and Fig. 5-13 for the MAVSD system is such a manner that the peak displacements are respectively 58.2 and 63.1 milliradians. The solid curve

in Fig. 5-16 represents the mean member motion of the MAVSD system. The next step is to dimensionalize Fig. 5-11 for the AVSD system and Fig. 5-14 for the MAVSD system. This is accomplished by making the mean member velocity first peaks 1524 milliradians per second and 1612 milliradians per second. The solid curve in Fig. 5-17 represents the mean member velocity of the MAVSD system. The next step is to determine the controlled-member velocity curve. It will be recalled that friction effects were neglected in this investigation. Therefore the controlled-member velocity is identical with mean member velocity until separation occurs. Separation occurs when the mean member velocity is a maximum or a minimum. At this instant of time the controlled-member velocity is at the maximum or minimum mean member velocity. The controlled-member continues at this velocity until the area between the mean motion velocity curve and the controlled-member velocity curve equals the controlled-member effective backlash. At this instant the controlled-member velocity assumes the mean member velocity. The controlled-member velocity curve for the MAVSD system with one quarter milliradian of effective backlash is shown in Fig. 5-17 as the solid curve including the shaded triangular areas. The hatched areas represent one quarter milliradian. The dashed curve of Fig. 5-16 is constructed by plotting the area of the hatched area of Fig. 5-17 as the ordinate difference from the solid curve of Fig. 5-16 from time of separation until the two velocity curves are identical. It is convenient to use a difference plot to show the variation of the difference ordinate. The difference plot for the MAVSD system is shown in Fig. 5-18 for an effective controlled-member backlash of one fourth milliradian. This difference is defined as $(\mathcal{E})f(t)$.

The method of determining the controlled-member angular displacement and velocity responses for one value of pulse height and one value of effective backlash for the MAVSD system has been explained and illustrated. These steps must be repeated for each value of effective backlash at each pulse strength desired. No curves are included for other values of pulse height or effective backlash.

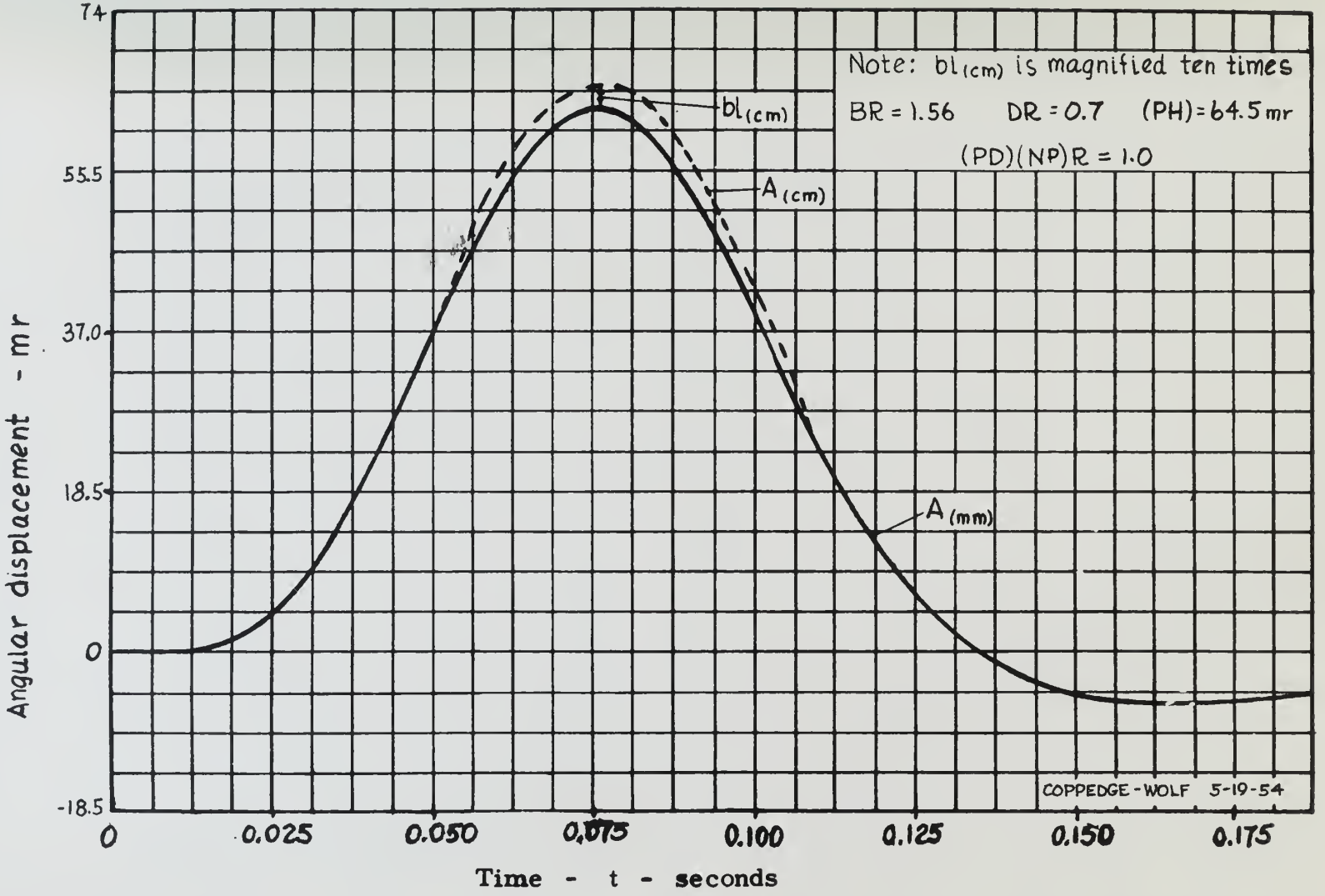

Fig. 5-16 Plot of angular displacement of mean member and controlled-member of MAVSD system for displaced cosine pulse function input showing effect of backlash.

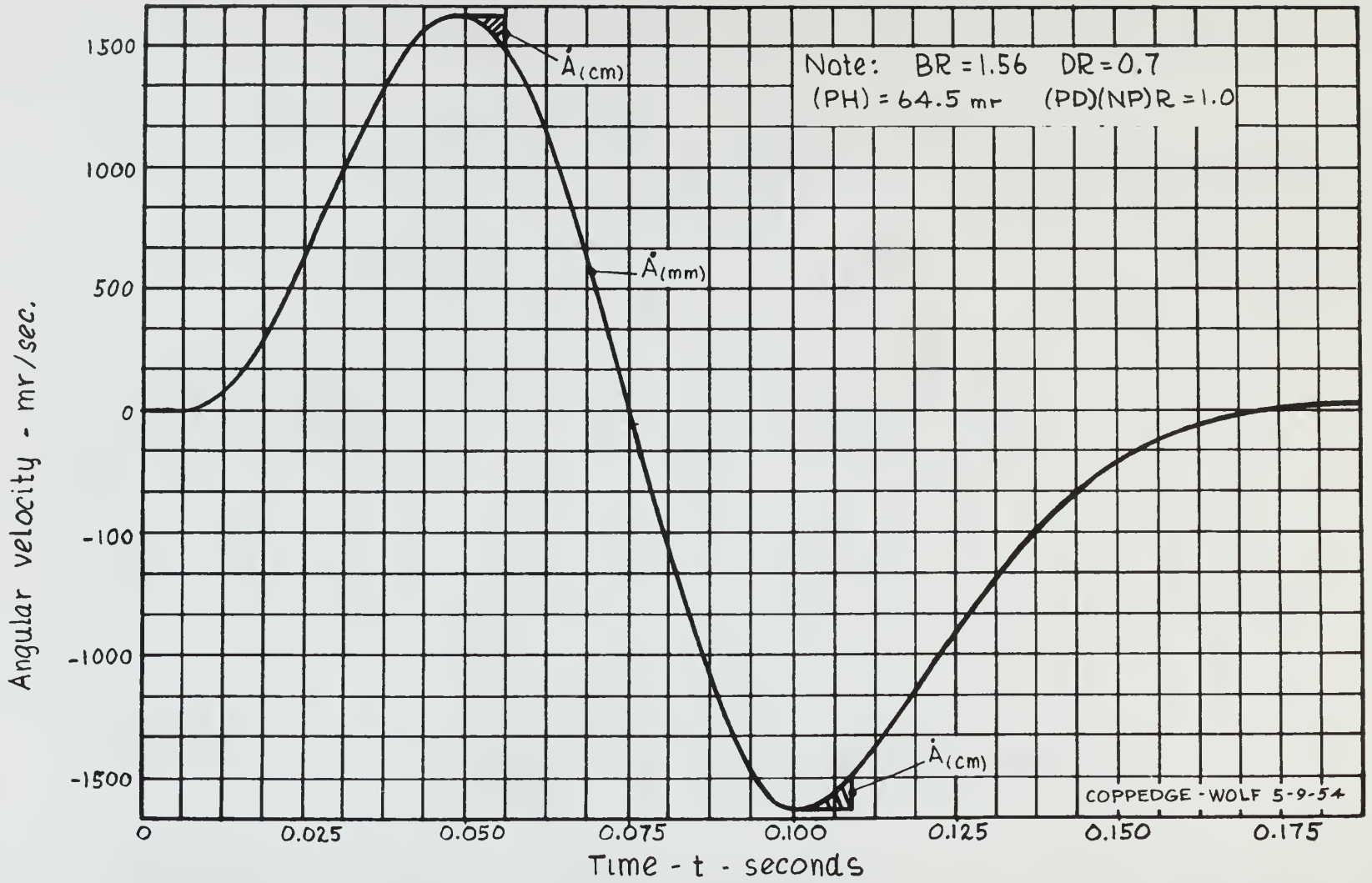

Fig. 5-17 Plot of angular velocity of mean member and controlled member of MAVSD system for displaced cosine pulse function input showing effect of backlash.

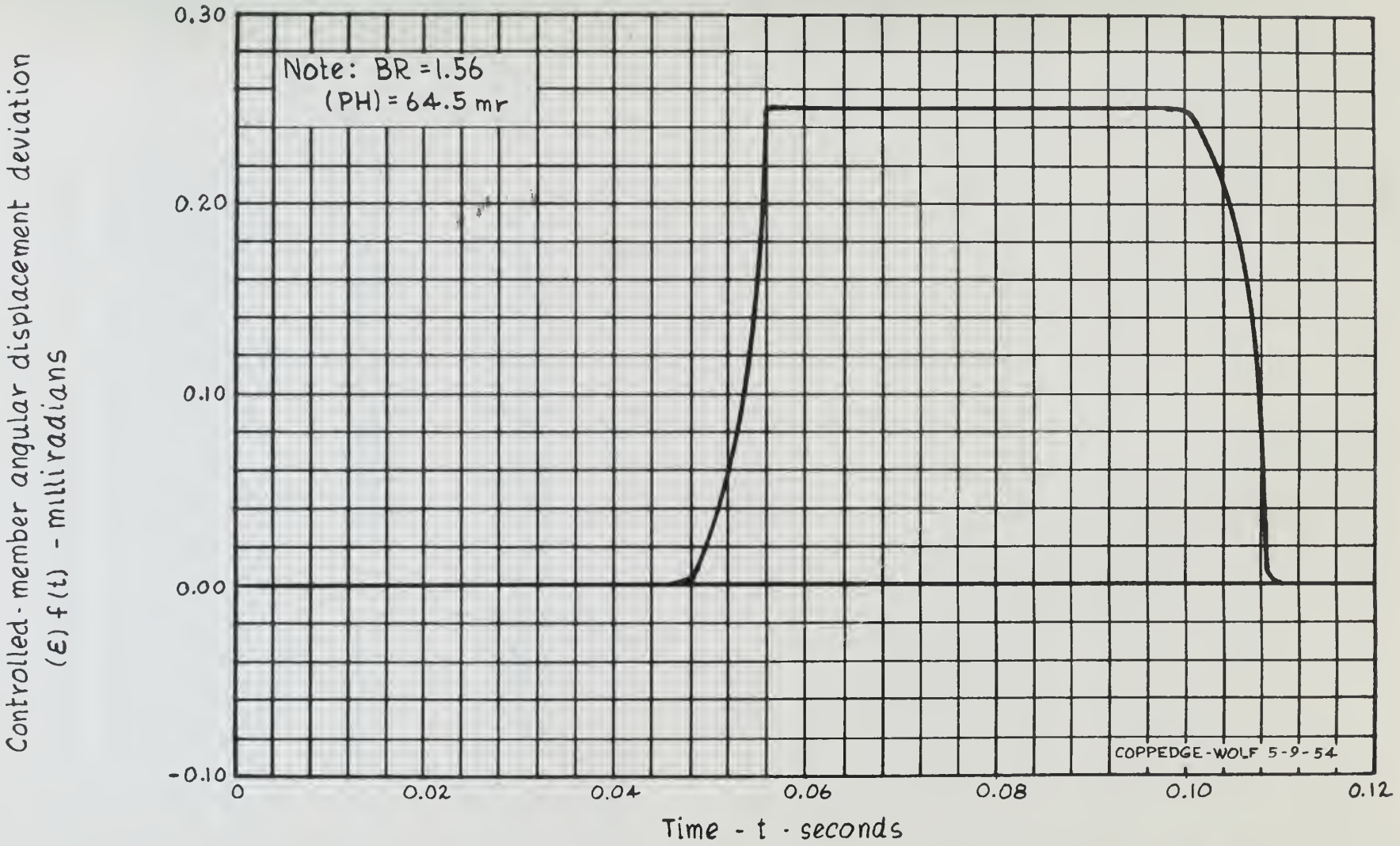

Fig. 5-18 Plot of controlled-member angular displacement deviation due to backlash in the MAVSD system with DR = 0.7 for displaced cosine pulse function input (PD/NP)R = 1.0

5-4 Calculation of Average Percentage Error

The final phase of this investigation consists of the calcualtion of the average percentage error in magnitude of the angular displacement of the controlled-member time response and frequency response. These functions are defined and derived in Derivation Summary 5-1.

The angular displacement time response of a physical system with limited nonlinearities may be written in the form

$$ADTTR_{(ps)} = f(t) + (\mathcal{E})f(t) \qquad (1)$$

where $ADTTR_{(ps)}$ = angular displacement transient time response of the physical system

$f(t)$ = angular displacement transient time response of the ideal linear system with same parameters as the physical system but with no nonlinearities

$(\mathcal{E})f(t)$ = angular displacement deviation of $ADTTR_{(ps)}$ from $f(t)$

Each quantity defined above is a function of time (t). $(\mathcal{E})f(t)$ is calculated as outlined in Chapter 3.

(a) Angular displacement time response

Cramer [9] shows that Schwarz inequality may be written in the form

$$\int_{-\infty}^{\infty} \left|(f)t+(\mathcal{E})f(t)\right|^2 dt \leq \int_{-\infty}^{\infty} \left\{ \left|f(t)\right|^2 + 2\left|(\mathcal{E})f(t)\right|\left|f(t)\right| + \left|(\mathcal{E})f(t)\right|^2 \right\} dt \qquad (2)$$

Neglect the term $\int_{-\infty}^{\infty} \left|(\mathcal{E})f(t)\right|^2 dt$ as small compared to other terms.

Derivation Summary 5-1. Derivation of error describing functions for a physical system with limited non-linearities. (Page 1 of 5.)

Subtract $\int_{-\infty}^{\infty} |f(t)|^2 dt$ from both sides of equation (2)

$$\int_{-\infty}^{\infty} |f(t)+(\mathcal{E})f(t)|^2 dt - \int_{-\infty}^{\infty} |f(t)|^2 dt \leq \int_{-\infty}^{\infty} |2\ (\mathcal{E})f(t)||f(t)| dt \qquad (3)$$

Divide Equation (3) by $\int_{-\infty}^{\infty} |f(t)|^2 dt$ and multiplying by 100%

$$\frac{100\% \int_{-\infty}^{\infty} |f(t)+(\mathcal{E})f(t)|^2 dt - 100\% \int_{-\infty}^{\infty} |f(t)|^2 dt}{\int_{-\infty}^{\infty} |f(t)|^2 dt} \leq \frac{100\% \int_{-\infty}^{\infty} 2|(\mathcal{E})f(t)||f(t)| dt}{\int_{-\infty}^{\infty} |f(t)|^2 dt} \qquad (4)$$

Define

$$APEM_{(ttr)} \triangleq \frac{100 \int_{-\infty}^{\infty} |f(t)+(\mathcal{E})f(t)|^2 dt - 100 \int_{-\infty}^{\infty} |f(t)|^2 dt}{\int_{-\infty}^{\infty} |f(t)|^2 dt} \qquad (5)$$

where

$APEM_{(ttr)}$ = average percentage error in amplitude of the transient time response of a physical system

Therefore

$$APEM_{(ttr)} \leq \frac{200 \int_{-\infty}^{\infty} |(\mathcal{E})f(t)||f(t)| dt}{\int_{-\infty}^{\infty} f(t)^2 dt} \quad \text{in percent} \qquad (6)$$

(b) Expression of average percentage error in amplitude of the transient time response of a physical system

Derivation Summary 5-1 Derivation of error describing functions for a physical system with limited non-linearities. (Page 2 of 5.)

The angular displacement frequency response of a physical system with limited non-linearities may be written in the form

$$ADFR_{(ps)} = F(\beta) + (\mathcal{E})\, F(\beta) \tag{7}$$

where

$ADFR_{(ps)}$ = angular displacement frequency response of the physical system

$F(\beta)$ = angular displacement frequency response of the ideal linear system with same parameters as the physical system but with no non-linearities

$(\mathcal{E})\, F(\beta)$ = deviation of $ADFR_{(ps)}$ from $F(\beta)$

β = frequency ratio and is the forcing frequency divided by some arbitrary reference frequency

(c) Angular displacement frequency response

Applying the steps outlined in section (b) it can be shown that

$$\frac{100\int_{-\infty}^{\infty}\left|F(\beta)+(\mathcal{E})F(\beta)\right|^2 d\beta \;-\; 100\int_{-\infty}^{\infty}\left|F(\beta)\right|^2 d\beta}{\int_{-\infty}^{\infty}\left|F(\beta)\right|^2 d\beta} \leq \frac{200\int_{-\infty}^{\infty}\left|(\mathcal{E})F(\beta)\right|\left|F(\beta)\right| d\beta}{\int_{-\infty}^{\infty}\left|F(\beta)\right|^2 d\beta} \tag{8}$$

The mathematical expression $F(\beta)$ is used to describe a physical relationship. In nearly all physical systems $F(\beta)$ is an even function. Negative frequencies do not exist. Therefore

Derivation Summary 5-1 Derivation of error describing functions for a physical system with limited non-linearities. (Page 3 of 5.)

$$\frac{100\int_{-\infty}^{\infty}|F(\beta)+(\mathcal{E})F(\beta)|^2 d\beta - 100\int_{-\infty}^{\infty}|F(\beta)|^2 d\beta}{\int_{-\infty}^{\infty}|F(\beta)|^2 d\beta} \leq \frac{400\int_{0}^{\infty}|(\mathcal{E})F(\beta)||F(\beta)|d\beta}{2\int_{0}^{\infty}|F(\beta)|^2 d\beta} \quad (9)$$

Define

$$APEM_{(fr)} \triangleq \frac{100\int_{-\infty}^{\infty}|F(\beta)+(\mathcal{E})F(\beta)|^2 d\beta - 100\int_{-\infty}^{\infty}|F(\beta)|^2 d\beta}{\int_{-\infty}^{\infty}|F(\beta)|^2 d\beta} \quad (10)$$

where

$APEM_{(fr)}$ = average percentage error in amplitude of the frequency response of a physical system

Therefore

$$APEM_{(fr)} \leq \frac{200\int_{0}^{\infty}|(\mathcal{E})F(\beta)||F(\beta)|d\beta}{\int_{0}^{\infty}|F(\beta)|^2 d\beta} \quad \text{in percent} \quad (11)$$

(d) Expression of average percentage error in amplitude of the frequency response of a physical system

Morse and Feshback[10] show that Parseval's formula may be written

$$\int_{-\infty}^{\infty}|F(\beta)|^2 d\beta = \int_{-\infty}^{\infty}|f(t)|^2 dt \quad (12)$$

From Equation (12) it may be seen that

Derivation Summary 5-1 Derivation of error describing functions for a physical system with limited non-linearities. (Page 4 of 5.)

$$\frac{\int_{-\infty}^{\infty} |F(\beta)+(\mathcal{E})F(\beta)|^2 d\beta - \int_{-\infty}^{\infty} |F(\beta)|^2 d\beta \int_{-\infty}^{\infty} |f(t)+(\mathcal{E})f(t)|^2 dt - \int_{-\infty}^{\infty} |f(t)|^2 dt}{\int_{-\infty}^{\infty} |F(\beta)|^2 \, d\beta} = \frac{}{\int_{-\infty}^{\infty} |f(t)|^2 \, dt}$$

Therefore

$$APEM_{(fr)} = APEM_{(ttr)}$$

(e) Relationship between average percentage error in amplitude of the transient time response and average percentage error in amplitude of the frequency response of a physical system

Derivation Summary 5-1 Derivation of error describing functions for a physical system with limited non-linearities. (Page 5 of 5.)

The deviation plots described in 5.3 are plots of $(\mathcal{E})f(t)$ as stated. Plots similar to the solid curve of Fig. 5-10 are constructed for each value of pulse strength to be considered for each system. A plot of $2|(\mathcal{E})f(t)||f(t)|$ is then constructed for each effective backlash value by multiplying the ordinates of the $(\mathcal{E})f(t)$ and $f(t)$ curves together. A plot of $|f(t)|^2$ is constructed for each pulse height for each system. These curves are integrated. Graphical methods were used by the authors. By combining the integrated functions as shown in section of Derivation Summary 5-1 $APEM_{(ttr)}$ is obtained.

Fig. 5-19 is a nondimensional plot of $APEM_{(ttr)}$ as a function of pulse strength and effective backlash for the AVSD system. Fig. 5-20 is a similar plot for the MAVSD system. The quantities used to nondimensionalize these curves are effective backlash ratio-BR- and reference pulse strength -$(PS)_{ref.}$ These two quantities are defined below.

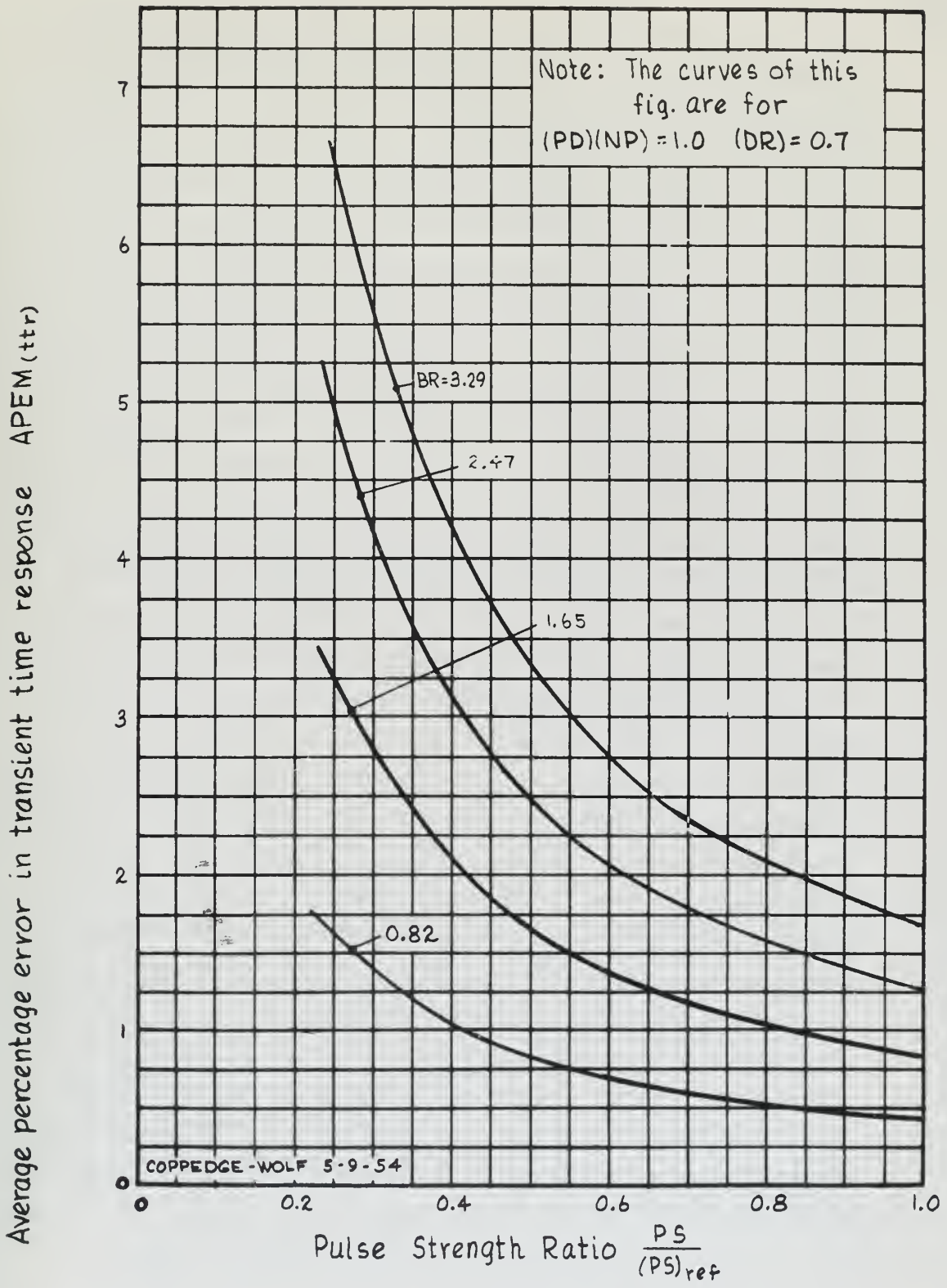

Fig. 5-19 Angular displacement average error produced by backlash in the AVSD system with DR=0.7 and (PD)(NP)R = 1.0

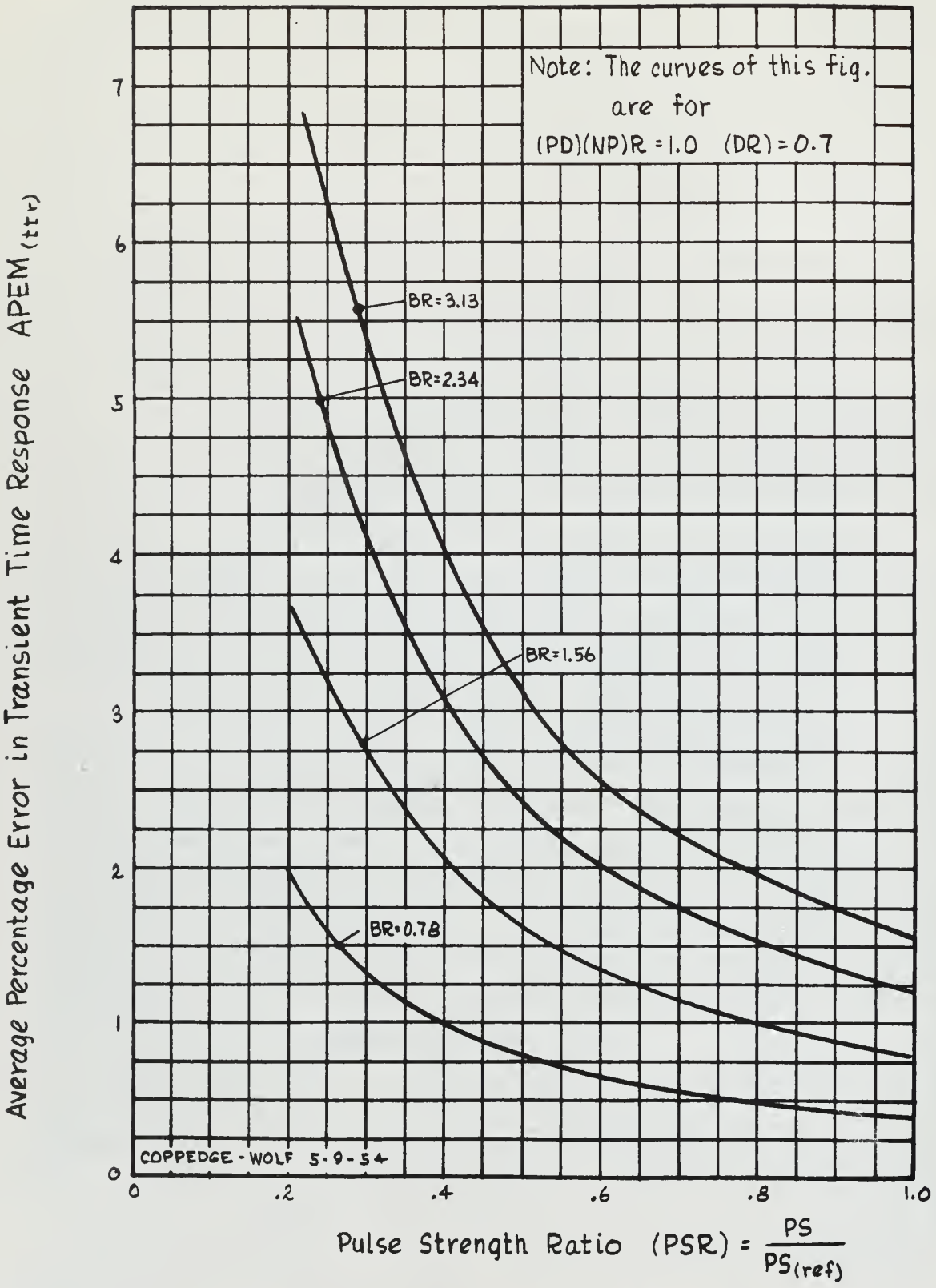

Fig. 5-20 Angular displacement average error produced by backlash in the MAVSD system with (DR) = 0.7 and (PD)(NP)R = 1.0.

$$BR \triangleq \frac{bl_{(cm)}\, n}{\dot{A}_m\, T_n}$$

where

$bl_{(cm)}$ = controlled-member effective backlash

n = gear ratio motor to controlled-member

$\dot{A}_m$ = maximum motor velocity

T_n = natural period of AVSD system

$$(PS)_{ref} = \int_0^{(PD)} \frac{(PH)_{max}}{2} \left(1 - \cos \frac{2\pi}{\omega_n} t\right) dt$$

where (PH) = pulse duration

$(PH)_{max}$ = maximum pulse height possible avoiding motor saturation

t = time

ω_n = natural angular frequency of AVSD system.

Table 5-4 lists the numerical values from which Fig. 5-19 was constructed. Table 5-5 tabulates the same information for Fig. 5-20.

From Derivation Summary 5-1 it may be seen that $APEM_{(ttr)}$ is equal to $APEM_{(fr)}$. Therefore although not so labelled, Figs. 5-19 and 5-20 show the variation in $APEM_{(fr)}$ for different values of BR and $(PS)_{(PS)_{ref}}$ for the AVSD and MAVSD systems respectively.

The effect of the uncertainty level in a system is handled in an analogous manner. It is apparant that the uncertainty level is present continuously throughout the motion. For this case, $(\mathcal{E})f(t)$ remains constant and is equal to the magnitude of the uncertainty level $(U)f(t)$. To compare the effect of uncertainties and backlash, a sample computation of the average percent error due to an uncertainty level of one half milliradian in the MAVSD system is included in Appendix D.

Table 5-4 Average percentage error in transient time response of the AVSD system due to backlash.

$A_{(bl)(cm)(mr)}$ \ PSR →	1.0	0.75	0.5	0.25
	APEM	APEM	APEM	APEM
0.500	1.676	2.22	3.32	6.59
0.375	1.25	1.67	2.49	4.94
0.250	0.83	1.11	1.66	3.30
0.125	0.42	0.55	0.83	1.65

Table 5-5 Average percentage error in transient time response of the MAVSD system due to backlash.

$A_{(bl)(cm)(mr)}$ \ PSR →	1.0	0.75	0.5	0.25
	APEM	APEM	APEM	APEM
0.500	1.550	2.065	3.10	6.20
0.375	1.202	1.602	2.404	4.81
0.250	0.798	1.064	1.596	3.19
0.125	0.394	0.525	0.788	1.576

The results indicate that an average error of 2.42 percent will exist due to the uncertainty level. Fig. 5-20 shows the average error for a total backlash of one half milliradian to be 0.798 percent for a pulse strength ratio of 1.0. It is concluded from this comparison that when the magnitudes of the backlash and uncertainties are equal, the response deviations due to backlash are negligible.

Investigation of the technique of pulse distrubance testing of feedback control systems discolses several significant considerations. Velocity and acceleration limitations of a given system must not be exceeded. The peak amplitude of the displacement response of the system must be large relative to the backlash. These requirements can be met simultaneously by proper choice of the pulse function. In this connection, pulse shape and duration, as well as pulse strength, are important. Utilization of the correct pulse function minimizes the response deviations due to backlash, and these deviations are negligible for nominal amounts of backlash.

CHAPTER 6

CONCLUSIONS AND RECOMMENDATIONS FOR FURTHER STUDY

Responses of physical systems to pulse functions are used for evaluating the linear properties of the systems. The intent of this study is to determine how to apply pulse function inputs which yield information about the linear properties of systems having some significant non-linearities.

Physical systems may exhibit a wide range and variety of non-linearities. In order to develop methods for studying such systems, the non-linearities have been restricted to backlash in the gear train and saturation of the torque source. Velocity saturation exists when the torque source output member has a maximum velocity it cannot exceed. Similarly, acceleration saturation implies the existence of an upper acceleration limit. These are quite general since every physical system possesses maximum velocity and acceleration limits. The procedures described in the previous chapters are adaptable to other types of non-linearities.

Two representative physical systems have been studied here. The AVSD system is a second order type, characterized by angular velocity signal feedback damping. Modifying the angular velocity feedback signal converts it into the third order, MAVSD system. Non-linearities in the form of small amounts of backlash as well as velocity and acceleration limits on the motor are introduced in the ideal systems. Rectangular and displaced cosine pulse function inputs are applied and the system responses studied. The effects of pulse shape, duration and strength on the system responses are examined. The following conclusions are derived from this study.

6-1 Conclusions

(a) Velocity and acceleration limits of the motor must not be exceeded. Saturation of any component can distort the transient response beyond usable limits. Correlation with the ideal responses determined from linear analysis is then impossible.

(b) The pulse function input must have continuous derivatives to avoid infinite inputs. This is first described in the theoretical analysis of Derivation Summary 3-1 of Chapter 3. The components of a physical system are incapable of accepting an infinite input. They may be driven into saturation by such an input.

(c) The pulse strength must be adequate to force an output large compared to backlash and uncertainties. A ratio of the peak amplitude of the transient response to the effective controlled-member backlash of one hundred to one is desirable. If this is achieved without saturation distortion, the deviations from the ideal response are negligible.

(d) The pulse duration should be approximately equal to the undamped natural period of the dominant mode of the system. Under this condition the pulse strength may be adequate without inducing saturation.

(e) A rectangular pulse function is unsuitable for the systems in this study. This is discussed from a theoretical point of view in Derivation Summary 3-1 of Chapter3 and verified numerically in Chapter 5. The discontinuous nature of this function and its derivatives makes it impossible to avoid saturation of the acceleration and velocity for the investigated systems. This condition is true regardless of pulse duration.

(f) Functions such as the displaced cosine pulse may meet the requirements stated above. They possess continuous derivatives. Further, it is possible to introduce adequate pulse strength by adjusting the pulse duration without inducing saturation.

(g) The average non-dimensional error in amplitude due to backlash and uncertainties is the same in both the time and frequency domains. This is shown in Derivation Summary 5-1 of Chapter 5. Since the correct choice of a pulse function results in a negligible average amplitude error

in the transient response, the average error in the amplitude of the calculated frequency response will also be negligible.

(h) When the backlash and the uncertainties are of the same order of magnitude, the average amplitude error due to backlash is smaller than that due to the uncertainties.

6-2 Recommendations for further study

The investigation reported in this thesis is limited to a study of the non-dimensional error in the frequency response amplitude. The effect of backlash, uncertainties and saturation upon the dynamic response angle has not been determined. However, the necessary information can be obtained by an extended study of the kind used herein. It is recommended that this be done.

Further study of the problem of calculating the frequency response from the transient response is suggested. Cognizance of the character of transient response errors arising from backlash and other uncertainties is important here. The distribution of errors in the frequency response may be ascertained from carrying out this recommendation.

A theoretical investigation of the sinusoidal responses of systems having backlash and saturation effects will be useful in comparing direct frequency response testing methods with pulse techniques.

Experimental verification of the conclusions described above is strongly recommended. More convincing conclusions may then be drawn as to the relative merits of pulse techniques versus direct frequency response testing methods.

APPENDIX A

DERIVATION OF THE PERFORMANCE EQUATIONS OF THE SYSTEMS INVESTIGATED

The performance equations of the positional servomechanisms described in Chapter 4 are derived by summing the torques acting on the controlled-member.

A-1. Positional Servomechanism with Angular Velocity Feedback Damping.-AVSD System

Consider the components of the functional diagram of Fig. 4-1. Notation used is defined there.

(a.) (Sc) = angle signal comparator

$$e_{(sc)} = S_{(sc)}\left[A;e\right]\left[\overline{A}_{(in)} - A_{(cm)}\right]$$

$$e_{(sc)} = S_{(sc)}\left[A;e\right]^{(C)} A_{(cm)} \qquad (A-1)$$

(b.) (pa) = Preamplifier

$$e_{(pa)} = S_{(pa)}\left[e;e\right] e_{(sc)} \qquad (A-2)$$

(c.) (vsc) = Velocity signal comparator

$$e_{(vsc)} = S_{(vsc)}\left[e;e\right]\left[e_{(pa)} - e_{(vsa)}\right] \qquad (A-3)$$

(d.) (da) = Drive amplifier

$$e_{(da)} = S_{(da)}\left[e;e\right] e_{(vsc)} \qquad (A-4)$$

(e.)

(tg) = Torque Generator

$$M_{(tg)} = S_{(gt)}\left[A_{cm};\ A_{tsm}\right]\ S_{(tg)}\left[e;\ M\right]\ e_{(da)}$$

$$- S^{2}_{(gt)}\left[A_{cm};\ A_{tsm}\right] S_{(tg)}\left[\dot{A};M\right]\ \dot{A}_{(cm)} \qquad (A-5)$$

Reduction of the output of the torque generator indicated in equation (A-5) is the result of motion of the torque generator rotor relative to its case.

(f.)

(avsg) = Angular Velocity Signal Generator

$$e_{(avsg)} = S_{(avsg)}\left[\dot{A};e\right]\ \dot{A}_{(tsm)}$$

$$e_{(avsg)} = S^{2}_{(gt)}\left[A_{cm};\ A_{tsm}\right] S_{(avsg)}\left[\dot{A};e\right]\ \dot{A}_{(cm)} \qquad (A-6)$$

(g.)

(vsa) = Velocity Signal Amplifier

$$e_{(vsa)} = S_{(vsa)}\left[e;e\right]\ e_{(avsg)} \qquad (A-7)$$

Combining the above relationships for the inner and outer loops of the functional diagram, Fig. 4-1. yields:

$$M_{(tg)} = S_{(gt)}\left[A_{cm};A_{tsm}\right]\ S_{(tg)}\left[e;M\right]\ S_{(da)}\left[e;e\right]\ S_{(vsc)}\left[e;e\right] S_{(pa)}\left[e;e\right]$$

$$S_{(sc)}\left[A;e\right]{}^{(C)}A_{(cm)} - S^{2}_{(gt)}\left[A_{cm};A_{tsm}\right] S_{(avsg)}\left[\dot{A};e\right]\ S_{(vsa)}\left[e;e\right]$$

$$S_{(vsc)}\left[e;e\right]\ S_{(da)}\left[e;e\right]\ S_{(tg)}\left[e;M\right]\ \dot{A}_{(cm)} - S^{2}_{(gt)}\left[A_{cm};A_{tsm}\right] S_{(tg)}\left[\dot{A};M\right]\ \acute{A}_{(cm)} \qquad (A-8)$$

An inertia reaction torque is present when the controlled-member is accelerated with respect to inertial space.

$$M_{(ir)} = - I_{(cm)(eq)} \ddot{A}_{[I - cm]} \qquad (A-9)$$

If the base does not move with respect to inertial space,

$$\ddot{A}_{[I - cm]} = \ddot{A}_{(cm)}$$

$$M_{(ir)} = - I_{(cm)(eg)} \ddot{A}_{(cm)} \qquad (A-10)$$

A basic damping torque exists due to the relative motion between the controlled-member and the supporting base. It is partially due to friction in the bearings and gear train, and to air damping.

$$M_{(d)} = - C_d \dot{A}_{[b - cm]} \qquad (A-11)$$

This reduces to

$$M_{(d)} = - C_d \dot{A}_{(cm)} \qquad (A-12)$$

if the base does not move with respect to inertial space.

Torque Summing Equation at the controlled-member

$$M_{(tg)} + M_{(ir)} + M_{(d)} + M_{(intfr)} = 0 \qquad (A-13)$$

Substituting equation (A-8), (A-9), and (A-12) in equation (A-13) gives the following performance equation of the AVSD system:

$$S_{(gt)}[A_{cm};A_{tsm}]\, S_{(tg)}[e;M]\, S_{(da)}[e;e]\, S_{(vsc)}[e;e]\, S_{(pa)}[e;e]\, S_{(sc)}[A;e]\, (C)\, A_{(cm)}$$
$$-\left\{S_{(gt)}^{2}[\dot{A}_{cm};A_{tsm}]\left[S_{(avsg)}[\dot{A};e]\, S_{(vsa)}[e;e]\, S_{(vsc)}[e;e]\, S_{(da)}[e;e]\, S_{(tg)}[e;M]\right.\right.$$
$$\left.\left.+S_{(tg)}[\dot{A};M]\right| + C_d\right\} \dot{A}_{cm} - I_{(cm)(eq)} \ddot{A}(cm) + M_{(intfr.)} = 0 \qquad (A-14)$$

Define:

$$S_{(ps)\,A;M} = S_{(gt)}\left[A_{cm};A_{tsm}\right] S_{(tg)}\left[e;M\right] S_{(da)}\left[e;\dot{e}\right] S_{(vsc)}\left[e;\dot{e}\right] S_{(pa)}\left[e;e\right]$$

$$S_{(sc)}\left[A;e\right] = \text{elastic coefficient} \qquad \text{(A-15)}$$

$$S_{(fb)(av)}\left[\dot{A};M\right] = S_{(avsg)}\left[\dot{A};e\right] S_{(vsa)}\left[e;\dot{e}\right] S_{(vsc)}\left[e;\dot{e}\right] S_{(da)}\left[e;\dot{e}\right] S_{(tg)}\left[e;M\right] \qquad \text{(A-16)}$$

$$S_{(ps)}\left[\dot{A};M\right] = S_{(gt)}^{2}\left[A_{cm};A_{tsm}\right]\left\{S_{(tg)}\left[A;M\right] + S_{(fb)(av)}\left[\dot{A};M\right]\right\} + C_d \qquad \text{(A-17)}$$

Substitution of equations (A-15) through (A-17) into equation (A-14) and rewriting the result in operator form yields:

$$\left\{I_{(cm)(eq)}\,p^2 + S_{(ps)}\left[\dot{A};M\right] p\right\} A_{(cm)} = S_{(ps)}\left[A;M\right]^{(C)} A_{(cm)} + M_{(intfr)} \qquad \text{(A-18)}$$

A-2. Positional Servomechanism with Modified Angular Veolcity Feedback Damping - MAVSD System.

Consider the components of the functional diagram of Figure 4-2. Note that the only difference in components from those of Figure 4-1 is the addition of a velocity signal modifier in the angular velocity feedback path. The velocity signal modifier is a simple passive network differentiating circuit which has the following performance function:

$$PF_{(vsm)}\left[e;\dot{e}\right] = \frac{(CT)_{(vsm)}\,p}{1+(CT)_{(vsm)}\,p} \qquad \text{(A-19)}$$

With the velocity signal modifier in the angular velocity feedback path the torque generator equation is as follows:

$$M_{(tg)} = S_{(ps)}[A;M](C)A_{(cm)} - \frac{(CT)_{(vsm)}p}{1+(CT)_{(vsm)}p} S^{2}_{(gt)}[A_{cm};A_{tsm}]$$

$$S_{(fb)(av)}[\dot{A};M]\ \dot{A}_{(cm)} - S^{2}_{(gt)}[A_{cm};A_{tsm}]\ S_{(tg)}[\dot{A};M]\ \dot{A}_{(cm)}$$

(A-20)

The inertia reaction and damping torques derived in equations (A-10) and (A-12) are unaffected by the velocity signal modifier. Subsituting the expressions for the torques into the torque summing equation (A-13), simplifying and writing in operator form produces the performance equation of the MASVD system.

$$I_{(cm)(eq)}p^{2} + S^{2}_{(gt)}[A_{cm};A_{tsm}]\ S_{(tg)}[\dot{A};M] + \frac{(CT)_{(vsm)}p}{1+(CT)_{(vsm)}p} S_{(fb)(av)}[\dot{A};M]\ p\ A_{(cm)}$$

$$= S_{(ps)}[A;M](C)A_{(cm)} + M_{(intfr)} \qquad \text{(A-21)}$$

Attention is invited to the fact that the coefficients of equations (A-18) and (A-21) may be kept constant while permitting the sensitivity of the gear train to vary. This is accomplished by adjusting amplifier sensitivities where necessary to compensate for a change in gear train sensitivity. As a consequence, it is possible to use the gear train sensitivity as a variable parameter in the study of pulse testing techniques for systems with backlash.

A-3 Numerical Performance Equations for the AVSD and MAVSD Systems

Numerical values for the coefficients of the performance equations derived above were selected from Lees[10] for a system damping ratio of seven-tenths critical at high frequencies. Coefficients were then determined for critical damping and one-tenth critical damping without changing the undamped natural frequency. Interference torques were not

considered in this investigation. These equations are shown below.

AVSD System - undamped natural frequency $w_{n(ps)} = 63.3$ rad/sec

(1) Critical Damping, $(DR)_{(ps)} = 1.0$

$$(p^2 + 126.6p + 4007)\, A_{(cm)} = 4007\, A_{(in)} \qquad (A\text{-}22)$$

(2) Seven-tenths critical damping, $(DR)_{(ps)} = 0.7$

$$(p^2 + 88.7p + 4007)\, A_{(cm)} = 4007\, A_{(in)} \qquad (A\text{-}23)$$

(3) One-tenth critical damping $(DR)_{(ps)} = 0.1$

$$(p^2 + 12.66p + 4007)\, A_{(cm)} = 4007\, A_{(in)} \qquad (A\text{-}24)$$

MAVSD System - undamped natural frequency $w_{n(ps)} = 53.6$ rad/sec

$$(CT)_{(vsm)} = 0.0993 \text{ sec.}$$

(1) Critical Damping $(DR)_{(ps)} = 1.0$

$$(p^3 + 127.4p^2 + 4030p + 40350)\, A_{(cm)} = (40350 + 4010p)A_{(in)} \qquad (A\text{-}25)$$

(2) Seven-tenths critical damping $(DR)_{(ps)} = 0.7$

$$(p^3 + 99.4p^2 + 4030p + 40350)A_{(cm)} = (40350 + 4010p)A_{(in)} \qquad (A\text{-}26)$$

(3) One-tenth critical damping $(DR)_{(ps)} = 0.1$

$$(p^3 + 22.83p^2 + 4030p + 40350)A_{(cm)} = (40350 + 4010p)A_{(in)} \qquad (A\text{-}27)$$

APPENDIX B

REAC INSTRUMENTATION

The instrumentation of the second order linear differential equation of motion of the AVSD system for REAC simulation was accomplished using standard techniques. For this reason, a discussion of the problem is not deemed necessary. The third order, linear differential equation for the MAVSD system required a somewhat different approach to effect correct REAC simulation due to the presence of the derivative of the input quantity. The method of instrumentation is developed below and a diagram of the basic REAC setup is shown in Fig. B-1.

The MAVSD performance equation, as derived in Appendix A, is of the following general form

$$(p^3 + a_2 p^2 + a_1 p + a_0) A_{(cm)} = (b_0 + b_1 p) A_{(in)} \qquad \text{(B-1)}$$

To obtain the solution of equation (B-1), where $A_{(in)}$ represents the desired pulse function input, instrument the following equation by standard REAC methods. (See Fig. B-1)

$$(p^3 + a_2 p^2 + a_1 p + a_0) A'_{(cm)} = b_0 A_{(in)} \qquad \text{(B-2)}$$

Let

$$y = \frac{A_{(in)}}{(p^3 + a_2 p^2 + a_1 p + a_0)} \qquad \text{(B-3)}$$

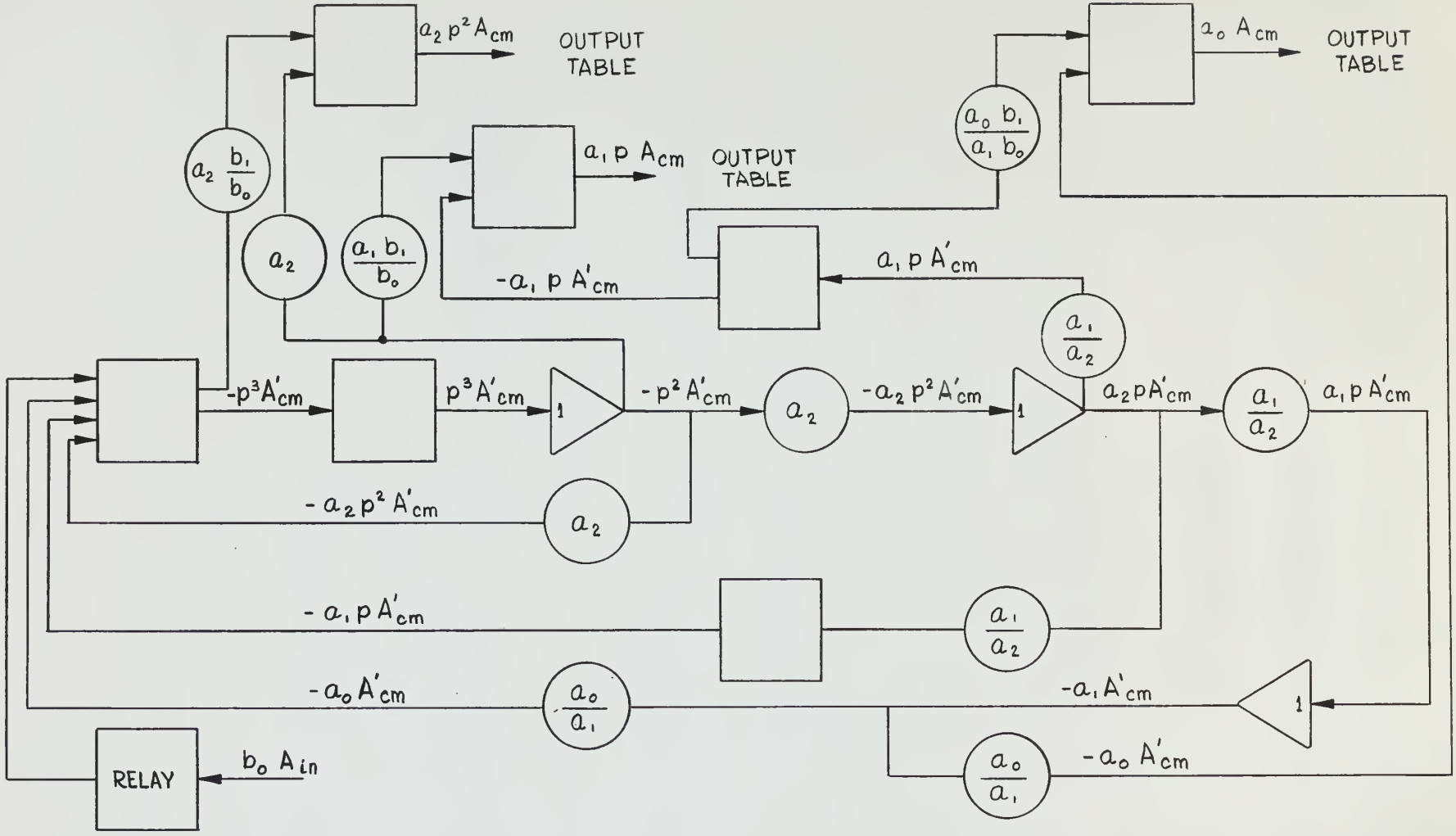

Note: Time scale change and amplifier gains not included in this diagram.

Fig. B-1 Basic REAC setup for the MAVSD system.

Then from (B-1),

$$A_{(cm)} = b_0 y + b_1 p y \qquad \text{(B-4)}$$

The first and second derivatives of equation (B-4) in operator form are:

$$p A_{(cm)} = b_0 p y + b_1 p^2 y \qquad \text{(a) (B-5)}$$

$$p^2 A_{(cm)} = b_0 p^2 y + b_1 p^3 y \qquad \text{(b) (B-5)}$$

From equation (B-2),

$$A'_{(cm)} = \frac{b_0 A_{(in)}}{(p^3 + a_2 p^2 + a_1 p + a_0)} = b_0 y \qquad \text{(B-6)}$$

The derivatives of (B-6) are,

$$p A'_{(cm)} = b_0 p y \qquad \text{(a) (B-7)}$$

$$p^2 A'_{(cm)} = b_0 p^2 y \qquad \text{(b) (B-7)}$$

Then,

$$b_1 p y = \frac{b_1}{b_0} p A'_{(cm)} \qquad \text{(a) (B-8)}$$

$$b_1 p^2 y = \frac{b_1}{b_0} p^2 A'_{(cm)} \qquad \text{(b) (B-8)}$$

Substituting in equations (B-4) and (B-5) gives:

$$A_{(cm)} = A'_{(cm)} + \frac{b_1}{b_0} p A'_{(cm)} \qquad \text{(a) (B-9)}$$

$$pA_{(cm)} = p A'_{(cm)} + \frac{b_1}{b_0} p^2 A'_{(cm)} \qquad \text{(b) (B-9)}$$

$$p^2 A_{(cm)} = p^2 A'_{(cm)} + \frac{b_1}{b_0} p^3 A'_{(cm)} \qquad \text{(c) (B-9)}$$

Multiply the equations of (B-9) by the appropriate coefficients from the characteristic equation of (B-1).

$$a_0 A_{(cm)} = a_0 A'_{(cm)} + a_0 \frac{b_1}{b_0} p A'_{(cm)} \qquad \text{(a) (B-10)}$$

$$a_1 p A_{(cm)} = a_1 p A'_{(cm)} + a_1 \frac{b_1}{b_0} p^2 A'_{(cm)} \qquad \text{(b) (B-10)}$$

$$a_2 p^2 A_{(cm)} = a_2 p^2 A'_{(cm)} + a_2 \frac{b_1}{b_0} p^3 A'_{(cm)} \qquad \text{(c) (B-10)}$$

Note that in the basic REAC setup of Fig. B-1 the quantities $(a_0 A'_{(cm)})$ and $(a_1 p A'_{(cm)})$ are present. Then to determine $(a_0 A_{(cm)})$ from equation (B-10)(a), it is necessary to multiply (a_1) by a factor (k_1) such that,

$$a_1 k_1 = a_0 \frac{b_1}{b_0}$$

or

$$k_1 = \frac{a_0 b_1}{a_1 b_0} \qquad \text{(a) (B-11)}$$

Similarly for (B-10)(a) and (b),

$$k_2 = \frac{a_1 b_1}{a_2 b_0} \qquad \text{(b) (B-11)}$$

$$k_3 = \frac{a_2 b_1}{b_0} \qquad \text{(c) (B-11)}$$

By the above procedure of instrumenting equation (B-2) and correctly summing quantities at pertinent points, it is possible to obtain the displacement, velocity and acceleration responses of equation (B-1) to a desired pulse input to the system. The method avoids REAC differentiation of the pulse input and gives reproduceable time

function responses.

Rectangular pulse generation was accomplished using a step input which was returned to zero magnitude at the end of the desired pulse duration by a relay. Displaced cosine pulse function generation was simply obtained by intrumenting an undamped second order system. Pulse amplitude was controlled by varying the initial condition on the second integrator. Pulse duration was established by a relay, and the undamped natural frequency was adjusted through proper choice of equation coefficients to give one cycle of the oscillation for the period of the pulse duration. Scale factors to meet loop gain limitations of the REAC were such as to make any minor deviation in pulse shape insignificant in their effect on system response.

APPENDIX C
TABULATION OF NUMERICAL VALUES OF THE RESPONSES FOR IDEAL LINEAR AVSD AND MAVSD SYSTEMS

Table C-1 Values of controlled-member displacement ratio for rectangular pulse function input to AVSD system (PD)(NP)R = 0.1

T(NP)R	A_{cm}/A_{ref}		
	DR = 0.1	DR = 0.7	DR = 1.0
0.000	0.000	0.000	0.000
0.050	0.095	0.090	0.079
0.151	0.654	0.462	0.390
0.252	0.978	0.523	0.420
0.352	0.915	0.420	0.333
0.453	0.524	0.267	0.235
0.554	0.000	0.135	0.155
0.655	-0.472	0.045	0.099
0.755	-0.714	0.000	0.061
0.856	-0.671	-0.021	0.037
0.957	-0.388	-0.024	0.022
1.057	0.000	-0.019	0.014
1.158	0.363	-0.011	0.009
1.260	0.518	-0.006	0.006
1.360	0.488	-0.002	0.004
1.460	0.287	0.000	0.003
1.510	0.157	0.000	0.002

$$A_{ref} = A_{cm(max)(DR = 0.1)}$$

Table C-2 Values of controlled-member velocity ratio for rectangular pulse function input to AVSD system (PD)(NP)R = 0.1

T(NP)R	$\dot{A}_{cm}/\dot{A}_{ref}$		
	DR = 0.1	DR = 0.7	DR = 1.0
0.000	0.000	0.000	0.000
0.053	0.553	0.476	0.430
0.101	0.994	0.659	0.566
0.151	0.766	0.324	0.213
0.252	0.203	-0.068	-0.081
0.352	-0.368	-0.216	-0.149
0.453	-0.741	-0.224	-0.136
0.554	-0.803	-0.167	-0.103
0.655	-0.568	-0.100	-0.072
0.755	-0.147	-0.047	-0.046
0.856	0.259	-0.138	-0.029
0.957	0.535	0.003	-0.016
1.057	0.589	0.010	-0.013
1.158	0.420	0.010	-0.008
1.260	0.110	0.008	-0.006
1.360	-0.184	0.007	-0.005
1.460	-0.380	0.000	-0.002
1.510	-0.430	0.000	-0.001

$$\dot{A}_{ref} = \dot{A}_{cm(max)(DR = 0.1)}$$

Table C-3 Value of controlled-member acceleration ratio for rectangular pulse function input to AVSD system (PD)(NP)R = 0.1

T(NP)R	$\ddot{A}_{cm}/\ddot{A}_{ref}$		
	DR = 0.1	DR = 0.7	DR = 1.0
0.000	0.000	0.000	0.000
0.025	1.000	0.810	0.797
0.095	0.760	0.334	0.228
0.121	-0.334	-0.633	-0.659
0.201	-0.494	-0.337	-0.258
0.302	-0.494	-0.122	-0.006
0.403	-0.314	0.000	0.005
0.503	-0.051	0.057	0.022
0.605	0.208	0.057	0.020
0.705	0.357	0.051	0.009
0.806	0.359	0.033	0.004
0.907	0.235	0.020	0.000
1.007	0.038	0.006	0.000
1.108	-0.152	0.000	0.000
1.208	-0.258	0.000	0.000
1.310	-0.268	0.000	0.000
1.410	-0.177	0.000	0.000
1.510	-0.033	0.000	0.000

$$\ddot{A}_{ref} = \ddot{A}_{cm\ (max)(DR = 0.1)}$$

Table C-4 Values of controlled-member displacement ratio for rectangular pulse function input to MAVSD system (PD)(NP)R = 0.1

T(NP)R	A_{cm}/A_{ref}		
	DR = 0.1	DR = 0.7	DR = 1.0
0.000	0.000	0.000	0.000
0.063	0.152	0.095	0.101
0.101	-----	0.259	0.127
0.126	0.514	0.368	0.346
0.189	0.817	0.535	0.471
0.246	-----	-----	0.498
0.252	0.976	-----	-----
0.258	-----	0.583	-----
0.289	1.000	-----	-----
0.314	-----	-----	0.467
0.315	-----	0.554	-----
0.327	0.967	-----	-----
0.378	0.837	0.483	0.411
0.503	0.270	0.303	0.288
0.630	-0.339	0.147	0.185
0.693	-0.556	-----	-----
0.755	-0.664	0.041	0.104
0.794	-0.679	-----	-----
0.882	-0.560	-0.001	0.050
1.007	-0.173	-0.038	0.016
1.132	0.263	-0.043	-0.007
1.126	0.462	-0.041	-0.018
1.285	0.490	-----	-----
1.385	0.405	-0.034	-0.026
1.510	0.118	-0.027	-0.028

$A_{ref} = A_{cm\ (max)(DR = 0.1)}$

Table C-5 Values of controlled-member velocity for rectangular pulse function input to MAVSD system (PD)(NP)R = 0.1

T(NP)R	$\dot{A}_{cm}/\dot{A}_{ref}$		
	DR = 0.1	DR = 0.7	DR = 1.0
0.0000	0.000	0.000	0.000
0.0126	-----	0.083	0.108
0.0252	0.277	-----	-----
0.0378	-----	0.298	0.301
0.0630	0.650	0.552	0.441
0.0910	-----	0.678	-----
0.1010	1.000	-----	-----
0.1110	-----	-----	0.581
0.1260	0.900	0.524	0.425
0.1510	-----	-----	0.255
0.1890	0.577	0.193	0.086
0.2520	0.202	-0.014	-0.078
0.3140	-----	-0.130	-----
0.3780	-0.499	-0.187	-0.175
0.4400	-0.710	-----	-----

(continued on next page)

Table C-5 - con't.

T(NP)R	$\dot{A}_{cm}/\dot{A}_{ref}$		
	DR = 0.1	DR = 0.7	DR = 1.0
0.4530	-----	-0.209	-----
0.5030	-----	-0.198	-0.157
0.5280	-0.809	-----	-----
0.5670	-0.776	-----	-----
0.6300	-0.632	-0.145	-0.118
0.7550	-0.127	-0.086	-0.070
0.8820	0.352	-0.041	-0.052
0.9440	0.499	-----	-----
1.0070	-----	-0.016	-0.019
1.0200	0.562	-----	-----
1.1320	0.433	-----	-----
1.1950	-----	0.000	-0.002
1.2600	0.083	-----	-----
1.3850	-0.249	0.004	0.009
1.4500	-0.355	-----	-----
1.5100	-0.394	0.004	0.011

$$\dot{A}_{ref} = \dot{A}_{cm(max)(DR = 0.1)}$$

Table C-6 Values of controlled-member acceleration ratio for rectangular pulse function input to MAVSD system (PD)(NP)R = 0.1

T(NP)R	$\ddot{A}_{cm}/\ddot{A}_{ref}$		
	DR = 0.1	DR = 0.7	DR = 1.0
0.000	0.000	0.000	0.000
0.013	0.405	0.127	-----
0.025	1.000	-----	0.200
0.045	-----	0.279	-----
0.063	-----	0.206	0.122
0.076	-----	0.110	-----
0.101	0.716	-0.022	0.064
0.113	-----	-0.178	-----
0.126	-0.378	-----	-----
0.138	-----	-----	-0.163
0.189	-0.505	-0.106	-0.092
0.252	-0.550	-0.063	-0.047
0.314	-0.507	-----	-----
0.378	-0.394	-0.014	-0.006
0.503	-0.047	0.007	0.004
0.630	0.270	0.012	0.007
0.755	0.380	-----	0.006
0.882	0.270	0.007	-----
1.007	0.027	-----	0.003
1.132	-0.195	0.007	-----
1.260	-0.270	----	0.001
1.385	-0.195	-----	-----
1.510	-0.014	-0.001	0.000

$$\ddot{A}_{ref} = A_{cm\ (max)(DR = 0.1)}$$

Table C-7 Values of controlled-member displacement ratio for displaced cosine pulse function input to AVSD system (PD)(NP)R = 0.1

T(NP)R	A_{cm}/A_{ref}		
	DR = 0.1	DR = 0.7	DR = 1.0
0.000	0.000	0.000	0.000
0.015	-----	-----	-----
0.020	0.000	-----	-----
0.025	-----	0.000	-----
0.050	0.050	0.044	0.048
0.075	-----	0.153	-----
0.100	0.328	0.276	0.253
0.151	0.627	0.442	0.383
0.176	-----	0.490	-----
0.201	0.840	0.514	0.423
0.222	-----	0.523	0.426
0.252	0.960	0.520	0.413
0.292	1.000	-----	-----
0.302	-----	0.480	0.375
0.352	0.908	0.414	-----
0.402	0.758	0.330	0.279
0.503	0.280	0.188	0.190
0.554	-----	0.130	-----

0.605	-0.239	0.083	0.125
0.655	-0.454	0.043	-----
0.705	-0.609	0.015	0.076
0.755	-0.695	-0.004	-----
0.806	-0.717	-0.015	0.036
0.856	-0.666	-----	-----
0.906	-----	-0.026	0.028
0.957	-0.380	-0.029	-----
1.007	-----	-0.026	0.017
1.061	0.000	-----	-----
1.110	-----	-0.019	-----
1.158	0.331	-0.015	-----
1.210	0.444	-0.011	-----
1.260	0.514	-----	-----
1.300	0.528	-0.008	-----
1.310	-----	-----	-----
1.350	0.490	-0.006	0.000
1.410	0.409	-----	
1.460	-----	0.000	
1.510	0.158		

$$A_{ref} = A_{cm(max)(DR = 0.1)}$$

Table C-8 Values of controlled-member velocity ratio for displaced cosine pulse function input to the AVSD system (PD)(NP)R = 0.1

T(NP)R	$\dot{A}_{cm}/\dot{A}_{ref}$		
	DR = 0.1	DR = 0.7	DR = 1.0
0.000	0.000	0.000	0.000
0.010	0.000	0.000	0.000
0.025	0.084	0.081	0.081
0.040	0.304	0.284	-----
0.050	0.508	0.450	0.440
0.060	-----	0.621	-----
0.070	0.880	0.730	0.676
0.079	0.975	0.770	0.695
0.090	1.000	0.746	0.649
0.100	0.982	0.675	0.554
0.126	-----	0.489	0.365
0.151	0.779	0.338	0.223
0.201	0.516	0.097	0.027
0.252	-----	-0.061	-0.080
0.302	-0.076	-0.162	-0.130
0.352	-----	-0.214	-0.149
0.402	-0.571	-0.230	-0.149

0.453	-0.726	-0.226	-----
0.503	-0.800	-0.203	-0.138
0.504	-0.811	-----	-----
0.554	-----	-0.169	-----
0.605	-0.717	-0.135	-0.088
0.655	-0.571	-0.102	-----
0.705	-----	-0.074	-0.058
0.755	-0.169	-0.049	-----
0.806	-----	-0.028	-0.038
0,856	0.245	-0.014	-----
0.957	0.528	0.002	-0.019
1.007	-----	0.007	-----
1.032	0.592	-----	-----
1.057	-----	0.014	-----
1.110	0.528	-----	-----
1.210	0.287	-----	-0.008
1.260	-----	0.011	-----
1.310	-0.032	-----	-----
1.360	-----	0.007	-----
1.410	-0.297	-----	-----
1.460	-0.381	-----	-----
1.510	-0.426	0.000	0.000

$$\dot{A}_{ref} = \dot{A}_{cm(max)(DR = 0.1)}$$

Table C-9 Values of controlled-member acceleration ratio for displaced cosine pulse function input to AVSD system (PD)(NP)R = 0.1

T(NP)R	$\ddot{A}_{cm}/\ddot{A}_{ref}$		
	DR = 0.1	DR = 0.7	DR = 1.0
0.000	0.000	0.000	0.000
0.010	0.071	0.090	0.077
0.020	0.345	0.315	0.283
0.030	0.651	0.606	0.554
0.040	0.901	-----	0.739
0.048	-----	0.850	0.782
0.050	1.000	-----	-----
0.055	-----	-----	0.721
0.060	0.901	0.696	0.605
0.070	0.630	0.374	0.309
0.080	0.258	0.000	-0.013
0.090	0.000	-0.258	-0.350
0.095	-0.118	-----	-----
0.097	-----	-0.386	-----
0.100	-----	-----	-0.463
0.111	-----	-0.345	-----
0.126	-0.188	-0.310	-0.329

0.151	-----	-0.273	-0.257
0.176	-----	-0.227	-----
0.201	-0.263	-0.188	-0.144
0.252	-0.280	-0.121	-----
0.302	-0.270	-0.071	-0.031
0.352	-----	-0.028	-----
0.392	-----	-----	0.000
0.402	-0.176	0.000	-----
0.504	--- -	0.028	-----
0.523	0.000	-----	0.010
0.604	-----	0.031	-----
0.655	0.165	-----	0.008
0.705	-----	0.026	-----
0.77-	0.212	-----	-----
0.805	-----	0.018	-----
0.856	0.180	-----	-----
0.906	-----	0.008	-----
0.957	0.088	-----	0.004
1.007	-----	0.000	-----
1.107	-0.072		0.000
1.210	-0.129		
1.270	-0.148		
1.360	-0.126		
1.510	-0.021		

$$\ddot{A}_{ref} = \ddot{A}_{cm(max)(DR = 0.1)}$$

Table C-10 Values of controlled-member displacement ratio for displaced cosine pulse function input to MAVSD system with (PD)(NP)R = 0.1

T(NP)R	A_{cm}/A_{ref}		
	DR = 0.1	DR = 0.7	DR = 1.0
0.0000	0.000	0.000	0.000
0.0252	0.000	-----	-----
0.0504	0.043	-----	0.038
0.0630	-----	0.094	-----
0.0756	0.161	-----	0.131
0.1007	0.326	-----	0.246
0.1260	0.483	0.332	0.330
0.1890	0.794	0.497	0.433
0.2520	0.939	0.529	0.451
0.3150	0.991	0.497	0.421
0.3780	0.855	0.429	0.371
0.4410	0.607	0.344	0.313
0.5040	0.296	0.267	0.259
0.5670	-0.029	0.195	0.208
0.6300	-0.329	0.126	0.163
0.6930	-0.570	0.071	0.125
0.7560	-0.701	0.036	0.089

0.8180	-0.718	0.006	0.065
0.8820	-0.622	-0.012	0.043
0.9440	-0.450	-0.026	0.027
1.0070	-0.219	-0.036	0.012
1.1320	0.245	-0.038	-0.008
1.2600	0.505	-0.036	-0.018
1.3830	0.455	-0.030	-0.025
1.5100	0.159	-0.025	-0.028
1 6360	-0.178	-0.019	-0.029
1.7630	-0.362	-----	-0.027
1.888	-.330	-0.012	-0.024
2.0150	-0.112	-----	-0.022

$$A_{ref} = A_{cm(max)(DR = 0.1)}$$

Table C-11 Values of controlled-member velocity ratio for displaced cosine pulse function input to MAVSD system with (PD)(NP)R = 0.1

T(NP)R	$\dot{A}_{cm}/\dot{A}_{ref}$		
	DR = 0.1	DR = 0.7	DR = 1.0
0.0000	0.000	0.000	0.000
0.0126	0.007	-----	0.000
0.0252	0.082	0.082	0.082
0.0378	0.249	-----	0.247
0.0504	0.481	0.470	0.436
0.0630	0.719	-----	0.640
0.0756	0.898	0.754	0.713
0.0882	0.996	-----	0.713
0.1007	0.996	0.685	0.613
0.1133	0.930	-----	0.507
0.1260	0.878	0.533	0.420
0.1890	0.530	0.178	0.119
0.2520	0.137	-0.014	-0.031
0.3150	-0.242	-0.129	-0.106
0.3780	-0.555	-0.187	-0.137
0.4410	-0.754	-0.206	-0.144
0.5040	-0.825	-----	-0.132

0.6300	-0.781	-0.174	-0.120
0.6930	-0.600	-0.144	-0.108
0.7560	-0.352	-----	-0.090
0.8820	-0.069	-0.085	-0.073
1.0070	0.411	-0.041	-0.051
1.1320	0.600	-0.014	-0.033
1.2600	0.452	0.000	-0.020
1.3830	0.078	-----	-0.012
1.5100	-0.279	0.010	-0.009
1.6360	-0.434	-----	0.000
2.0150	-----	0.007	
		0.000	

$$\dot{A}_{(ref)} = \dot{A}_{cm(max)(DR = 0.1)}$$

Table C-12 Values of controlled-member acceleration ratio for displaced cosine pulse function input to MAVSD system with (PD)(NP)R = 0.1

T(NP)R	$\ddot{A}_{cm}/\ddot{A}_{ref}$		
	DR = 0.1	DR = 0.7	DR = 1.0
0.0000	0.000	0.000	0.000
0.0126	0.171	0.163	0.150
0.0252	0.479	0.458	0.226
0.0378	0.845	0.751	0.763
0.0504	1.000	0.830	0.782
0.0630	0.875	0.611	0.531
0.0756	0.475	0.494	0.090
0.0882	0.028	-0.190	-0.240
0.1007	-0.205	-0.347	-0.393
0.1133	-0.217	-0.328	-0.341
0.1260	-0.232	-0.294	-0.308
0.1890	-0.291	-0.196	-0.158
0.2520	-0.304	-0.120	-0.082
0.3150	-0.262	-0.065	-0.025
0.3780	-0.194	-0.026	0.000
0.4410	-0.101	0.000	0.020

0.5040	0.000	0.006	0.025
0.5670	0.091	0.019	0.020
0.6300	0.161	0.022	-----
0.6930	0.201	0.021	-----
0.7560	0.211	0.018	-----
0.8180	0.207	0.013	-----
0.8820	0.150	0.010	0.000
0.9440	0.076	0.003	
1.0070	0.000	0.000	
1.0700	-0.079		
1.1320	-0.079		
1.1960	-0.148		

$$\ddot{A}_{ref} = \ddot{A}_{cm(max)(DR = 0.1)}$$

Table C-13 Values of controlled-member displacement ratio for displaced cosine pulse function input to AVSD system DR = 0.7

T(NP)R	A_{cm}/A_{ref}				
	(PD)(NP)R = 0.1	(PD)(NP)R = 0.3	(PD)(NP)R = 0.7	(PD)(NP)R = 0.7	(PD)(NP)R = 1.0
0.000	0.000	0.000	0.000	0.000	0.000
0.047	0.013	0.000	-----	-----	-----
0.075	0.048	0.013	-----	-----	-----
0.100	0.085	-----	-----	-----	-----
0.126	-----	0.061	0.025	0.015	0.000
0.151	0.137	------	-----	-----	-----
0.176	0.152	-----	-----	-----	-----
0.189	0.156	0.213	0.107	0.063	0.030
0.227	0.162	----	-----	-----	-----
0.252	0.161	0.380	0.256	0.162	0.087
0.302	0.148	-----	-----	-----	-----
0.315	-----	0.464	0.442	0.304	0.178
0.340	0.131	0.468	-----	-----	-----
0.378	-----	0.457	0.616	-----	-----
0.403	0.102	-----	-----	-----	-----
0.438	-----	0.398	0.702	0.670	0.465

0.453	0.079	-----	-----	-----	-----
0.472	-----	-----	0.710	-----	-----
0.504	0.058	0.317	0.687	0.802	-----
0.566	0.033	0.231	0.597	0.862	0.783
0.605	0.026	-----	-----	-----	-----
0.629	-----	0.154	0.474	0.836	0.908
0.655	0.013	-----	-----	-----	-----
0. 692	-----	0.093	0.350	0.733	0.982
0.705	0.005	-----	-----	-----	-----
0.743	-----	-----	-----	-----	1.000
0.755	-0.001	0.046	0.232	-----	0.996
0.806	-0.005	-----	-----	-----	-----
0.818	-----	0.013	0.141	0.433	0.950
0.882	-0.007	-0.008	0.071	0.300	0.848
0.945	-----	-0.018	0.022	0.181	-----
0.957	-0.009	-----	-----	-----	-----
1.007	-0.008	-0.023	-0.008	0.097	0.544
1.070	-----	-0.023	-0.023	0.034	-----
1.132	-----	-0.020	-0.029	-0.005	0.251
1.158	-0.005	-----	-0.032	-----	-----
1.196	-----	-----	-0.031	-0.026	0.142
1.210	-0.004	-----	-0.0026	-0.035	-----
1.310	-0.003	-0.010	-0.022	-0.035	0.021
1.400	-0.001	-0.005	-0.011	-0.030	-0.024

$A_{ref} = A_{cm(max)}[(PD)(NP)R = 1.0]$

Table C-14 Values of controlled-member velocity ratio for displaced cosine function input to AVSD system DR = 0.7

T(NP)R	$\dot{A}_{cm}/\dot{A}_{ref}$				
	(PD)(NP)R = 0.1	(PD)(NP)R = 0.3	(PD)(NP)R = 0.5	(PD)(NP)R = 0.7	(PD)(NP)R = 1.0
0.000	0.000	0.000	0.000	0.000	0.000
0.025	0.055	-----	0.000	0.000	0.000
0.040	0.193	-----	-----	-----	-----
0.050	0.306	-----	-----	-----	-----
0.063	0.430	0.103	0.037	0.018	-----
0.080	0.524	0.218	-----	-----	-----
0.094	0.507	0.291	-- --	-----	0.034
0.126	0.333	0.547	0.250	0.138	-----
0.157	0.210	0.783	-----	-----	0.129
0.189	0.076	0.920	0.608	0.368	-----
0.201	0.066	0.936	-----	-----	-----
0.221	0.009	0.903	-----	-----	-----
0.252	-0.041	0.718	0.920	0.652	0.368
0.296	-0.109	0.419	1.000	-----	-----
0.333	-0.141	0.101	0.917	0.927	-----
0.372	-0.155	-0.191	0.703	0.973	0.733
0.403	-0.156	-0.239	-----	0.941	-----

0.438	-0.155	-0.381	0.202	0.838	0.849
0.483	-0.148	-0.421	-0.098	-----	0.866
0.523	-0.127	-0.443	-0.452	0.382	0.816
0.566	-0.099	-0.427	-0.585	0.077	0.752
0.629	-0.080	-0.357	-0.670	-0.350	0.547
0.692	-0.055	-0.291	-0.645	-----	0.262
0.755	-0.033	-0.211	-0.552	-0.807	-0.062
0.819	-0.015	-0.134	-----	-0.783	-0.381
0.882	-0.001	-0.082	-0.309	-0.677	-0.641
0.945	0.000	-0.037	-----	-----	-0.805
1.007	0.005	-0.011	-0.118	-0.390	-0.851
1.057	0.009	0.009	-0.023	-----	-0.743
1.132	0.008	0.018	-----	-0.149	-----
1.160	0.008	-----	0.000	-----	-0.655
1.260	0.007	0.018	0.029	-0.022	-0.378
1.386	0.004	0.016	0.037	0.034	-0.120
1.510	0.000	-----	-----	0.018	0.000
1.575	0.000	0.004	0.018	-----	0.024
1.700	0.000	0.000	0.013	0.009	0.040
1.890	0.000	0.000	0.000	0.000	0.028

$$\dot{A}_{ref} = \dot{A}_{cm(max)} \left[(PD)(NP)R = 0.5 \right]$$

Table C-15 Values of controlled-member acceleration ratio for displaced cosine function input to AVSD system DR = 0.7

T(NP)R	$\ddot{A}_{cm}/\ddot{A}_{ref}$				
	(PD)(NP)R = 0.1	(PD)(NP)R = 0.3	(PD)(NP)R = 0.5	(PD)(NP)R = 0.7	(PD)(NP)R = 1.0
0.000	0.000	0.000	0.000	0.000	0.000
0.010	0.106	------	------	------	------
0.020	0.370	------	------	------	------
0.031	0.712	0.144	0.039	0.023	0.009
0.048	1.000	------	------	------	------
0.063	0.781	0.372	0.145	0.079	0.038
0.070	0.439	------	------	------	------
0.081	0.000	0.551	0.218	0.123	0.060
0.097	-0.455	------	------	------	------
0.120	-0.376	0.687	0.454	0.219	0.114
0.156	-0.318	0.518	0.479	0.306	0.166
0.188	-0.244	0.151	0.490	0.356	0.206
0.204	-0.219	0.000	------	------	------
0.219	-0.197	-0.297	0.424	0.375	0.236
0.250	-0.141	-0.478	0.287	0.363	0.255
0.281	-0.101	-0.750	0.083	0.310	0.260
0.313	-0.793	-0.628	-0.147	0.223	0.251
0.344	-0.391	-0.480	-0.375	0.112	0.227

0.376	-0.161	-0.348	-0.568	-0.026	0.189
0.438	0.015	-0.148	-0.719	-0.303	0.076
0.504	0.033	-0.015	-0.524	-0.519	-0.060
0.562	0.034	0.060	-0.219	-0.605	-0.209
0.630	0.035	0.097	-0.024	-0.525	-0.330
0.692	0.032	0.106	0.094	-0.291	-0.410
0.755	0.261	0.099	0.145	-0.042	-0.430
0.819	0.019	0.082	0.160	0.101	-0.386
0.882	0.012	0.064	0.148	0.174	-0.283
0.944	0.005	0.045	0.126	0.194	-0.133
1.007	0.000	0.029	0.097	0.182	0.032
1.070	------	0.015	0.067	0.154	0.150
1.196	------	0.000	0.022	0.085	0.204
1.320	0.000	-0.006	0.000	0.032	0.147
1.385	------	-0.007	-0.006	0.012	0.110
1.510	------	-0.006	-0.009	-0.005	0.048
1.762	------	0.000	-0.006	-0.008	0.011
1.890	0.000	------	0.000	-0.003	-0.006

$$\ddot{A}_{ref} = \ddot{A}_{cm(max)}[(PD)(NP)R = 0.1]$$

Table C-16 Values of controlled-member displacement ratio for displaced cosine pulse function input to MAVSD system with DR=0.7

T(NP)R	A_{cm}/A_{ref}				
	(PD)(NP)R = 0.1	(PD)(NP)R = 0.3	(PD)(NP)R = 0.5	(PD)(NP)R = 0.7	(PD)(NP)R = 1.0
0.000	0.000	0.000	0.000	0.000	0.000
0.063	0.026	0.006	0.000	0.000	------
0.126	0.099	0.054	0.021	0.014	0.000
0.189	0.140	0.178	0.093	0.054	0.033
0.252	0.149	0.329	0.223	0.143	0.063
0.315	0.140	0.419	0.397	0.282	0.147
0.378	0.120	0.429	0.553	0.448	0.264
0.441	0.097	0.388	0.641	0.615	------
0.504	0.075	0.330	0.645	0.744	0.560
0.567	0.056	0.263	0.586	0.810	------
0.630	0.036	0.197	0.494	0.805	0.836
0.693	0.020	0.132	0.378	0.716	0.929
0.756	0.010	0.088	0.283	0.602	0.965
0.818	0.002	0.048	0.200	------	0.943
0.882	-0.004	0.018	0.121	0.347	0.858
0.944	-0.007	-0.004	------	------	------
1.007	-0.010	-0.017	0.019	0.152	0.600
1.132	-0.011	-0.030	-0.034	0.023	0.316

1.196	------	------	-0.046	-0.014	------
1.260	-0.010	-0.033	-0.051	-0.041	0.107
1.383	-0.009	-0.030	-0.053	-0.063	-0.014
1.447	------	------	------	-0.067	------
1.510	-0.007	-0.024	-0.048	-0.067	-0.074
1.573	------	------	------	-0.064	------
1.636	-0.005	-0.018	-0.039	------	-0.091
1.699	------	------	------	------	-0.091
1.763	------	------	------	------	-0.086
1.888	-0.004	-0.011	-0.024	-0.036	-0.073
2.015	------	------	------	------	------
2.265	------	-0.006	-0.014	------	------
2.390	------	------	------	-0.014	-0.028
2.520	-0.002	------	------	------	------
2.765	------	-0.003	-0.007	------	------
2.895	------	------	------	-0.006	------
3.145	-0.001	------	------	------	-0.014
3.400	0.000	0.000	0.000	------	------
3.525				0.000	------
3.770					0.000

$$A_{(ref)} = A_{in_{(max)}}$$

Table C-17 Values of controlled-member velocity ratio for displaced cosine pulse function input to MAVSD system with DR=0.7

T(ND)R	$\dot{A}_{cm}/\dot{A}_{ref}$				
	(PD)(NP)R = 0.1	(PD)(NP)R = 0.3	(PD)(NP)R = 0.5	(PD)(NP)R = 0.7	(PD)(NP)R = 1.0
0.0000	0.000	0.000	0.000	0.000	0.000
0.0252	0.055	------	------	------	------
0.0504	0.309	------	------	------	------
0.0630	------	0.088	0.036	0.020	0.000
0.0756	0.495	------	------	------	------
0.1007	0.450	------	------	------	------
0.1260	0.350	0.504	0.248	0.132	0.055
0.1890	0.117	0.885	0.598	0.360	0.182
0.2520	-0.009	0.736	0.918	0.641	0.360
0.3150	-0.085	0.241	0.990	0.894	0.566
0.3780	-0.123	-0.100	0.732	0.990	0.741
0.4410	-0.135	-0.291	0.256	0.897	0.868
0.5040	------	-0.386	-0.202	0.599	0.900
0.5670	-0.114	-0.396	-0.480	0.180	0.828
0.6300	-0.094	-0.382	-0.587	-0.270	0.630
0.6930	------	------	-0.599	-0.594	0.360
0.7560	-0.056	-0.259	-0.554	-0.735	0.018
0.8180	------	------	-0.468	-0.749	-0.299

0.8820	-0.027	-0.148	-0.382	-0.685	-0.594
0.9440	------	------	-0.300	-0.588	-0.781
1.0070	-0.009	-0.072	-0.216	-0.469	-0.857
1.0700	------	------	-0.144	-0.368	-0.826
1.1320	0.000	-0.020	-0.095	-0.270	-0.727
1.260	------	0.000	-0.031	-0.122	-0.481
1.3220	0.007	------	-0.007	------	------
1.3830	------	0.014	------	-0.031	-0.231
1.4470	------	------	0.018	-0.005	------
1.5100	------	0.015	------	0.011	-0.090
1.5730	------	------	0.018	------	------
1.6360	0.004	0.014	------	------	-0.014
1.6990	------	------	------	0.027	------
1.7630	------	0.008	------	------	0.025
1.8880	------	------	------	------	0.040
2.0150	0.000	0.00	------	0.018	------
2.1400			0.009	------	------
2.3900			0.000	0.000	0.022
3.2720					0.000

$$\dot{A}_{(ref)} = \dot{A}_{cm(max)}[(PD)(NP)R = 0.5]$$

Table C-18 Values of controlled-member acceleration ratio for displaced cosine function input to MAVSD system with DR = 0.7

T(NP)R	$\ddot{A}_{cm}/\ddot{A}_{ref}$				
	(PD)(NP)R = 0.1	(PD)(NP)R = 0.3	(PD)(NP)R = 0.5	(PD)(NP)R = 0.7	(PD)(NP)R = 1.0
0.0000	0.000	0.000	0.000	0.000	0.000
0.0126	0.206	0.032	------	------	------
0.0252	0.552	0.095	0.025	0.013	0.000
0.0378	0.905	0.177	------	------	------
0.0504	1.000	0.284	0.101	0.058	0.020
0.0630	0.700	0.394	------	------	------
0.0756	0.595	0.498	0.205	0.110	0.049
0.0882	-0.232	0.600	------	------	------
0.1007	-0.418	0.663	0.316	0.178	0.083
0.1133	-0.396	0.698	------	------	------
0.1260	-0.354	0.698	0.418	0.240	0.120
0.1890	-0.236	0.158	0.521	0.366	0.207
0.2520	-0.144	-0.606	0.312	0.379	0.266
0.2835	------	-0.718	------	------	------
0.3150	-0.078	-0.605	-0.118	0.242	0.270
0.3780	-0.032	-0.350	-0.552	0.000	0.214
0.4410	0.000	-0.178	-1.710	-0.279	0.111
0.5040	0.008	-0.060	-0.521	-0.501	-0.024

0.5670	0.023	0.017	-0.248	-0.593	-0.176
0.6300	0.026	0.062	-0.134	-0.531	-0.316
0.6930	0.025	0.076	0.035	-0.316	-0.401
0.7560	0.022	0.079	0.095	-0.087	-0.448
0.8180	0.016	0.076	0.120	0.034	-0.421
0.8820	0.012	0.065	0.126	0.112	-0.252
0.9440	0.004	0.055	0.115	0.144	-0.194
1.0070	0.000	0.043	0.101	0.152	-0.026
1.0700		------	------	------	0.095
1.1325		0.022	0.065	0.142	0.152
1.1960		------	------	------	0.173
1.2600		0.008	0.035	0.122	0.170
1.3830			0.016	0.044	0.128
1.5100			0.000	0.017	0.077
1.6360				0.004	0.039
1.7630				0.000	0.014
1.8880				-0.004	0.000
2.2060				0.000	-0.008
3.7750					0.000

$$\ddot{A}_{(ref)} = \ddot{A}_{cm(max)[(PD)(NP)R = 0.1]}$$

APPENDIX D

TYPICAL CALCULATION OF ERROR

The purpose of the following computation is to illustrate the application of the methods of Chapters 3 and 5 to determine the average response error resulting from backlash. Tables 5-4 and 5-5 summarize the results of similar calculations. Figures 5-19 and 5-20 show the variation of the average percentage error with pulse strength.

1. Pulse Function: MAVSD System
   Displaced Cosine

   $(PD)(NP)R = 1.0$

2. Motor Limitations: At the torque summing member, maximum
   acceleration = 9300 rad/sec^2

   maximum velocity = 415.0 rad/sec

3. Gear Train: $A_{(tsm)}/A_{(cm)} = 100$

   Total backlash = 0.5 milliradian = $A_{(bl)}$

   Effective backlash = 0.25 milliradian = $A_{(bl)(cm)}$

4. Pulse Strength:
   (a) From Table 5-3, a pulse height of 1 mr. gives

   $$\ddot{A}_{(cm)} = 1441 \ mr/sec^2$$

   (b) From motor characteristics and gear ratio,

$$\ddot{A}_{(cm)(max)} = 93000 \text{ mr./sec}^2$$

(c) $(PH)_{max} = \frac{93000}{1441} = 64.5$ mr.

(d) $(PS) = \frac{(PH)(T_n)}{2} = \frac{(64.5)(.0993)}{2} = 3.21$ mr. sec.

5. Peak amplitude of displacement response:

From Table 5-3,

$$A_{(cm)(max)} = (PH) \times 0.967$$

$$A_{(cm)(max)} = 64.5 \times 0.967 = 62.4 \text{ mr.}$$

6. Peak amplitude of velocity response

From Table 5-3,

$$\dot{A}_{(cm)} = (PH) \times 25 = 64.5 \times 25 = 1612 \text{ mr./sec.}$$

From motor characteristics and gear ratio,

$$\dot{A}_{(cm)(max)} = 4150 \text{ mr./sec.}$$

Therefore the velocity is well below it's limit.

7. Application of the effective backlash to the velocity response of the mean point. (Shaded triangular areas of Fig. 5-17.)

$$A_{(bl)(cm)} \approx \frac{\Delta Vel \times Time}{2} = 0.25 \text{ mr.}$$

Note: As the velocity peaks decrease in amplitude, a greater period of time is required to take up the effective backlash.

8. Deviation due to backlash Fig. 5-16

   (a) During time the backlash is taken up the deviation rises parabolically.

   (b) Deviation remains constant at the value of the effective backlash until the velocity reaches a negative maximum.

   (c) Deviation falls parabolically to zero as backlash is taken up in the opposite direction.

9. Average error in percent

$$\text{APEM} \leq \frac{2\int_{-\infty}^{\infty} |f(t)||(\mathcal{E})f(t)|\,dt}{\int_{-\infty}^{\infty} |f(t)|^2\,dt} \times 100$$

where $(\mathcal{E})f(t)$ = ordinate of deviation curve, Fig. 5-18

$f(t)$ = ordinate of displacement curve, Fig. 5-16

(a) Integrating graphically,

$$\int_{-\infty}^{\infty} |f(t)|^2 = 173\ (\text{mr})^2\ \text{sec}$$

$$2\int_{-\infty}^{\infty} |f(t)||(\mathcal{E})f(t)|\,dt = 1.38\ (\text{mr})^2\text{sec}$$

(b) $$\text{APEM}_{(\text{ttr})} = \frac{1.38}{173} \times 100 = 0.798\%$$

10. Average error for uncertainty level $(U)f(t)$ of 0.5 mr.

$$2\int_{-\infty}^{\infty} |f(t)||(U)f(t)|\,dt = 4.18\ (\text{mr})^2\text{sec}$$

$$\text{APEM}_{(\text{ttr})} = \frac{4.18}{173} \times 100 = 2.42\%$$

GLOSSARY OF SYMBOLS AND NOTATIONS

Self-defining notation developed by Draper et al[5] has been used throughout this thesis.

a - amplitude

A - angular displacement

$\dot{A}$ - angular velocity

$\ddot{A}$ - angular acceleration

ADFR - angular displacement frequency response

ADTTR - angular displacement transient time response

APEM - average percentage error in magnitude

AVSD - angular velocity signal damping

β - non-dimensional frequency ratio

bl - backlash

bl(cm) - effective controlled-member backlash

BR - backlash ratio

(C) - correction

cm - controlled-member

DAR - dynamic amplitude ratio

DCPF - displaced cosine pulse function

DRA - dynamic response angle

DR - damping ratio

e - natural logarithm base

eq - equivalent

$(\mathcal{E})f(t)$ - error in the function of time

$F(\mathcal{E})$ - working variable form for frequency response

f(t) - working variable form for transient time response

fr - frequency response

FR - frequency ratio

I - inertia

id - identified

IFF - input forcing function

j - imaginary component

MAVSD - modified angular velocity signal damping

M - torque

mr - milliradian

n - frequency in cycles per second

n_f - forcing frequency in cycles per second

n_{ref} - reference frequency in cycles per second

OR - output response

p - derivative operator

PF - performance function

PD - pulse duration

(PD)(NP)R - pulse duration natural period ratio

PH - pulse height

PS - pulse strength

ps - positional servomechanism or physical system

PSR - pulse strength ratio

q - quantity

REAC - Reeves Electronic Analogue Computer

S - sensitivity - dimensional similarity factor

t - time

T_n - undamped natural period

(T)(NP)R - time natural period ratio

T_p/T_n - working variable expression for (PD)(NP)R

tsm - torque summing member

ttr - transient time response

(U)f(t) - uncertainty in the transient time response

w_f - angular forcing frequency

w_n - angular undamped natural frequency

μ - working variable form for DAR

ϕ - working variable form for DRA

σ - working variable form for S

BIBLIOGRAPHY

1. Bromberg, B. G. "Graphical Methods of Fourier Series to Automatic Tracking Systems", (D. Sc. Thesis, Department of Aeronautical Engineering, Massachusetts Institute of Technology, 1947) Report No. 6445-T-7 Instrumentation Laboratory, Massachusetts Institute of Technology, Cambridge, Massachusetts. 1948 (Confidential)

2. Seamans, R. C. Jr., Blasingame, B. P., and Clementson, G. C. "The Pulse Method for the Determination of Aircraft Dynamic Performance", Journal of the Aeronautical Sciences, Vol. 17, No. 1. page 22, January, 1950

3. Bollay, W., "Aerodynamic Stability and Automatic Control", Journal of the Aeronautical Sciences, Vol. 18, No. 9, page 569, September, 1951

4. Gardner, M. T., and Ross, C. W., "Comparison of Sinusoidal Forcing Function and Pulse Forcing Function Techniques for Obtaining Dynamic Performance Characteristics of Fire Control Systems" (S. M. Thesis, Department of Aeronautical Engineering, Massachusetts Institute of Technology, May, 1953) Report No. T-30, Instrumentation Laboratory, Massachusetts Institute of Technology, Cambridge, Massachusetts, 1953 (Confidential)

5. Draper, C. S., McKay, W., Lees, S., "Instrument Engineering - Vol. I - Methods for Describing the Situations of Instrument Engineering" McGraw-Hill Book Company, Inc., New York, First Edition, 1952

6. Draper, C.S., McKay, W., Lees, S., "Instrument Engineering Vol. II - Methods for Associating Mathematical Solutions with Common Forms", McGraw-Hill Book Company, Inc., New York, First Edition, 1953

7. Tustin, A., "The Effects of Backlash and of Speed-Dependent Friction on the Stability of Closed-Cycle Control Systems", The Journal of the Institution of Electrical Engineers, Vol. 94, Part IIA, No. 1, 1947 page 143

8. Lees, S., "Stabilization of a Simple Positional Servomechanism with Negative Unity Feedback" Unpublished Class Notes, Course 16:42, Aeronautical Engineering Department, Massachusetts Institute of Technology, Cambridge, Massachusetts, March, 1952

9. Cramer, H., "Mathematical Methods of Statistics", Princeton University Press, Princeton, New Jersey, 1946

10. Morse, P.M., and Feshbach, H., "Methods of Theoretical Physics", McGraw - Hill Book Company, Inc., New York, 1953

11. Lees, S., "Design Study of a Positional Servomechanism with Unity Feedback" Unpublished problem, Course 16:41, Aeronautical Engineering Department, Massachusetts Institute of Technology Cambridge, Massachusetts, Fall, 1953.

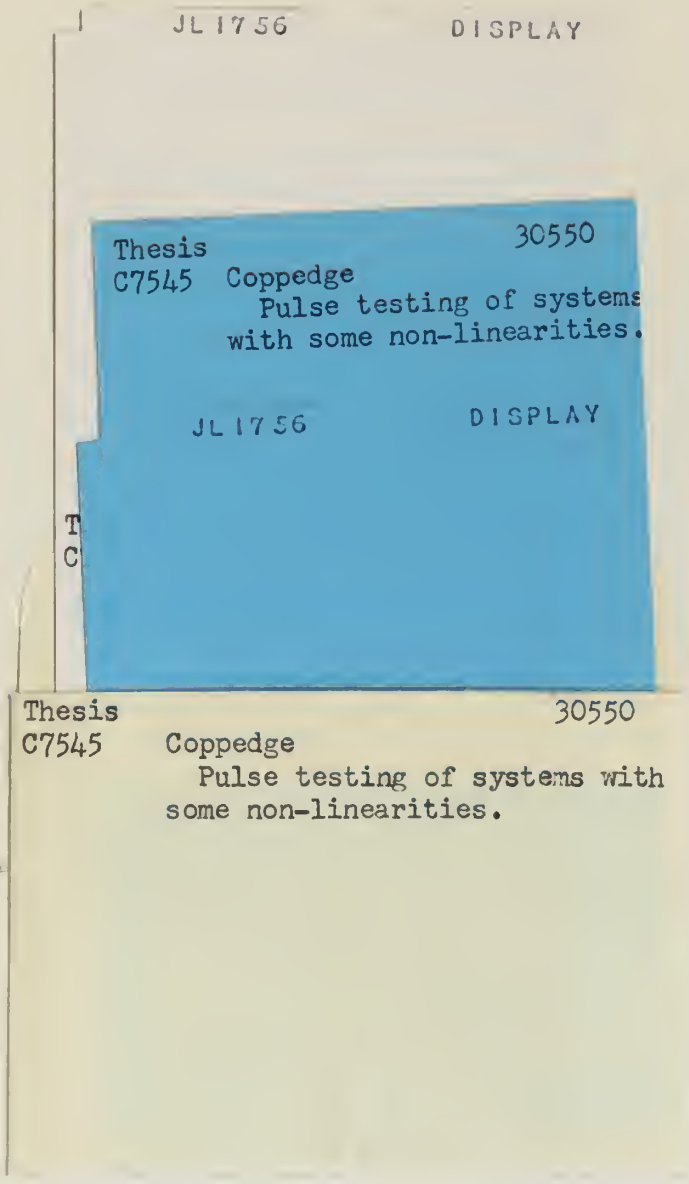
JL 1756
DISPLAY
Thesis
30550
C7545 Coppedge
Pulse testing of systems
with some non-linearities.
JL 1756
DISPLAY
Thesis
30550
C7545 Coppedge
Pulse testing of systems with
some non-linearities.